UNIVERSIDADE ESTADUAL DE CAMPINAS

LEONARDO FERNANDES FRACETO

"ANESTÉSICOS LOCAIS: INTERAÇÃO COM MEMBRANAS E FRAGMENTO DO CANAL DE SÓDIO VOLTAGEM DEPENDENTE"

Tese apresentada ao Instituto de Biologia da Universidade Estadual de Campinas, para obtenção do título de Doutor em Biologia Funcional e Molecular na área de Bioquímica.

Orientadora: Profa. Dra. Thelma de Aguiar Pertinhez

Co-orientadora: Profa. Dra. Eneida de Paula

2003

Data da Defesa: 07/11/2003

Banca Examinadora

Profa. Dra. Thelma de Aguiar Pertinhez (Orientadora)
CeBiME/ Laboratório Nacional de Luz Síncrotron

Prof. Dr. Francisco Pessine
Instituto de Química/Universidade Estadual de Campinas

Prof. Dr. José Daniel Figueroa Villar
Instituto Militar de Engenharia

Profa. Dra. Maria Teresa Lamy Freund
Instituto de Física/Universidade de São Paulo

Profa. Dra. Maria Terêsa Machini de Miranda
Instituto de Química/Universidade de São Paulo

Profa. Dra. Nilce Correa Meirelles
Instituto de Biologia/Universidade Estadual de Campinas

Prof. Dr. Eduardo Maffud Cilli
Instituto de Química/Universidade Estadual Paulista

AGRADECIMENTOS

À Fundação de Amparo à Pesquisa do Estado de São Paulo (FAPESP) pela concessão da bolsa e ajuda financeira para o andamento do projeto.

As Profa. Dra. Thelma de Aguiar Pertinhez e Profa. Dra. Eneida de Paula pelo profissionalismo, oportunidade, estímulo a visão crítica e pelo grande lado humano que permitiram meu crescimento profissional e pessoal, vocês terão minha eterna gratidão.

Ao Prof. Dr. Alberto Spisni por sua colaboração direta no trabalho com sugestões, críticas e pela amizade.

Ao Prof. Dr. Clóvis R. Nakaie, pela síntese do peptídeo sem o qual parte deste trabalho não teria sido realizado.

A todos do Laboratório Nacional de Luz Síncrotron, em especial aos colegas do Centro de Biologia Molecular e Estrutural e todos do Departamento de Bioquímica/Unicamp (alunos, funcionários e professores) que dividiram parte deste trabalho mesmo que de maneira indireta.

A todos os amigos do Grupo da Ressonância Magnética Nuclear em especial para Ângela, Alberto, Aline, Maurício, Sérgio e Thelma, obrigado por tudo e por me aguentarem por todo este tempo.

Aos amigos do laboratório de Biomembranas, em especial para Bispo (Marcelo), Morango (Daniele), Nono (Eleonora), Eneida e Nilce por todos os momentos durante minha iniciação científica e pós-graduação.

Em especial a meus pais Agda e Benedito e meu irmão Leandro, pelo apoio, incentivo, educação, confiança, mesmo muitas vezes não entendendo bem o que faço.

Aos amigos da Universidade de Sorocaba: Amouni, Raquel, Sílvio, Marli, Eni e em especial a Renata. Agradeço ainda a todos meus alunos pela amizade e ambiente agradável para se trabalhar.

A todos que acompanharam este trabalho de maneira direta e indireta, em especial para Márcio (Bioquímica), Elano, Leandro, Rodrigo (Zap), Maurício (RPG), Nina e Carla (USP).

Enfim, gostaria de agradecer a oportunidade de ter conhecido pessoas importantes para minha formação científica, cultural, tecnológica, em um ambiente muito agradável ao longo de todos estes anos. Ah, detalhe, não pensem que vou desaparecer, pois vou perturbar vocês por um bom tempo ainda.

Bom, é isso aí pessoal..... Valeu.

“ Não ande pelo caminho
traçado; ele conduz
somente até onde
os outros já foram ”

Albert Einstein

Dedico essa Tese às minhas orientadoras:

Eneida e Thelma

RESUMO

Várias teorias sobre o mecanismo de ação de anestésicos locais (AL) são descritas na literatura. Podemos destacar as que propõem explicar efeitos diretos dos AL sobre a proteína canal de sódio e as que levam em conta a interação dos anestésicos com a fase lipídica membranar.

Também é bem conhecido que a hidrofobicidade dos anestésicos locais está diretamente relacionada com a potência anestésica clínica. Portanto, o mecanismo de ação dos anestésicos locais, seja via interação com a fase lipídica da membrana ou com a proteína canal de sódio, deve ser analisado com base nessa característica.

A primeira etapa deste trabalho foi direcionada ao estudo da interação dos anestésicos, lidocaína e benzocaína, com sistemas modelos de membranas: lipossomos e *ghosts* de eritrócitos. Várias técnicas espectroscópicas foram empregadas na caracterização dos sistemas de estudo: ressonância paramagnética eletrônica (RPE), fluorescência, infravermelho e ressonância magnética nuclear (RMN) de hidrogênio e fósforo.

Considerando que os anestésicos locais atravessam rapidamente a bicamada lipídica, a localização destes na membrana é representada por uma função de distribuição (em relação à normal da bicamada), isto é, onde os anestésicos se encontram na maior parte do tempo. O estudo da localização preferencial dos anestésicos locais nas vesículas de fosfatidilcolina de ovo e nos *ghosts* de eritrócitos mostrou que a lidocaína se posiciona próximo ao grupamento fosfato da cabeça polar dos lipídios, enquanto que a benzocaína está mais inserida na membrana junto a região do glicerol e primeiros carbonos da cadeia acila.

Na segunda parte da tese estudamos, por RMN e dicroísmo circular, a interação dos AL benzocaína e lidocaína com um fragmento pertencente à alça citoplasmática S4-S5, do domínio IV, do canal de sódio voltagem-dependente, de cérebro humano (resíduos 1644-1664, KGIRTLLFALMMSLPALFNIG-NH_2, *p*IV/S4-S5), que está envolvido na estabilização do estado inativado do canal. Este estudo compreendeu a determinação estrutural do peptídeo *p*IV/S4-S5 em presença do co-solvente trifluoretanol, considerado um sistema mimético de membrana, e a caracterização da interação com os AL.

O peptídeo *p*IV/S4-S5 apresenta uma estrutura helicoidal com uma dobra na região do resíduo de prolina e uma face hidrofóbica formada pelos resíduos hidrofóbicos de leucina, isoleucina e metionina, importantes para o processo de estabilização do estado inativado do canal de sódio voltagem dependente.

O anestésico local benzocaína apresentou maior interação com o fragmento *p*IV/S4-S5, sendo que o resíduo mais afetado foi a metionina 1655 identificada como importante para o processo de inativação do canal.

Desta forma, demonstramos que os AL apresentam uma localização preferencial no interior da bicamada de acordo com suas propriedades químicas, ou seja, a benzocaína (mais hidrofóbica) se posiciona mais profundamente, enquanto a lidocaína (mais hidrofílica) se insere próximo à cabeça polar dos lipídios. Portanto, a localização, assim como o caráter hidrofóbico destes anestésicos, está diretamente correlacionada com a potência anestésica.

Os resultados apresentados neste trabalho fornecem embasamenteo para um melhor entendimento ao nível molecular, do processo de interação de anestésicos locais com membranas e com a proteína canal de sódio, ambos importantes no mecanismo de ação destes compostos, além de auxiliar no desenvolvimento de novos compostos com tal potencial.

As estratégias utilizadas neste trabalho podem, ainda, ser aplicadas a outros tipos de sistemas, onde a interação molecular de um ligante, fármaco, cofator enzimático, substrato com uma proteína ou membrana lipídica seja importante para o mecanismo de ação.

ABSTRACT

Many theories about the mechanism of action of local anesthetics (LA) are described in the literature. We can highlight those that focus on the direct effects of LA on the voltage gated sodium channel protein and the ones that take into account the interaction of the anesthetic molecules with the lipid membrane phase.

The direct correlation between local anesthetic hydrophobicity and anesthetic potency is well know. In this context, this property is crucial to the understanding of the LA mechanisms of action through their interaction with the membrane or with the sodium channel protein.

In the first part of this work we have employed different spectroscopic techniques such as electron paramagnetic resonance, fluorescence, infrared and nuclear magnetic resonance of hydrogen and phosphorus to obtain information about the specific interaction of local anesthetic with the membranes: lipossomes and *ghosts*.

Considering that local anesthetic crosses the membrane in a fast way and that its location inside the bilayer is best represented by a distribution function (against the bilayer normal), we have brought together clear evidences of regions with greater probabilities of finding the local anesthetic, i.e., where the local anesthetic stay most of the time.

The study of preferential location between local anesthetic and egg phosphatidylcholine model membranes and human erythrocyte membranes indicates that lidocaine molecules are inserted across the polar and liquid interface of the membrane, establishing both electrostatic (charged form) and hydrophobic (neutral form) interactions. Benzocaine locates itself a little deeper in the bilayer, between the interfacial glycerol region and the hydrophobic core.

In the second part of this work we have determined the solution structure of the peptide: KGIRTLLFALMMSLPALFNIG-NH_2, 1644-1664 (in trifluorethanol as a membrane mimetic solvent) that encompasses the cytoplasmic linker connecting the S4-S5 helices in domain IV (*p*IV/S4-S5) of the human brain voltage-gated sodium channel, studied by circular dichroism (CD) and nuclear magnetic resonance (NMR). The interaction

between the local anesthetic and this peptide has been accessed by nuclear magnetic resonance.

The peptide exhibits a α-helical structure extending over most of its length with a bend at the proline position. In the central part of the helix it is evident the existence of a hydrophobic surface involving one side of the helix surface formed by leucine, isoleucine and methionine residues, important to the stabilization of the inactivation sodium channel state. The higher level of complexation is observed for benzocaine and the interaction occurs with the methionine 1655, a residue that plays an important role in the inactivation of the channel.

In conclusion, we have shown that the local anesthetics have a preferential location inside the bilayer and this behavior can be explained on the basis of the physical-chemical properties of the two local anesthetics, i.e., benzocaine (more hydrophobic) deep inside, while lidocaine (more hydrophilic) inside near the polar head of lipids. The location of both local anesthetics is related with the anesthetic potency. The interaction of benzocaine with the peptide suggests a possible action site to this local anesthetic with the sodium channel protein.

The results here presented provide new insights on the understanding of the molecular processes involved in the interaction of local anesthetics with the membrane and the sodium channel protein. In addition, they can be useful in the development of novel compounds with anesthetic properties.

The methods and strategies employed in this work can be applied in different systems were the interaction of a drug, an enzymatic cofactor or a substrate with proteins or membranes could be important to their mode of action.

ÍNDICE página

1 - INTRODUÇÃO

1.1 – TRANSMISSÃO DO IMPULSO NERVOSO

Em todas as células excitáveis, o potencial para a condução do impulso nervoso provém do desequilíbrio iônico dentro e fora da membrana plasmática (Hodgkin & Huxley, 1952). O processo de excitação-condução do estímulo nervoso em nervos periféricos e terminais nervosos se deve a um potencial eletronegativo (potencial de repouso) de aproximadamente –60 a –90 mV, que existe através da membrana celular, durante o período de repouso do nervo. Ocorrendo uma excitação, uma seqüência completa de fenômenos se inicia com a despolarização da membrana. Durante essa fase, o potencial elétrico no interior da célula nervosa torna-se progressivamente menos negativo (Covino & Vassalo, 1985; Butterworth & Strichartz, 1990). Quando a diferença de potencial entre a superfície interna e externa da membrana celular atinge um nível crítico, o potencial de disparo ou limiar de excitabilidade, uma fase de despolarização extremamente rápida se inicia, levando a uma reversão do potencial da membrana celular, tornando-se o interior da membrana eletropositivo em relação à face externa. Ao atingir o máximo do potencial de ação, o interior da célula tem um potencial elétrico positivo de aproximadamente de +30 a +40 mV, em relação ao exterior da célula. Terminada a fase de despolarização, inicia a repolarização. Nesta fase, o potencial elétrico dentro da célula torna-se progressivamente mais negativo em relação ao exterior, até que o potencial de repouso, de –60 a –90 mV, se restabeleça. Sob condições normais, todo o processo de despolarização e repolarização dura cerca de 1 ms. A fase de despolarização dura aproximadamente 30% de todo tempo do potencial de ação, enquanto que a repolarização consome os 70% restantes (Covino & Vassalo, 1985).

Fisiologicamente, a excitação da membrana nervosa causa ativação da proteína canal de sódio voltagem dependente, que se abre, fazendo com que haja influxo de íons sódio – para re-equilibrar o potencial e as concentrações desiguais desse íon dentro e fora da célula - levando à despolarização da membrana (**Figura 1**). A ativação dos canais de sódio envolve uma série de transições entre o estado de repouso (não condutor) e aberto (condutor), responsável pelo influxo de sódio. Essa diminuição de cargas ou despolarização

é o sinal para que os canais de sódio voltagem-dependente dos axônios se abram, permitindo assim a propagação do impulso nervoso, no qual o sinal elétrico é transmitido ao longo do axônio, unidirecionalmente. Os canais de sódio fecham-se (inativação) espontaneamente após alguns milisegundos e, portanto, a duração do fluxo de entrada de íons sódio na célula é limitada (Butterworth & Strichartz, 1990).

O canal voltagem-dependente é a principal proteína do axônio, chegando a representar mais de 90% das proteínas de membrana. Diferentemente de outros canais, esta proteína não possui um sítio receptor, e sua ativação é feita pela alteração do potencial elétrico da membrana, que causa alterações conformacionais na proteína, provocando a ativação (Marban *et al.*, 1998).

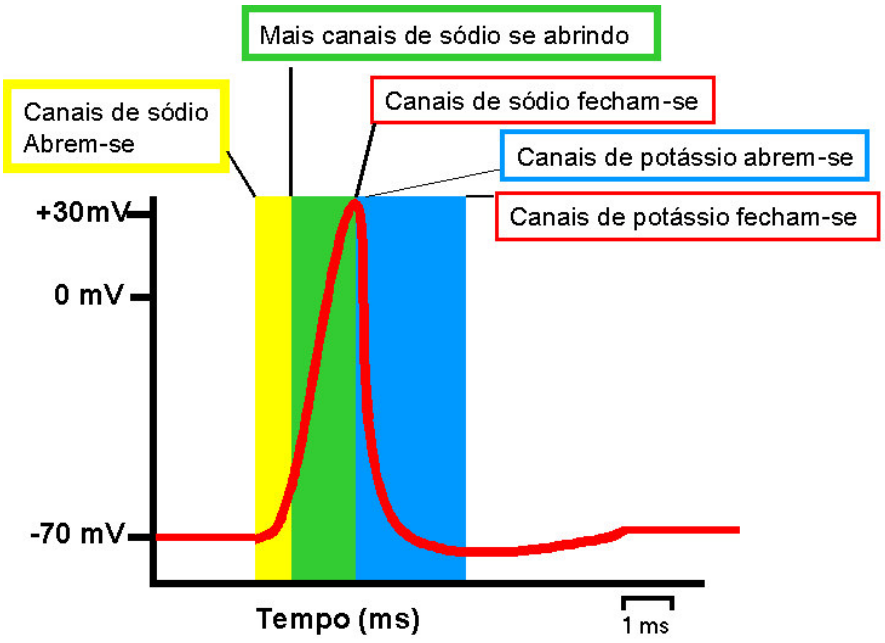

Figura 1: *Potencial de ação no axônio.* O aumento rápido no potencial de membrana de -70mV para aproximadamente +30mV é descrito como despolarização. Esta despolarização é causada por um rápido aumento na permeabilidade ao íon Na^+. Quando a permeabilidade ao íon Na^+ diminui, a permeabilidade ao íon K^+ aumenta e o potencial de membrana cai, muitas vezes abaixo do potencial de repouso, seguido de um retorno lento ao nível de repouso.

Mais lentamente que a abertura dos canais de sódio, desenvolve-se o efluxo de íons potássio, através de canais de potássio eletricamente sensíveis, o que auxilia o período de repolarização da membrana. Durante a repolarização a concentração de cátions é rapidamente restaurada; porém, com um excesso de sódio no meio intracelular e um excesso de potássio no meio extracelular. Nas células nervosas como em outras, o desequilíbrio iônico é criado e mantido pela Na^+, K^+ ATPase (a bomba de sódio/potássio), uma proteína de membrana que, às custas de ATP bombeia 3 íons Na^+ para fora contra 2 íons K^+ para dentro da célula restabelecendo, assim, as concentrações iônicas dentro e fora da célula (Voet & Voet, 1995).

Várias substâncias químicas são conhecidas pela capacidade de agir sobre as espécies envolvidas no processo de excitação-condução do estímulo nervoso (principalmente canais de sódio); dentre elas podemos destacar as drogas anti-arrítimicas (Katz, 1998), anestésicos locais (Scholz, 2002), antiepiléticas (Ragsdale & Avoli, 1998) e as neurotoxinas (Cestèle & Catterall, 2000), entre outras.

1.2 ANESTÉSICOS LOCAIS

Anestésicos locais (AL) diferem dos anestésicos gerais por sua ação regional e pelo modo de aplicação, sendo os últimos aplicados via sistêmica, direta (no sangue) ou indiretamente (pulmões). Além disso, os anestésicos locais agem sobre os axônios, enquanto os anestésicos gerais atuam nas transmissões sinápticas (Covino & Vassalo, 1985; Strichartz & Ritchie, 1987; de Jong, 1994).

Anestésicos locais compreendem um grande número de moléculas, de diferentes estruturas químicas: amino-ésteres, amino-amidas, amino-cetonas, amidas, álcoois, tio-ésteres, tio-amidas, derivados de uréia, poliéteres, etc (Gupta, 1991), capazes de bloquear a condução do estímulo nervoso.

No final do século XIX foram descobertas acidentalmente as propriedades anestésicas da cocaína, o primeiro anestésico local. A cocaína existe em grandes quantidades em folhas do arbusto coca (*Erythroxylon coca*). Durante séculos, os nativos dos Andes mascaram um extrato alcalino dessas folhas devido a suas ações estimulatórias e

euforizantes. A cocaína foi isolada pela primeira vez em 1860, por Albert Niemann que, assim como muitos químicos daquela época, provaram do composto isolado e constataram que o mesmo causava entorpecimento da língua. Sigmund Freud estudou as ações fisiológicas da cocaína e, em 1884, Carl Koller a introduziu na prática clínica como um anestésico tópico para cirurgia oftalmológica. Os muitos anestésicos locais utilizados na prática clínica atual originam-se dessas observações antigas (Covino & Vassalo, 1985; Guyton & Hall, 1996). A cocaína é um éster do ácido benzóico que, devido à sua toxicidade foi rapidamente substituída por análogos sintéticos. Em 1905 foi sintetizada a procaína, que se tornou o protótipo dos anestésicos locais durante quase meio século. Atualmente, os agentes mais amplamente utilizados são a bupivacaína e a lidocaína. A **Figura 2** apresenta a estrutura química dos anestésicos locais típicos que possuem regiões hidrofílicas (normalmente um grupamento amina) e hidrofóbicas (em geral um anel aromático) que são separadas por um éster intermediário ou por uma ligação amídica.

Por serem moléculas anfifílicas, os anestésicos locais têm grande afinidade pela membrana celular. Em membranas excitáveis, eles diminuem a velocidade de despolarização, inativando os canais de sódio voltagem-dependente dos axônios, impedindo assim o influxo de íons necessários à despolarização da membrana (Covino & Vassalo, 1985).

ANESTÉSICO	pKa	R_1
Lidocaina	7.8	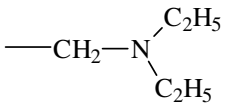
Etidocaina	7.7	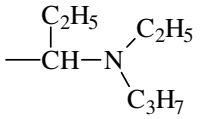 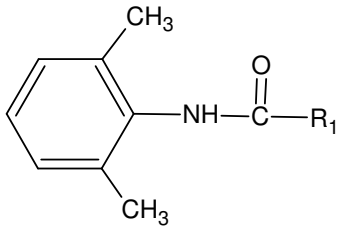
Mepivacaina	7.6	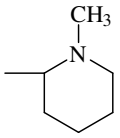
Bupivacaina	8.1	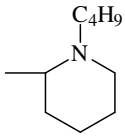
Tetracaína	8.5	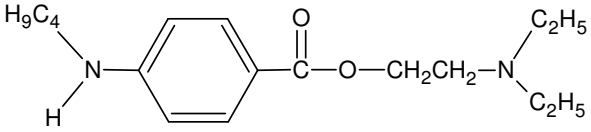
Procaína	9.2	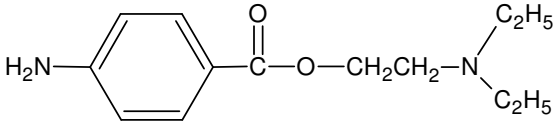
Benzocaína	2.3	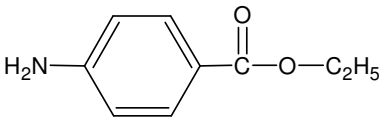

Figura 2: Estrutura química de alguns anestésicos locais.

Na clínica, as amino-amidas como a lidocaína e a bupivacaína e amino-ésteres como a tetracaína e benzocaína são os mais usados (de Jong, 1994). Os amino-ésteres são, em geral, mais potentes que as amino-amidas, no entanto, a tendência atual é a de desenvolver-se amino-amidas mais potentes, pelo fato de serem menos tóxicas e mais resistentes à

hidrólise quando comparadas com os amino-ésteres (de Jong, 1994). A importância clínica da lidocaína (amino-amida, ionizável) e a baixa solubilidade aquosa da benzocaína (um amino-éster, de caráter neutro e empregado somente em anestesia tópica) nos levaram a escolher essas duas moléculas para este estudo.

Abaixo são descritas algumas propriedades destes anestésicos locais:

1.2.1 - BENZOCAÍNA

A benzocaína (**Figura 2**) é um anestésico local com baixa solubilidade em água limitando sua utilização na forma injetável. Em conseqüência, este composto permaneceu esquecido por muitos anos. Finalmente, a benzocaína, foi reconhecida como anestésico tópico eficaz, permanecendo atualmente como um fármaco valioso para obtenção de anestesia de superfície das membranas mucosas, sendo recomendada para alívio da dor dérmica, causada pelas pequenas abrasões ou queimadura solar (Covino & Vassalo, 1985; de Jong, 1994). Sua metabolização hepática envolve a interação com citocromo P_{450} e o primeiro passo seria a N-hidroxilação do grupo amino-benzoato. Outro provável passo metabólico seria a hidrólise a ácido p-amino benzóico e etanol, ainda não comprovada; o ácido p-amino benzóico pode, também, ser metabolizado em ácido amino hipúrico, que está envolvido na formação de meta-hemoglobina (de Jong, 1994).

Eventos celulares, como a inibição do aumento dos níveis de cálcio intracitoplasmático e fisiológicos, como a alteração na curva de resposta dos barorreceptores em indivíduos com pressões mais altas, têm sido associados ao uso da benzocaína. O efeito indesejável mais grave, porém, está relacionado ao aumento dos níveis de metahemoglobina, induzido pela benzocaína em várias espécies (Martin *et al.*, 1995).

1.2.2 - LIDOCAÍNA

É atualmente o anestésico local mais amplamente utilizado e sua estrutura química está ilustrada na **Figura 2**. A lidocaína produz anestesia de início mais rápido, mais intensa e de maior duração que uma igual concentração de procaína (Catterall & Mackie, 1996). A lidocaína é rapidamente absorvida após administração parenteral e pelos tratos gastrintestinal e respiratório. Embora seja eficaz quando utilizada sem qualquer vasoconstritor, com a adição de adrenalina a taxa de absorção e a toxicidade são reduzidas e a duração da ação é, em geral, prolongada. A lidocaína é desalquilada no fígado por oxidases de função mista, que podem ser metabolizadas em monoetilglicina e glicina xilidida. Monoetilglicina xilidida e glicina xilidida retêm a atividade anestésica local. Nos seres humanos cerca de 75% da xilidida é excretada na urina, como o metabólito 4-hidróxi-2,6-dimetilanilina (Catterall & Mackie, 1996).

Os efeitos colaterais da lidocaína incluem sonolência, zumbido e tontura. À medida que aumenta a dose, podem ocorrer convulsões, coma, depressão e parada respiratória. Em geral, níveis séricos de lidocaína que produzem efeitos acentuados no sistema nervoso central também provocam depressão cardiovascular clinicamente importante. Os metabólitos monoetilglicina xilidida e glicina xilidida contribuem para alguns desses efeitos colaterais (Goodman & Gilman, 1996).

A lidocaína tem vários usos clínicos como anestésico local. Sua duração não é tão grande quanto a da bupivacaína, etidocaína ou tetracaína; porém, é útil em quase toda aplicação em que é necessário um anestésico de duração intermediária e também é utilizada como agente antiarrítmico (Goodman & Gilman, 1996).

1.3 – HIPÓTESE DE MECANISMO DE AÇÃO DOS AL

Podemos classificar as teorias propostas para explicar os mecanismos de ação dos anestésicos locais em duas categorias: a que atribui o efeito anestésico à ligação destes à proteína canal de sódio e a que considera a interação dos AL com os lipídios da membrana (conhecida como "hipótese do lipídio") como o mecanismo responsável pelas alterações no canal.

Na primeira categoria enquadram-se inúmeras tentativas de explicar a ligação direta dos anestésicos locais em um ou mais sítios específicos do canal de sódio voltagem-dependente, alterando sua conformação e levando à inativação temporária do canal (Strichartz & Ritchie, 1987).

Várias observações já foram feitas em favor da interação específica entre anestésicos e o canal de Na^+. Primeiramente encontramos na literatura inúmeras descrições da interação dos AL com proteínas, como: calmodulina, canais de potássio, receptores de acetilcolina, ATPases microssomais e mitocondriais, citocromo oxidase, proteína G, proteína EnvZ que age na transdução de sinais por ativação da porina e proteína quinase Cα (de Paula & Schreier, 1996; Arias, 1998; Slater, *et al.*, 1997).

Desde os trabalhos pioneiros de Hodgkin & Huxley (1952) sabe-se que os anestésicos têm efeito direto nos canais de sódio e que interagem com diferentes afinidades com essas proteínas, dependendo do estado funcional (ativado, inativado, em repouso). Uma possível interpretação para essas diferentes afinidades estaria na presença das formas ionizada e neutra dos anestésicos, em pH fisiológico. Na década de 70, Frazier e col. verificaram que análogos quaternários de anestésicos locais bloqueavam a condução nervosa quando aplicados internamente em axônios gigantes de lula perfundidos. Esses autores entenderam esses resultados como indicativos de que a forma carregada dos AL seria a responsável pelo efeito no canal, e que o sítio de ligação seria acessível apenas a partir da face citoplasmática da membrana (Narahashi & Yamada, 1969; Frazier *et al.*, 1970).

No entanto, a grande potência anestésica de compostos como a benzocaína, que não se protona em pH próximo ao fisiológico, causava controvérsia para a descrição deste sítio único de ação para os anestésicos locais protonados. Além disso, a grande variedade estrutural de moléculas com ação anestésica local, levava a crer na existência de mais de um sítio receptor ou mecanismo de ação (Strichartz & Ritchie, 1987). O desenvolvimento quase simultâneo das técnicas de mutação sítio-específico e de *patch-clamp* permitiu, na década de 1980 um crescimento enorme nas pesquisas envolvendo proteínas-canal (Noda *et al.*, 1986). Em 1994 Catterall e colaboradores, usando técnicas de biologia molecular, conseguiram demonstrar a existência de um "sítio hidrofóbico" para a forma neutra dos anestésicos locais, situado no interior da bicamada, isto é, em uma α-hélice transmembranar (S6, do domínio IV, da subunidade α) da proteína canal de sódio. A substituição de resíduos hidrofóbicos como a fenilalanina (1764) por alanina faz decrescer, de 10 a 100 vezes, o bloqueio causado por anestésicos locais em canais de sódio de cérebro de ratos (Ragsdale *et al.*, 1994; 1996) .

Talvez a teoria de anestesia mais compreensiva e abrangente seja a "receptor-modulated", que admite a existência de um ou mais sítios de ligação no canal de sódio para os anestésicos locais. As diferentes afinidades dos anestésicos locais por esse(s) sítio(s) seriam moduladas pelo estado conformacional do canal, sendo maior a afinidade pelo canal inativado ou em repouso (na membrana despolarizada) do que pelo estado ativado, na membrana hiperpolarizada (Hille, 1977; Hondeghem & Katzung, 1977).

Na hipótese do lipídio considera-se que as alterações causadas pelos anestésicos nas propriedades estruturais e dinâmicas da matriz lipídica como a separação lateral de fases (Trudell, 1977; Hornby & Cullis, 1981), aumento da fluidez (Hubbel & McConnell., 1971; Boulanger *et al*., 1981; Bianconi & Schreier, 1991) ou lise celular (Seeman, 1966) levariam a mudanças conformacionais no canal de sódio, causando sua inativação (Lee, 1976a).

Nesta linha, temos estudado em nosso laboratório a interação de anestésicos locais com membranas modelo, tendo em vista as alterações estruturais e dinâmicas provocadas pelos anestésicos na fase lipídica (de Paula & Schreier, 1995, 1996; Malheiros *et al.*, 1999; Pinto *et al.,* 2000; Fraceto, *et al.*, 2002).

1.3.1 - INTERAÇÃO DE ANESTÉSICOS LOCAIS COM MEMBRANAS

Estudos clássicos da literatura mostram que os anestésicos locais agem sobre sistemas membranares, alterando-os de diversas maneiras. Analisando somente a fase lipídica membranar foram observados efeitos de expansão da bicamada, aumento da fluidez da membrana e alteração da temperatura de transição de fase, entre outros (de Paula & Schreier, 1996).

A incorporação de anestésicos locais causa uma expansão da área superficial de monocamadas (Skou, 1954) e bicamadas (Seeman, 1966; Seelig, 1987); esta expansão seria favorecida pela diferença entre o comprimento do anestésico local (mais curto) e o dos fosfolipídios; assim, abaixo do seu ponto de inserção o anestésico criaria um "volume livre" que seria compensado com aumento de conformações gauche das cadeias lipídicas, causando diminuição no comprimento total dos lipídios (Trudell, 1977; Gallová & Balgavý, 1997). De fato, Hill (1974) observou uma diminuição da espessura da bicamada, seguindo alterações da temperatura de transição de fase causadas por anestésicos gerais e álcoois. Essa alteração seria resultante da maior mobilidade das moléculas lipídicas, causada pela expansão da membrana.

Diminuições na temperatura de transição de fase foram observadas por diferentes grupos de pesquisadores utilizando várias técnicas. Lee (1976b, 1978), empregando calorimetria, registrou diminuição da temperatura de transição de fase de vesículas de fosfatidilcolina (PC) causada pela partição dos AL benzocaína, procaína, tetracaína, lidocaína e dibucaína, em concentrações iguais às necessárias para 50% de bloqueio na condução do estímulo nervoso. Esses achados foram confirmados para a forma neutra da procaína, tetracaína, lidocaína e bupivacaína, por espalhamento de luz (Ueda *et al.*, 1977). O fato de que os anestésicos locais perturbam o empacotamento dos fosfolipídios em membranas modelo e biológicas foi bastante estudado por experimentos de ressonância paramagnética eletrônica e também por outras técnicas espectroscópicas como ressonância magnética nuclear, infravermelho e fluorescência, (revisão em de Paula & Schreier, 1996),

trazendo enorme contribuição para o entendimento da interação de anestésico local com membrana.

Através da técnica de absorção no infravermelho, Schöpflin e col. (1987) demonstraram a incorporação da dibucaína e procaína em monocamadas de palmitoiloleil fosfatidilcolina, estudando as bandas de absorção dos compostos, entre 1400 e 1800 cm^{-1}. A combinação de estudos de infravermelho com variação de pressão possibilitou a Auger e col. demonstrar que a tetracaína, incorporada em membranas de PC, fosfatidilserina e biológicas, é expulsa da bicamada por aumento da pressão (Auger *et al.*, 1987, 1990). Esse achado veio comprovar observações anteriores, *in vivo*, da reversão da ação de anestésicos gerais com aumento de pressão (Lever *et al.*, 1971) e por que os anestésicos locais penetram menos em membranas biológicas com a diminuição da temperatura (Bradley & Richards, 1984). A compactação da membrana deve ser o fator limitante da partição dos anestésicos locais à baixa temperatura, como observaram Kaminoh e col. (1988; 1989).

Medidas de fluorescência revelaram importantes informações sobre a localização de anestésicos locais em vesículas fosfolipídicas. Estudos utilizando o anestésico local tetracaína como supressor de marcadores fluorescentes incorporados em diferentes posições no interior da bicamada indicaram uma inserção do anestésico em regiões mais profundas da bicamada, além de verificar a diferente mobilidade local nas cadeias acilas dos fosfolipídios (Sikaris & Sawyer, 1982; Hutterer, *et al.,* 1997).

Medidas de Ressonância Paramagnética Eletrônica (RPE) foram realizadas com anestésicos locais modificados, isto é, covalentemente ligados a radicais nitróxido (Gargiulo *et al.*, 1973; Giotta *et al.*, 1974) e também empregando radicais nitróxido ligados a ácidos graxos ou a ésteres destes ácidos (Schreier *et al.,* 1984, 1986; Frezatti Jr. *et al.*, 1986; de Paula & Schreier, 1995; Gallová & Balgavý, 1997; Pinto *et al.*, 2000; Fraceto *et al.*, 2002). Esses estudos mostraram que a incorporação dos anestésicos locais na bicamada lipídica é acompanhada por uma diminuição de ordem e dinâmica membranar. Em um estudo sistemático envolvendo anestésicos locais das séries amino-amidas e amino-éster (de Paula & Schreier, 1995) foi observado que o efeito de diminuição da organização de membranas lipídicas não está relacionado diretamente à hidrofobicidade ou classe dos anestésicos locais. Esses resultados foram reforçados por outro estudo realizado em nosso laboratório,

que correlacionou resultados de ressonância magnética nuclear (RMN) e RPE na análise da interação de AL de três famílias distintas com membranas multilamelares de PC de ovo (Pinto *et al.*, 2000). Foram encontradas evidências de que parâmetros estéricos dos AL determinariam sua localização preferencial no interior da bicamada.

Os primeiros experimentos empregando RMN de hidrogênio detectaram imobilização da molécula do anestésico local quando intercalado na bicamada lipídica (Hauser & Dawson, 1968; Cerbon, 1972; Darke *et al.*, 1972; Finer *et al.*, 1972; Lee *et al.*, 1972), efeito semelhante ao observado por RPE com análogos paramagnéticos dos AL (Gargiulo *et al.*, 1973; Giotta *et al.*, 1974).

Com experimentos de RMN de deutério, ^{2}H-RMN e a utilização de anestésicos locais e lipídios seletivamente deuterados foi possível, pela primeira vez, identificar as regiões da membrana lipídica nas quais se localizam preferencialmente os anestésicos locais (Boulanger *et al.,* 1980, 1981; Westman *et al.*, 1982; Browning & Akutsu, 1982; Kelusky, 1983; Kelusky & Smith, 1984). O trabalho de Boulanger e col. (1981) tornou-se citação obrigatória e é, com certeza, o trabalho de maior reconhecimento na área, por ter demonstrado, inequivocamente, a localização diferencial das formas protonada (mais superficial) e neutra da tetracaína em vesículas de PC. Resultados semelhantes foram encontrados com anestésicos gerais; utilizando ^{2}H-RMN, foi demonstrado que o etanol interage com diversas regiões da bicamada em vesículas unilamelares (Barry & Gawrisch, 1994) e multilamelares de PC de ovo (Holte & Gawrisch, 1997), porém apresenta preferência pela região mais polar do lipídio. Já os anestésicos gerais halotano, isofurano e enfurano residem na região hidrocarbônica de vesículas fosfolipídicas apresentando, também, preferência pela interface membrana-solvente (Baber *et al.*, 1995).

Medidas de ^{1}H-RMN foram favorecidas com o desenvolvimento de espectrômetros de RMN de alta resolução e de novas técnicas de pulso, que possibilitaram a obtenção de informações sobre a proximidade entre núcleos e o mapeamento do interior hidrofóbico da bicamada. Em relação aos anestésicos locais, os resultados obtidos até aqui por ^{1}H-RMN com a forma protonada da tetracaína (Yokono *et al*., 1989) procaína, dibucaína e tetracaína (Kuroda & Fujiwara, 1987; Wakita *et al.*, 1992), estão de acordo com os achados de ^{2}H-RMN, quanto à localização e grau de perturbação da bicamada.

No entanto, poucos trabalhos na literatura tratam da forma neutra dos anestésicos locais, entre eles estão os do grupo de Smith (Boulanger *et al.*, 1980 e 1981; Westman *et al.*, 1982; Kelusky *et al.*, 1984), o trabalho de Sikaris & Sawyer (1982) e nossos (Lissi *et al.,* 1990; de Paula & Schreier, 1995 e 1996; Pinto *et al*., 2000; Fraceto *et al*., 2002), a despeito da maior interação desses com a fase lipídica da membrana. É provável que a dificuldade imposta pela baixa solubilidade aquosa dos AL desprotonados tenha limitado seu estudo, além da falsa idéia introduzida a partir dos trabalhos com análogos quaternários da lidocaína realizados nos anos 70 (Frazier & Narahashi, 1971; Frazier *et al.*, 1970) de que a forma protonada dos anestésicos locais seria a responsável pela ligação à proteína canal de Na^+. A importância da forma neutra dos anestésicos locais foi retomada depois dos trabalhos de Ragsdale e col. (1994 e 1996) que demonstraram a existência de um sítio hidrofóbico no canal de Na^+ para a ligação dos anestésicos locais desprotonados. Além disso, há evidências de que o pK aparente de anestésicos locais como a tetracaína (Schreier *et al.,* 1984) diminui significativamente na presença de membranas, o que leva a um aumento na fração de anestésicos desprotonados em pH fisiológico.

Nosso trabalho foi direcionado à questão da determinação da localização preferencial de AL no interior de bicamada, através de medidas de RMN, ^{1}H-NOE e tempo de relaxação longitudinal spin-rede (T_1). As medidas de RMN forneceram informações sobre a interação anestésico local/lipídio, que nos permitem ampliar o entendimento sobre o mecanismo de anestesia.

1.3.2- INTERAÇÃO DE ANESTÉSICOS LOCAIS COM A PROTEÍNA CANAL DE SÓDIO

A principal ação farmacológica dos AL é a de interromper o processo de excitação e condução do estímulo nervoso em fibras nervosas periféricas.

O canal de sódio (**Figura 3**), glicoproteínas de membrana formadas por dois tipos de subunidades a α e β, é seletivo ao íon sódio (a passagem de K^+ equivale à cerca de 8% da

de Na^+), mas somente a α é requerida para sua função. Experimentos usando anticorpos anti-peptídeos das subunidades β1 e β2 mostraram que a maior parte dos canais de sódio de cérebro de rato têm ambas as subunidades β. A subunidade α tem 260 kDa e as β têm 23 e 21 kDa cada, sendo que β2 está ligada à subunidade α por pontes dissulfeto, enquanto β1 liga-se não covalentemente à α (Noda et al., 1986). Cada subunidade β tem um grande segmento amino terminal extracelular, com várias regiões de consenso para N-glicosilação. Canais de músculo esquelético tem a subunidade α (260 kDa) e uma ou duas subunidades β (com 38 kDa cada), enquanto os canais voltagem-dependentes de enguia e de coração de galinha apresentam apenas a subunidade α (Catterall, 1992). Canais de sódio pertencem à mesma família dos canais de potássio e de cálcio voltagem-dependentes (Marban *et al.*, 1998).

O canal de sódio é o mais estudado dos canais voltagem-dependentes. Já em 1952, Hodgkin & Huxley demonstraram que os fenômenos de abertura ("gating") e permeação de íons estavam relacionados com mais de 2 estados funcionais: aberto, fechado e inativado (Hodgkin & Huxley, 1952). Essa proteína foi também o primeiro canal desse tipo a ser clonado (Noda *et al.*, 1986) e seu estudo beneficiou-se, ainda, do desenvolvimento, na mesma época, da técnica de *patch-clamp*, que permite a medida do potencial elétrico de canais isolados (Hamill *et al.*, 1981).

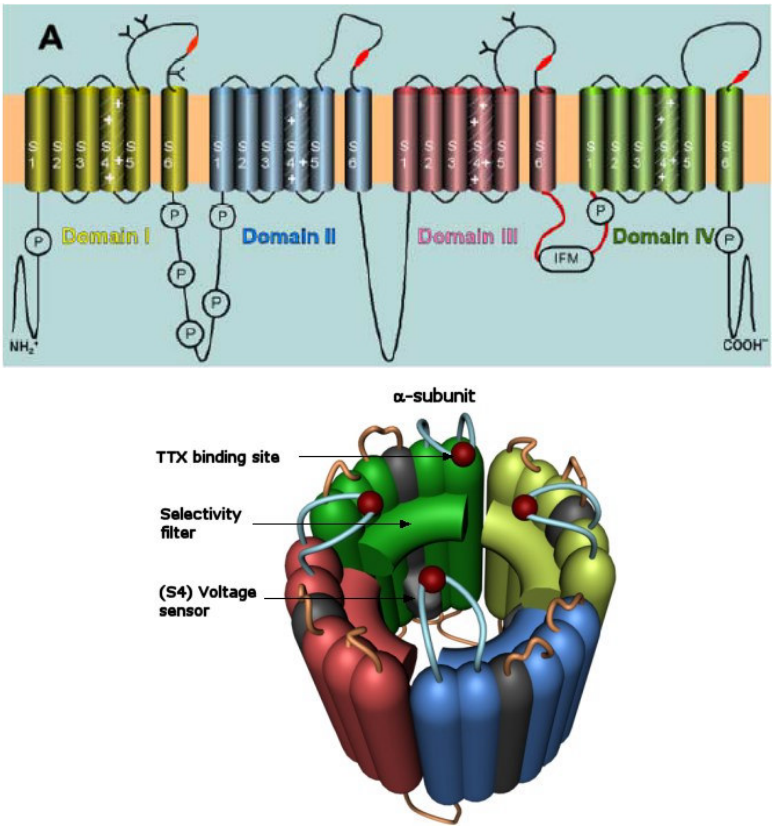

Figura 3: Subunidades do canal de sódio de cérebro de mamíferos e arranjo dos quatro domínios ao redor do poro central. Cada domínio apresenta seis α-hélices (S1-S6). (http://www.chemsoc.org/exemplarchem/entries/2002/Tim_Smith/channels/sodium)

A característica dessa família de canais voltagem-dependentes é a presença de 4 domínios transmembranares homólogos (canais de sódio e cálcio) ou quatro subunidades homólogas (canais de potássio), onde cada domínio ou subunidade apresenta seis segmentos em α-hélice, S1 a S6, como mostrado na **Figura 3** (Catterral, 1992; Marban *et al*., 1998; Scheuer, 1999). Os domínios ou subunidades se organizam de forma a apresentar um poro central seletivo ao sódio. Segundo Marban e col. (1998) os canais de sódio devem ter surgido a partir da mutação de canais de cálcio que, por sua vez, evoluíram por duplicação da informação gênica dos canais de potássio.

A estrutura do poro dos canais de potássio, com resolução de 3,2 angstrons foi determinada por cristalografia de Raios-X (Doyle *et al.*, 1998) e está apresentada na **Figura 4**. Os canais de potássio são muito similares aos de sódio, pois apresentam quatro domínios

(I a IV) compostos de seis α-hélices transmembranares (S1 a S6). Em cada domínio a α-hélice S4 - apresentando vários resíduos de aminoácidos carregados positivamente - tem importância fundamental no processo de abertura do poro em ambos os canais. Como esses canais voltagem-dependentes não possuem uma molécula ativadora específica, as α-hélices S4 formam a região "voltage-sensing" ou de disparo do canal (Scheuer, 1999). Acredita-se que a mudança do potencial da membrana desestabiliza o segmento S4, cujas cargas positivas são mantidas por pareamento com cargas negativas de outros segmentos transmembranares. Com a despolarização da membrana as forças que mantém as cargas positivas de S4 na sua posição são reduzidas e a hélice S4 sofre uma rotação (movimento espiral de cerca de 60 graus, projetando-se em 5 angstrons para fora da bicamada). Esse movimento deixa uma carga negativa não pareada no interior da bicamada e expõe uma carga positiva na superfície externa da membrana, resultando na transferência de carga líquida de +1 (Catterral, 1992).

Outra similaridade entre os canais é o segmento P (de poro), formado pela alça extracelular S5-S6, isto é, entre as α-hélices S5 e S6. Esse segmento é uma região bastante conservada entre os canais de Na^+, K^+ e Ca^{+2} e é considerado o "filtro" do canal (pois se dobra sobre o poro, **Figura 4**), como mostra a cristalografia de Raios-X dos canais de K^+ (Doyle *et al.*, 1998).

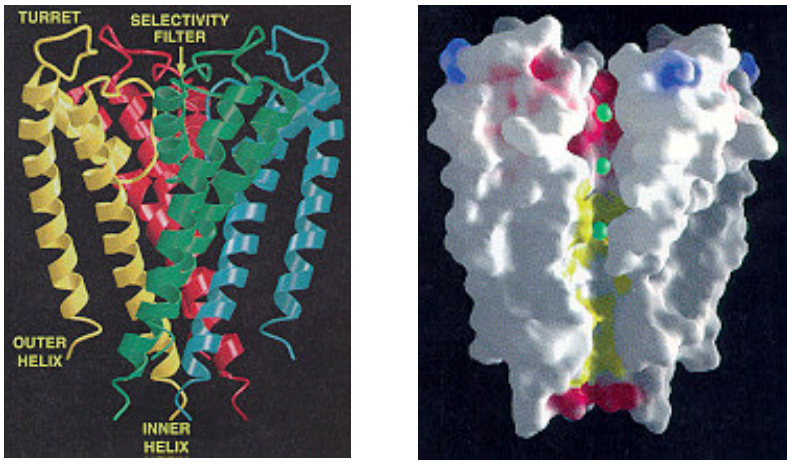

(A) (B)

Figura 4: Estrutura do canal de potássio. (A) Vista tridimensional do tetrâmero do canal de potássio (no qual as quatro subunidades apresentam cores diferentes); (B) Ilustração do poro iônico formado pelas diferentes subunidades do canal de potássio (de acordo com Doyle *et al.*, 1998).

Uma região extremamente importante para o funcionamento dos canais de sódio é o sítio de inativação ("*inativating gate*"), formado pela alça intramembranar entre os domínios III (S6) e IV (S1), que se projetam (como *tampa de dobradiça*) sobre o lúmem interno do poro, inativando-o. Anticorpos preparados contra esse segmento são capazes de inibir completamente a inativação do canal. Estudos de mutação sítio-específica mostraram que os resíduos I-F-M (posição 1488, 1489, 1490, Kuroda *et al.*, 1996) são fundamentais para a inativação espontânea do canal e formariam o *trinco* da fechadura, mantendo a tampa fechada sobre o poro (Rohl *et al.*, 1999; Scheuer, 1999), como ilustrado na **Figura 5**.

Sítios de regulação - por fosforilação - para a proteína quinase dependente de AMPc, foram encontrados na isoforma neuronal e em várias isoformas cardíacas do canal, especificamente na alça intracelular entre os domínios I e II (Marban *et al.*, 1998); a fosforilação diminui a amplitude da corrente e altera a condutância total da célula. A proteína quinase C também altera o funcionamento de todas as isoformas dos canais de sódio de mamíferos. O sítio de fosforilação é uma serina, altamente conservada, na alça entre os domínios III e IV; a fosforilação pela proteína quinase C reduz a condutância máxima do canal e altera sua ativação (Marban *et al.*, 1998).

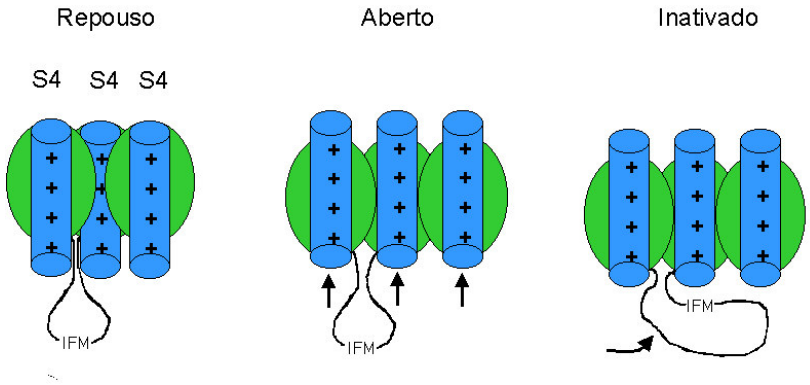

Figura 5: Modelo para ativação e inativação para o canal de sódio (adaptado de Ragsdale & Avoli, 1998).

A **Tabela 1** resume as informações específicas sobre funções relacionadas a diferentes porções do canal de sódio.

Tabela 1: Algumas regiões importantes do canal de sódio e suas funções.

Região	Função
Hélice S4 (Domínio IV)	"gating sensor" responsável pela ativação do canal
Alça S5-S6 (Domínio IV)	"Segmento P", filtro do poro.
Alça S6-S1 (Domínios III-IV)	"inactivating gate" ou tampa interna do canal; inclui também o sítio de fosforilação por proteína quinase C.
Alça S6-S1 (Domínio I e II)	Sítios de fosforilação pela proteína quinase dependente de AMPc.
Hélice S6 (Domínio IV)	Possível sítio de ligação de anestésicos locais.
Alça S4-S5 (Domínio IV)	Relacionada com a inativação do canal. Possível sítio de ação para anestésicos locais.

Evidências da interação dos anestésicos locais com a proteína canal de sódio vêm sendo obtidas há muitos anos. Frazier e col. (1970) verificaram que análogos quaternários

de AL bloqueiam a condução nervosa quando aplicados internamente aos axônios gigantes de lula perfundidos, porém são relativamente ineficazes quando aplicados externamente (Narahashi & Yamada, 1969; Frazier *et al.*, 1970). Ragsdale e col., (Ragsdale, *et al.*, 1994) demonstraram a existência de um "sítio hidrofóbico" para AL desprotonados no interior da α-hélice S6 do domínio IV da subunidade α da proteína canal de sódio de cérebro de rato. A α-hélice S6 estaria próxima ao lúmen interno do canal e constituiria o sítio de ação dos anestésicos locais, sendo que o resíduo de fenilalanina (1764), no meio da α-hélice transmembranar (correspondente à região de estreitamento do canal de K^+, revelada pelos estudos de Raios-X) e a tirosina (1771, próxima a face interna da membrana) são fundamentais para a interação com AL (Ragsdale *et al*., 1994). Os resultados desses pesquisadores fortalecem a hipótese de que os AL têm um efeito alostérico sobre o canal (Marban *et al*., 1998), podendo ligar-se a outras regiões do mesmo, como a alça extracelular S5-S6 ou segmento P.

Kuroda e col. empregando ^{1}H-RMN encontraram resultados que indicariam a interação dos AL com o sítio de inativação do canal, isto é, a alça entre o domínio III (α-hélice S6) e IV (α-hélice S1) que mantém o canal fechado durante o estado refratário e de repouso. Segundo esses autores a presença do anestésico nesta região prolonga o estado inativado do canal de sódio, tornando impossível à transmissão do impulso nervoso (Kuroda *et al.*, 1996).

Estudos mais recentes, empregando RMN e técnicas de biologia molecular, mostraram que os AL não agem no poro ou canal iônico propriamente dito, nem tampouco na alça entre o domínio III (S6) e IV (S1), sítio de inativação, vistos na **Figura 3** (região IFM)**.** A não evidência de sítios nessas regiões do canal corrobora a idéia de que os AL agiriam como reguladores alostéricos da proteína canal (Balser *et al*., 1996), podendo ligar-se a outras regiões da molécula como nos sítios hidrofóbicos descritos pelo grupo de Catterall (Ragsdale *et al.*, 1994 e 1996; Ragsdale & Avoli, 1998; Yarov-Yarovoy *et al.*, 2002) e afetar, indiretamente, as funções do canal.

Recentemente estudos de mutações sítio específicas (McPhee *et al.*, 1995 e 1996; Mitrovic *et al.*, 1996; Tang *et al.*, 1996; Lerche *et al.*, 1997; Filatov *et al.*, 1998), mostraram que a alça que liga as α-hélices S4 e S5 do domínio IV (**Figura 6**) seria também importante

para o processo de inativação do canal de sódio, constituindo um possível sítio de ação dos anestésicos locais, visto que as moléculas de anestésico têm interação preferencial pela forma inativada do canal de sódio (Mitrovic *et al.*, 1996; Lerche *et al.*, 1997; Filatov *et al.*, 1998; Scheuer, 1999).

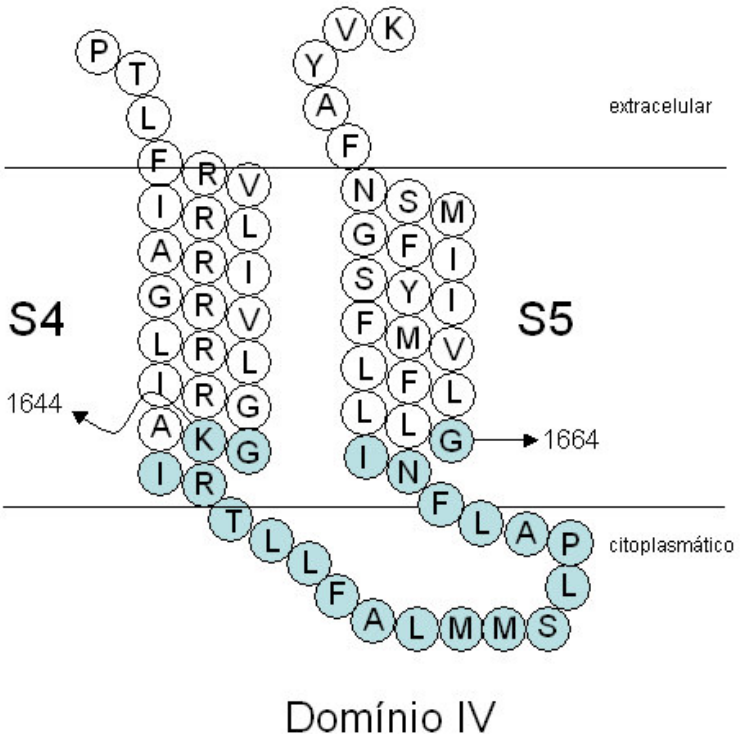

Figura 6: Esquema dos segmentos S4, S5 e alça citoplasmática S4-S5 no quarto domínio da subunidade α de canais de sódio de músculo humano (Mitrovic *et al.*, 1996). O segmento colorido em azul é o fragmento objeto de estudo nessa tese.

Nos últimos anos, o grupo de Kuroda publicou uma série de estudos com peptídeos de diversas regiões do canal de sódio. Em 1999, Kuroda e col. realizaram um estudo, por ^{1}H-RMN e dicroísmo circular, onde observaram efeito de um pentapeptídeo (KIFMK) em fragmentos do canal de sódio propondo que este pentapeptídeo interage com as alças S4-S5 dos domínios III e IV e com a alça III-IV (região da fechadura do canal). Este pentapeptídeo causa uma aceleração ou restaura o processo de inativação rápida em canais onde foram realizadas mutações no "*linker"* III-IV ou na alça S4-S5 do domínio IV (Kuroda *et al.*, 1999).

Em 2000, foi publicado pelo mesmo grupo um artigo no qual apresentaram a estrutura da alça entre os domínios III e IV (Ac-KKKFGGQDIFMTEEQKK-NH_2) contendo o motivo IFM por RMN e dicroísmo circular. O efeito da substituição da fenilalanina por uma glutamina (Ac-KKKFGGQDQFMTEEQKK-NH_2) foi estudado em condições que simulassem um meio hidrofóbico (trifluoretanol e micelas de dodecil sulfato de sódio, SDS). Em conclusão ao trabalho os autores propõem que o resíduo de Thr participa ativamente do processo de inativação. Entretanto, a mutação F/Q causa mudanças conformacionais que impedem o canal de inativar-se completamente (Kuroda *et al.*, 2000).

Em 2001, o mesmo grupo (Miyamoto *et al.*, 2001a) publicou um estudo onde foram investigadas as mudanças conformacionais com vários mutantes no *cluster* hidrofóbico formado pelo motivo IFM, em presença de micelas de SDS utilizando espectroscopias de RMN e dicroísmo circular. A partir dos resultados foi concluído que a Thr apresenta um papel importantíssimo na estabilização de um *cluster* hidrofóbico necessário para o processo de inativação. Ainda em 2001, Miyamoto e col. (Miyamoto *et al.*, 2001b) publicaram a estrutura de duas alças entre os segmentos S4 e S5 dos domínios III (Ac-AVVNALLGAIPSIM-NH_2) e IV (Ac-TLLFALMMSLPALFNIGLL-NH_2, mesma alça do nosso estudo, Figura 6, resíduos em azul) em micelas de SDS, determinadas por RMN. Neste artigo foi mostrado que a alça S4-S5 do domínio III apresenta estrutura em hélice e a alça S4-S5 do domínio IV apresenta um segmento helicoidal seguido de um *turn* formado pelos resíduos de prolina. Foi proposto, ainda, que estas duas alças formam, juntamente com o *linker* III – IV, um *cluster* hidrofóbico, que poderia ser estabilizado por interações hidrofóbicas, como mostra a **Figura 7.**

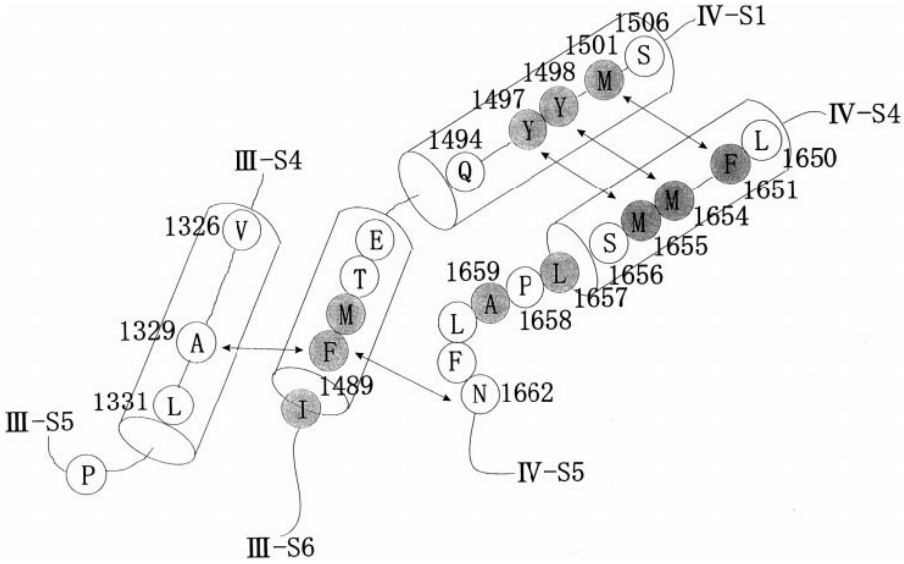

Figura 7: Representação esquemática da interação entre as alças S4-S5 dos domínios III e IV com o *linker* dos domínios III-IV. Estão representadas possíveis interações hidrofóbicas que formariam um *cluster* hidrofóbico, juntamente com o motivo IFM. As representações cilíndricas indicam estruturas em α-hélice (Miyamoto *et al.*, 2001b).

2- OBJETIVOS

Este trabalho teve como objetivo geral o estudo da interação de anestésicos locais com membranas lipídicas e com um fragmento do canal de sódio voltagem- dependente, com a finalidade de explorar as hipóteses de mecanismos de ação dos anestésicos locais ao nível molecular.

Como objetivos específicos para esta abordagem tivemos:

1) Estudar a interação dos anestésicos locais lidocaína e benzocaína com vesículas de fosfatidilcolina de ovo e membranas de eritrócito, empregando para isso técnicas espectroscópicas (ressonância magnética nuclear de ^{1}H e ^{31}P, ressonância paramagnética eletrônica, fluorescência e infravermelho).

2) Realizar estudo estrutural de um fragmento do canal de sódio voltagem-dependente (alça S4-S5/domínio IV, *p*IV/S4-S5, do canal de sódio voltagem dependente de cérebro humano) envolvido no processo de inativação, empregando RMN de ^{1}H e dicroísmo circular.

3) Estudar a interação dos anestésicos locais com peptídeo *p*IV/S4-S5, utilizando medidas de difusão e experimentos heteronucleares, de RMN (^{15}N-HSQC).

3. RESULTADOS

O corpo dos resultados obtidos compõem o material de 4 artigos publicados e/ou submetidos a revistas de política editoral seletiva e estão incluídos a seguir:

3.1 – Pinto, L.M.A., Yokaichiya, D.K., **Fraceto, L.F.**, de Paula, E. (2000) Interaction of benzocaine with model membranes. **Biophys. Chem**. **87**:213-223.

3.2 – **Fraceto, L.F.**, Pinto, L.M.A., Franzoni, L., Braga, A.A.C., Spisni, A., Schreier, S., de Paula, E. (2002) Spectroscopic evidence for a preferential location of lidocaine inside phospholipid bilayers. **Biophys. Chem. 99**:229-243.

3.3 – **Fraceto, L.F.**, de Paula, E. (2003) Anestésicos locais: interação com membranas de eritrócitos de sangue humano, estudada por ressonância magnética nuclear de ^{1}H e ^{31}P. **Química Nova** (no prelo).

3.4 – **Fraceto, L.F.**, Nakaie, C.R., Spisni, A., de Paula, E., Pertinhez, T.A. (2003) Selective interaction of local anesthetics with a peptide derived from the voltage-gated Na^{+} channel. A NMR study. **Submetido.**

3.1 – INTERACTION OF BENZOCAINE WITH MODEL MEMBRANES

ELSEVIER

Biophysical Chemistry 87 (2000) 213–223

Biophysical Chemistry

www.elsevier.nl/locate/bpc

Interaction of benzocaine with model membranes

Luciana de Matos Alves Pinto, Daniela Kiyoko Yokaichiya, Leonardo Fernandes Fraceto, Eneida de Paula*

Departamento de Bioquímica, Instituto de Biologia, Universidade Estadual de Campinas (Unicamp), Sao Paulo, Brazil

Received 30 May 2000; accepted 24 July 2000

Abstract

We measured the absorption properties, water solubility and partition coefficients (P) between n-octanol, egg phosphatidylcholine (EPC) liposomes and erythrocyte ghosts/water for benzocaine (BZC), an ester-type always uncharged local anesthetic. The interaction of BZC with EPC liposomes was followed using Electron Paramagnetic Resonance, with spin labels at different positions in the acyl chain (5, 7, 12, 16-doxylstearic acid methyl ester). Changes in lipid organization upon BZC addition allowed the determination of P values, without phase separation. The effect of BZC in decreasing membrane organization (maximum of 11.6% at approx. 0.8:1 BZC:EPC) was compared to those caused by the local anesthetics tetracaine and lidocaine. Hemolytic tests revealed a biphasic (protective/inductive) concentration-dependent hemolytic effect for BZC upon rat erythrocytes, with an effective BZC:lipid molar ratio in the membrane for protection (Re^{PROT}), onset of hemolysis (Re^{SAT}) and 100% membrane solubilization (Re^{SOL}) of 1.0:1, 1.1:1 and 1.3:1, respectively. The results presented here reinforce the importance of considering hydrophobic interactions in the interpretation of the effects of anesthetics on membranes.

Keywords: Benzocaine; Partition coefficient; EPR; Membranes; Erythrocytes; Hemolysis

Abbreviations: BZC, benzocaine; C^{PROT}, drug concentration for maximal protection against hypotonic hemolysis, C^{SAT}, drug concentration for the onset of hemolysis; C^{SOL}, drug concentration for total lysis; DMSO, dimethylsulfoxide; EPC, egg phosphatidylcholine; EPR, electron paramagnetic resonance; Ht, hematocrit; LA, local anesthetic; MeSL, doxylstearic acid methyl ester spin probes; P, partition coefficient; Re, effective drug/lipid molar ratio in the membrane

* Corresponding author. Fax: +55-19-788-7840.

E-mail address: depaula@unicamp.br (E. de Paula).

0301-4622/00/$ - see front matter
PII: S0301-4622(00)00196-4

1. Introduction

Among the theories for the mechanism of action of local anesthetics (LA), particularly important is the one that explains the inactivation effect of LA on the voltage-gated sodium channel of axons [1] as well as those focusing on the effects of LA interaction with the lipid membrane phase [2]. Possibly the best indication of the importance of LA interaction with the lipid phase is the direct correlation between LA hydrophobicity and clinical potency [3–5]. The neutral form of the anesthetic molecules plays a special role in this interpretation since it is more hydrophobic than the charged species [1,3,6].

Benzocaine (BZC, Fig. 1), an ester-type LA, attracted our attention because — different from the other clinically used local anesthetics — it is always uncharged at physiological pH and causes no use-dependent inhibition of the voltage-gated Na^+ channel [7]. BZC is used for topical anesthesia, since its low water solubility limits infiltrative administration [3,6,8].

Although the effect of BZC on membrane excitability has been extensively studied [1,7], there are only a few papers describing the interaction of benzocaine with model membranes [9–11] or the fundamental physicochemical properties of BZC in this interaction [12–14].

The purpose of the present study was to describe the interaction of BZC with phospholipid and erythrocyte membranes, and to correlate its effect with LA hydrophobicity and location inside the bilayer as one step to understand local anesthesia.

2. Materials and methods

Benzocaine was purchased from Hoeschst Marion Roussel S.A. and used without further purification. Egg phosphatidyl choline (EPC) and MeSL spin labels (methyl ester of doxyl stearic acids) labeled at carbons 5, 7, 12 and 16 were obtained from Sigma Chemical Co., St. Louis, MO. All other reagents were of analytical grade.

Because of the low solubility of BZC, a dimethylsulfoxide PBS solution was used as solvent, both in EPR and hemolytic experiments. The amount of DMSO in the solutions did not exceed 8.5% v/v (1 M) and blank controls were prepared throughout, to rule out the effect of the solvent.

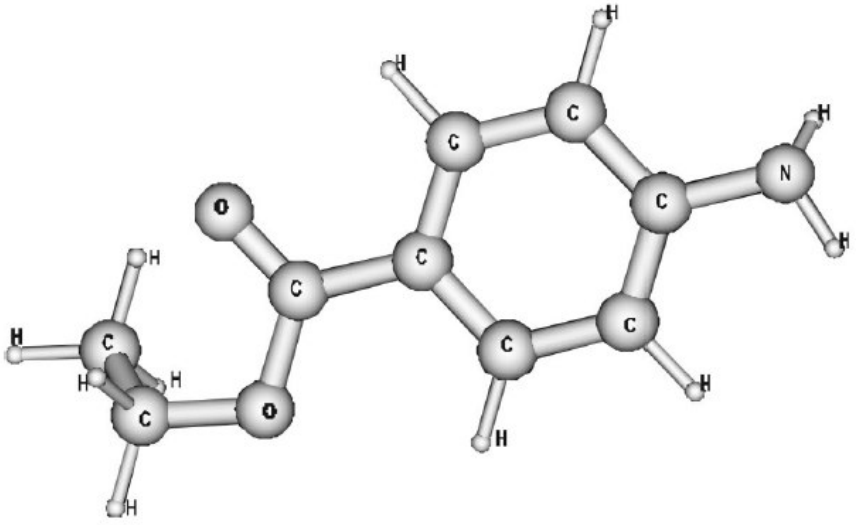

Fig. 1. Chemical structure of benzocaine (BZC).

2.1. Membrane preparation

EPC multilamellar vesicles were prepared by evaporating stock chloroform EPC solutions under a stream of nitrogen. The samples were left under vacuum for at least 2 h at room temperature (22°C). Vesicles were obtained by the addition of phosphate buffered saline, PBS (5 mM phosphate, 150 mM NaCl, pH 7.4), and vortexing for 5 min.

2.2. Erythrocyte membranes

Freshly obtained rat blood was collected into Alsever's solution (27 mM sodium citrate, 72 mM NaCl, 114 mM glucose, 2.6 mM citric acid) and washed three times in PBS, with centrifugation at $260 \times g$ for 3 min. Human erythrocyte ghosts were prepared as described by Dodge et al. [15].

2.3. EPR experiments

The experiments were conducted at room temperature (22°C) using a Bruker ER-200 spectrometer, operating at 9 GHz (3·4 kGauss) and 0.2 ml flat cells. From the spectra of the MeSL spin labels incorporated into multilamellar EPC membranes to a 1% molar ratio, we determined h_{+1}/h_0, the ratio of low to central-field heights of the nitroxide signal (Fig. 2). h_{+1}/h_0 measure changes in membrane organization [16,17], and is expressed on a percent basis relatively to the control (without LA), according to the following formula:

$$\%\,\text{Effect} = \frac{(h_{+1}/h_0)\text{sample} - (h_{+1}/h_0)\text{ control}}{(h_{+1}/h_0)\text{ control}} \times 100 \quad (1)$$

This parameter comprises the effect of order and molecular mobility in the bilayer. The difference between the low-field (h_{+1}) and the mid-field (h_0) height is high in the bilayer because of the anisotropy and slow molecular motion of the probe [16]. As membrane organization decreases, h_{+1}/h_0 approaches zero and % Effect increases.

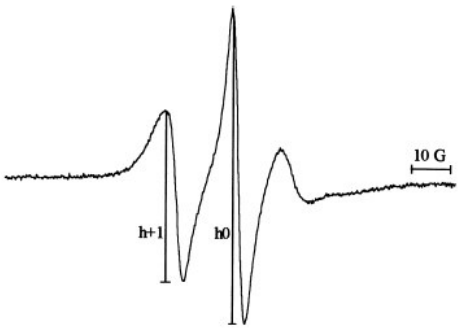

Fig. 2. EPR spectra of 5-MeSL (1 mol%) in EPC multilamellar vesicles showing the measurement of the h_{+1}/h_0 ratio: [EPC] = 8 mM, PBS buffer, pH 7.4, room temperature.

2.4. Partition coefficient between octanol and water (Poct)

PBS and *n*-octanol solutions were pre-equilibrated overnight. After BZC addition the mixture was vortexed for 5 min and incubated for an additional 15 min before centrifugation at 1000 × g for 5 min *P*oct was optically determined at 284 nm (ε_M BZC = 15 850).

The amount of drug bound to the lipid phase was obtained by subtracting the supernatant concentration from the total drug concentration, measured before phase mixing. The partition coefficient, P, was determined according to Eq. (2):

$$P = \frac{n_m/V_m}{n_w/V_w}, \quad (2)$$

where n denotes the number of BZC moles, V is the volume and the subscripts m and w refer to the membrane (or octanol) and aqueous phase, respectively.

2.5. Partition coefficient determination by phase separation

A known amount of BZC in PBS buffer was added to the membranes, followed by shaking and 10 min incubation at room temperature. After ultra centrifugation at $120\,000 \times g$ for 2 h, the

BZC concentration in the supernatant was optically detected at 284 nm, against a control (membrane in PBS). Partition coefficients were determined by this procedure for multilamellar EPC vesicles ($P_{p\text{-}s}$) and erythrocyte ghosts (P_{ghost}).

2.6. Partition coefficient determination by spectroscopic methods

The partition coefficient of BZC between EPC vesicles and PBS buffer was also determined by EPR without phase separation. Changes in the 5-MeSL spectra due to BZC partition and membrane saturation were used to determine P_{epr} and P_{sol}, as described before [17,18].

Briefly, in the first approach, the effect of BZC on membrane organization was determined at different (4–10 mM) EPC concentrations. For a given effect, plots of BZC total concentration, n_t — where $n_t = n_w + n_m$ in Eq. (2)-vs. membrane volume (taken from the lipid concentration, assuming density = 1 g/ml) give straight lines that allow direct P determination (P_{epr}) from the slope/intercept ratio [18].

The second method takes into account the limited solubility of BZC, leading to a fixed n_w value in Eq. (2). The hyperbolic EPR curves for the effect of BZC on membrane organization were used to determine n_t for membrane saturation (inflexion of Fig. 3b). As $n_t = n_m + n_w$, and n_w is equal to the water solubility of BZC [17], we calculated n_m and the partition coefficient, P_{sol}, for BZC between EPC/water according to Eq. (2).

2.7. Hemolytic assay under hypotonic conditions

Rat erythrocytes (hematocrit, Ht = 0.15%) were incubated in hypotonic PBS (5 mM sodium phosphate, 66 mM NaCl, pH 7.4) to induce approximately 50% hemolysis. BZC (0–21 mM) was added and the samples were incubated for 40 min. After centrifugation at $260 \times g$ for 3 min, released hemoglobin was measured in the supernatant at 412 nm. Results were expressed on a Relative Absorbance (RA) scale ranging from < 1 (protection) to > 1 (hemolysis). RA = 1 indicates 50% hemolysis induced by the 66 mM saline control. Each experiment was run in triplicate and RA values represent the mean of three independent experiments.

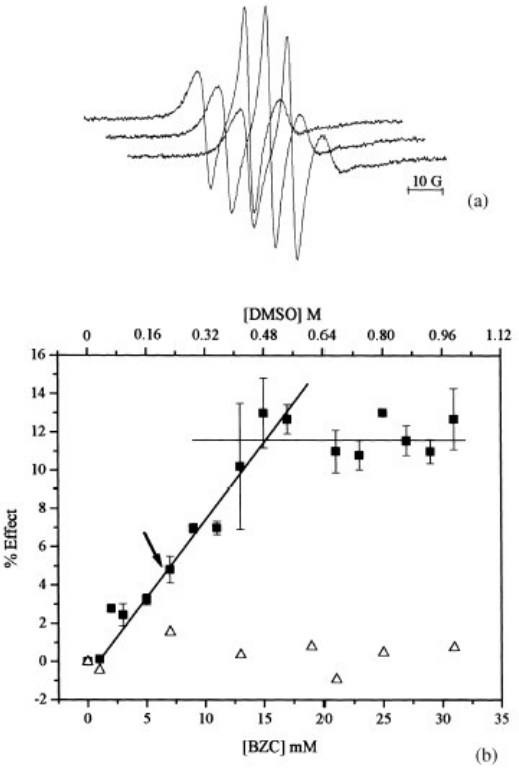

Fig. 3. (a) EPR spectra of 5-MeSL (1 mol%) in 8 mM EPC multilamellar vesicles (middle spectrum) in the presence of 0.5 M DMSO (lower) or 15 mM BZC (upper) solubilized in DMSO:PBS buffer, pH 7.4, room temperature. (b) BZC effect, as registered by the EPR spectra of 5-MeSL, on the lipid organization of EPC multilamellar vesicles (■). The effect of DMSO, used as a solvent for BZC, is also shown (Δ). The arrow indicates BZC concentration for Re = 0.33:1 (see text).

2.8. Isotonic hemolytic assay

Erythrocytes (Ht = 0.15%) in isotonic PBS solution were incubated with different BZC concentrations (0–25 mM) and the samples left at room temperature for 40 min before centrifugation at $260 \times g$ for 3 min. Hemoglobin released into the supernatant was detected at 412 nm. The hemo-

lytic effect, measured as Relative Hemolysis (RH), was determined on the basis of released hemoglobin [19]:

$$\mathrm{RH} = \frac{A_s - A_{c1}}{A_{c2} - A_{c1}}, \quad (3)$$

where A is the absorbance, s the sample, c_1 the mechanical hemolysis control (erythrocytes in PBS) and c_2 the 100% hemolysis (erythrocytes in water) control. Each experiment was run in triplicate and RH values represent the mean of three experiments.

Lichtenberg defined C^{SAT} and C^{SOL} as the amount of surfactant drugs needed for initial (membrane saturation) and total membrane solubilization, respectively [20]. Although BZC is not a surface active compound, we borrowed this definition and considered *solubilization* as the 100% release of hemoglobin into the supernatant. C^{SAT} and C^{SOL} were determined in the hemolytic experiments allowing the calculation of *Re*, the effective drug/lipid molar ratio in the membrane, for initial (Re^{SAT}) and total hemolysis (Re^{SOL}).

2.9. Re (drug / lipid ratio) calculation

Since the P value is known, *Re* can be calculated from the ratio between drug in the membrane [*nm* in Eq. (2)] and lipid membrane concentration, assuming a lipid density of 1 g/ml [19,21].

3. Results and discussion

Table 1 shows the partition coefficients of BZC between octanol (P_{oct}), erythrocyte ghosts (P_{ghost}) and multilamellar EPC vesicles ($P_{p\text{-}s}$) and water, determined at pH 7.4 by phase separation. Organic solvent–water systems have been used as models of membranes for the study of partition coefficients, although the absolute P_{oct} values rarely coincide with those found in the anisotropic lipid bilayers or biological membranes [18,22,23]. Nevertheless, a good correlation exists between P_{oct} values and P values from model membranes/water within homologous series of anesthetic compounds [5]. P_{oct} indicates that BZC is a mild hydrophobic LA; in the ester family it is not so hydrophilic as procaine, nor so hydrophobic as tetracaine [12,14].

P_{ghost} reveals that BZC partition inside ghosts membranes is very similar to that in the zwitterionic EPC bilayers ($P_{p\text{-}s}$). This result is quite peculiar for BZC since the high cholesterol content (30% in weight) of erythrocyte membranes [24] should restrict drug partition into them in comparison to the fluid EPC vesicles. The slightly higher P_{ghost} value may reflect the preferential binding of membrane proteins for the uncharged species of amphiphilic compounds, since dibucaine (an aminoamide LA) and trifluoperazine (a tricyclic phenothiazinic antipsychotic agent) which have an amine group with pK just above pH 7.4 show smaller P_{ghost} than $P_{p\text{-}s}$ [19,21].

Table 1 also shows values of P_{epr} and P_{sol}, taken from the EPR experiments, without phase separation. Although both methodologies provided similar results, the standard deviation for P_{epr} was smaller, justifying its adoption for the *Re* calculation (see below). Using nine different aminoester and aminoamide local anesthetics, we have shown before that there is a good correlation between the partition coefficient values determined by EPR (P_{epr} and P_{sol}) and those determined by phase separation ($P_{p\text{-}s}$) in EPC/water systems [17]. However, the values of P_{epr} and P_{sol}

Table 1
Partition coefficient for BZC (pH 7.4; room temperature) between octanol/water (P_{oct}), erythrocyte ghosts/water (P_{ghost}) and EPC liposomes/water obtained by phase separation ($P_{p\text{-}s}$) or spectrophotometrically (P_{epr}, P_{sol}). The results are the mean of at least five experiments

Benzocaine	P_{oct}	P_{ghost}	$P_{p\text{-}s}$	P_{epr}	P_{sol}
Mean ± S.D.	37.8 ± 6.1	287 ± 76	253 ± 43	115 ± 18	106 ± 40

for BZC determined here were lower than $P_{p\text{-}s}$, as explained by the fact that the first experiments were run in the presence of 0.5 M DMSO (DMSO:PBS buffer) to increase the water solubility of BZC (4.4 mM) and to reach suitable BZC:EPC ratios inside the membrane in the EPR measurements. We measured an increase in the water solubility of BZC in the presence of 0.5 M DMSO (11.3 mM), which explains the proportional decrease in the lipid hydrophobicity of the compound as detected by the P_{epr} and P_{sol} values.

In fact we are not the first to use DMSO to solubilize BZC [7,25]. DMSO is a water-miscible solvent, it forms hydrogen bonds with water molecules, shrinking the solvation shell of phospholipid membranes [26] and stabilizing their structure at low temperatures [27].

The ester linkage of benzocaine has good chemical stability in comparison to other ester-type LA [12,28] and no hydrolysis was detected at pH 7.4 up to 4 h (data not shown).

3.1. EPR experiments

Fig. 3a shows the EPR spectra of 5-MeSL inside EPC multilamellar vesicles with and without BZC. A plot of the effect on membrane organization [Eq. (1)] vs. BZC concentration is given in Fig. 3b. The figure shows that BZC decreased the membrane organization of phospholipid membranes until membrane saturation was reached and addition of the LA was not accompanied by further changes in fluidity. The maximum effect (11.6%) was reached at a benzocaine concentration of 15.4 mM (n_t), corresponding to a BZC:lipid molar ratio, *Re*, inside the membrane equal to 0.8:1. *Re* was calculated from Eq. (2) using P_{epr} (Table 1). For this we first calculated n_m, the amount of BZC in the membrane and then the ratio of n_m/ [lipid] gave *Re*, as explained in Section 2.

This behavior and the extent of maximal membrane perturbation detected with 5-MeSL was comparable to those determined for aminoester LA such as tetracaine, procaine and chloroprocaine and was more pronounced than those caused by the cyclic aminoamide LA mepivacaine and bupivacaine [17]. Fig. 3b highlights BZC's effect at 0.33:1 BZC:lipid molar ratio (arrow) and shows that DMSO, used to solubilize BZC in water, did not cause any change in membrane organization.

The values of P_{sol} in Table 1 were determined from plots like that illustrated in Fig. 3b, assuming a limiting water solubility, as described in Section 2 and [17]. Also, from plots like that illustrated in Fig. 3b, but using at least four different membrane concentrations, we determined P_{epr}, by the method of Lissi et al. [18].

Using different paramagnetic probes we could monitor the phospholipid acyl chain to detect the regions most affected by the presence of BZC. Fig. 4 is a plot of the effect (decrease in membrane organization) of BZC on EPC bilayers, as detected by 5, 7, 12 and 16-MeSL. Stearic acid spin labels do monitor different depths of the acyl chain, as demonstrated by Godici and Landsberger [29] using ^{13}C NMR relaxation times. The two curves represent the maximum perturbing effect and the effect at a fixed *Re* (0.33:1 BZC:EPC) inside the membrane. One can see that the disturbing effect of BZC is more evident when the probe monitors intermediate–C_5–C_7–positions in the acyl chain.

To understand these differential effects we compared the effect of BZC on membrane orga-

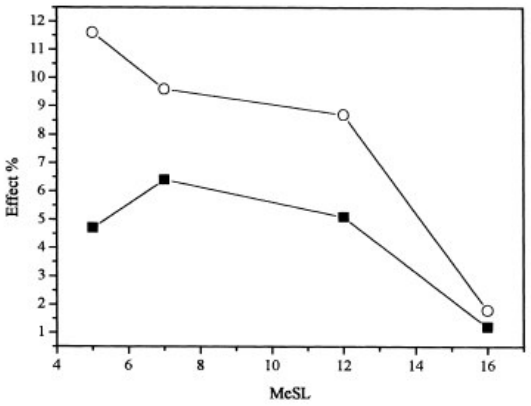

Fig. 4. Maximum effect of BZC on membrane organization (○) and effect at a fixed, *Re* = 0.33:1, BZC:EPC molar ratio in the membrane (■), as detected with 5, 7, 12 and 16-MeSL spin probes.

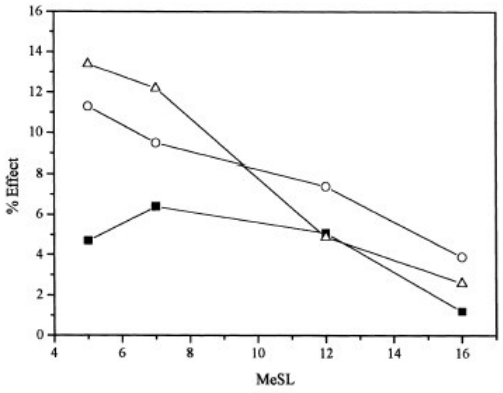

Fig. 5. Decrease in membrane organization caused by the local anesthetics benzocaine (■), lidocaine (○) and tetracaine (Δ) when present at a fixed molar ratio, *Re* = 0.33:1, in the membrane. Data obtained from the EPR spectra of 5, 7, 12 and 16-MeSL spin probes incorporated (1 mol%) into 8-mM EPC vesicles.

nization with that of lidocaine and tetracaine (Fig. 5) in their uncharged form, pH 10.5, and present at the same *Re* in the membrane. Lidocaine is a less hydrophobic LA that seems to lie preferentially in the glycerol neighborhood of EPC bilayers (Pinto, Fraceto, Spisni, Schreier and de Paula, in preparation). Tetracaine is a more hydrophobic LA whose uncharged species seems to position its benzenoid ring mainly at the level of C_2 in the acyl chain of phosphatidylcholine membranes, extending its *p*-butyl group up to C_8–C_{10}, as revealed by ^{2}H-NMR experiments [30].

Even considering that 16-MeSL experiences a more mobile/less ordered environment, due to the profile of the acyl chain dynamics [29–32] and order in the bilayers [33,34] — that could explain the low sensitiveness of the probe at that position, these results clearly show that BZC disturbs mainly the acyl chain core (5 < 7 > 12 MeSL), in a different manner than tetracaine (5 ≈ 7 > 12 MeSL) and lidocaine (5 > 7 > 12).

Desai and coworkers used the intrinsic fluorescence of LA molecules to determine the equivalent dielectric constants of their environment when inserted into micelles [11]. Inside SDS micelles they found a polarity of approximately 35 (Dielectric Constant) for BZC, comparable to that of uncharged tetracaine in the same micelles, indicating that the aromatic ring of both LA were located in a region of the micelles with a polarity equivalent to that of the interface glycerol/carbonyl region of phospholipid membranes (Dielectric Constant = 30 according to [35]).

In a previous work we have shown that lidocaine and tetracaine disturb the overall membrane organization to a 26.5% and 15% extent, respectively, as monitored by 5-MeSL in EPC vesicles [17]. Here we determined a maximum effect of 11.6% for BZC. The reason for this less pronounced effect of BZC on membrane organization may be due to the steric features of the molecule since benzocaine has a small van der Waals volume (147.4 Å^3) in comparison to lidocaine and tetracaine (227.3 and 250.8 Å^3, respectively) [5]. Besides, BZC lacks a polar amine group in the hydrophilic domain of the molecule (opposite to the aromatic ring) that would be able to establish either electrostatic (above pK) or hydrogen binding [14]. As a consequence, BZC is not anchored at the interface glycerol/polar head-group region and its effect seems to be more discrete, although deeper (in position) than the other LAs studied.

We obtained other indications of the discrete effect and not preferential positioning of BZC with ^{1}H-NMR ROESY experiments, since no LA:lipid intermolecular NOE peaks were detected for BZC in unilamellar EPC vesicles (unpublished data); lidocaine, tetracaine and other aminoamide LA established detectable cross-peaks with both the polar head group and acyl chain protons of the phospholipid membranes.

3.2. Hemolysis experiments

Seeman described the biphasic effect of many amphiphilic compounds upon erythrocyte membranes: at lower concentrations they protect the membranes against hypotonic hemolysis, while at higher concentrations they induce lysis [36]. Tertiary amine LA such as procaine, tetracaine, lidocaine [37] and dibucaine [21,37] present this biphasic behavior, although just tetracaine and

dibucaine have been shown to be surface active compounds [38]. Protection against hypotonic hemolysis is believed to result from the amphiphilic partition into the membrane, increasing the membrane area/volume ratio of the cell and thereby the critical hemolytic volume of the erythrocyte.

The effect of BZC on biological membranes was evaluated in hemolytic experiments under normal and hyposmotic condition. Fig. 6a shows a typical hemolytic curve obtained after 40 min incubation of BZC with rat erythrocytes under isotonic conditions. From the amount of drug for membrane saturation at the beginning of the hemolytic curve (C^{SAT} = 14.1 mM) and for complete membrane solubilization (C^{SOL} = 17.3 mM) at 100% hemolysis, we calculated *Re* values, using P_{epr} values, as explained before. P_{epr} was used since BZC partition into ghosts and EPC membranes are very similar (Table 1) and also because DMSO was used in the BZC solutions employed in the hemolytic tests. For BZC in a Ht = 0.15% (13.05 μM lipids [15,21]), we obtained Re^{SAT} and Re^{SOL} of 1.1:1 and 1.3:1, respectively.

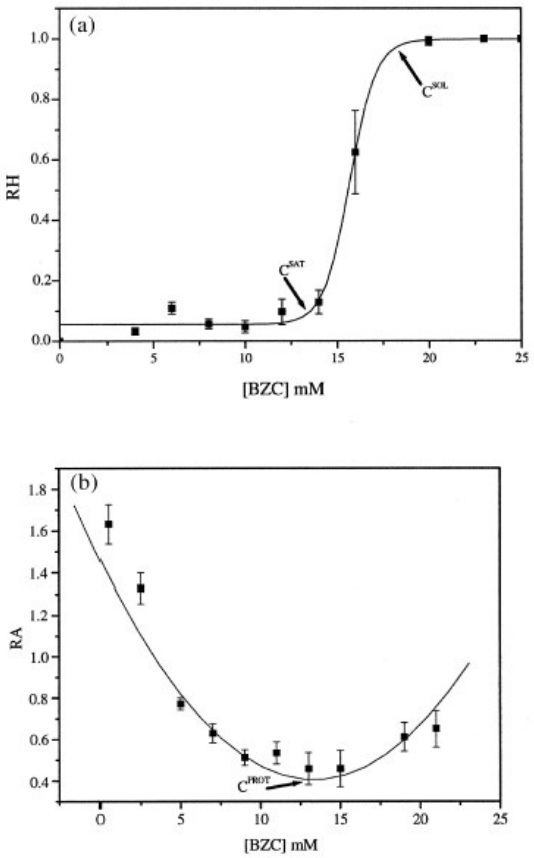

Fig. 6. (a) BZC-induced isotonic hemolysis; C^{SAT} and C^{SOL} (see text) determinations are shown. (b) BZC-induced protection against hypotonic hemolysis: Ht = 0.15%, PBS buffer, pH 7.4, incubation time: 40 min, room temperature.

For Dibucaine, a more hydrophobic LA, we have determined Re^{SAT} and Re^{SOL} of 0.34 and 0.69:1 [21], and for trifluoperazine Re^{SAT} and Re^{SOL} of 0.43 and 1.5:1 [19], ratios that suggest saturation of the membrane phase with the amphiphiles [2,39] leading to membrane solubilization.

Fig. 6b depicts the protective BZC effect on erythrocyte hemolysis under hypotonic conditions. The maximal protective BZC concentration (C^{PROT}) for a Ht = 0.15% was 13 mM, giving an Re^{PROT} value of 1.0:1 BZC:lipid.

Since there are some reports in the literature relating methemoglobin (MetHb) formation to BZC administration [40,41], we performed a control experiment using purified Hb solution and incubated it for 40 min with increasing amounts of BZC (Fig. 7). No significant increase in MetHb content was detected after BZC incubation up to 20 mM, excluding the possibility of the hemolytic effect being affected by Hb oxidation. The oxidative effect of BZC is related to its structural similarity to *p*-amine propyophenone (PAPP), a strong MetHb inducing agent [42].

4. Conclusions

The *P* values determined by EPR in Table 1 were smaller than that determined by phase separation ($P_{p\text{-}s}$), reflecting the lower partitioning of BZC into EPC bilayers when dissolved in DMSO:PBS solvent. In fact, the use of DMSO to solubilize BZC turns the water phase more attractive for the anesthetic, decreasing P_{epr} and P_{sol} values.

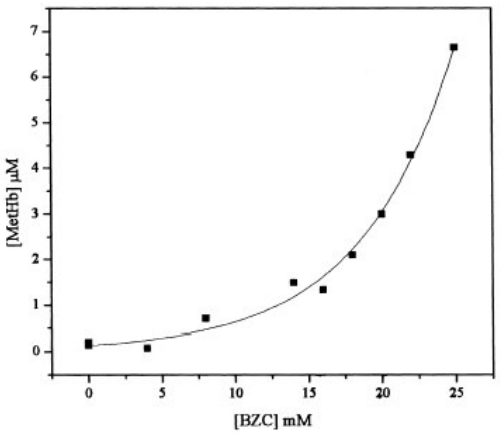

Fig. 7. MetHb formation induced by BZC in a purified Hb solution in PBS buffer, pH 7.4, at room temperature.

Since we knew the real partition coefficient for BZC in the EPR experiment, we could compare the effect of BZC with that of other commonly studied LA such as lidocaine and tetracaine. BZC decreased the overall membrane lipid organization, inserting itself into a deeper position in the bilayer, although its effect on membrane organization was less pronounced than the other LA, probably due to its smaller molecular size.

Knowledge of the P value allowed also the quantitative study of the hemolytic effect of benzocaine. As seen for other LA [36], BZC showed a biphasic (protective/inductive) concentration-dependent hemolytic effect on erythrocytes. The BZC:lipid molar ratio in the membrane for protection (Re^{PROT}) was lower than those required for lysis (Re^{SAT} and Re^{SOL}). On average, ca. 1:1 is the BZC:lipid ratio for hemolysis, a quite reasonable value for a true saturation of the membrane phase [39,43].

Re for maximum change in phospholipid membrane organization (0.8:1 BZC:lipids) is close to Re^{PROT} (1:1) in erythrocyte membranes, revealing that hydrophobic interaction rules both phenomena.

The importance of the hydrophobic parameters for anesthesia (potency and toxicity) justifies the study of the neutral LA interaction and effects on membranes and the results presented here reinforce this hypothesis, since the extent of changes in membrane organization (EPR) and hemolysis was determined by the hydrophobic interaction of the BZC molecule with the bilayer.

Besides, site-directed mutagenesis has revealed the existence of a hydrophobic binding site for LA inside Na^+ channels [44,45], reinforcing the relevance of uncharged (hydrophobic) LA species for the mechanism of anesthesia.

Acknowledgements

This work was supported by Fundação de Amparo à Pesquisa do Estado de São Paulo (FAPESP, Grant 96/1451-9) and Coordenação de Apoio ao Ensino Superior. L.M.A.P. (Grant. 96/9786-0), D.K.Y (Grant 97/02395-8) and L.F.F. (Grant 98/84-8) were the recipients of fellowships from FAPESP. We acknowledge Dr S. Schreier (Institute of Chemistry, University of São Paulo) for the access to the EPR facility and CENAPAD for the use of Moldem/Gamess Molecular Simulation programs.

References

[1] J.F. Butterworth, G.R. Strichartz, Molecular mechanisms of local anesthesia: a review, Anesthesiology 72 (1990) 711–734.
[2] E. de Paula, S. Schreier, Molecular and physicochemical aspects of local anesthetic-membrane interaction, Braz. J. Med. Biol. Res. 29 (1996) 877–894.
[3] B.G. Covino, H.G. Vassalo, Local anesthetics: mechanisms of action and clinical use, Grune and Stratton, New York, 1976.
[4] K.R. Courtney, Structure-activity relations for frequency-dependent sodium channel block in nerve by local anesthetics, J. Pharmacol. Exp. Ther. 213 (1980) 114–119.
[5] S.P. Gupta, Quantitative structure-activity relationship studies on local anesthetics, Chem. Rev. 91 (1991) 1109–1119.
[6] R.H. de Jong, Local anesthetics, Mosby, St. Louis, 1994.
[7] C. Quan, W.M. Mok, G.K. Wang, Use-dependent inhibition of Na^+ currents by benzocaine homologs, Biophys. J. 70 (1996) 194–201.
[8] G.R. Strichartz, J.M. Ritchie, in: G.R. Strichartz (Ed.), Local anesthetics, Handbook of Experimental Pharmacology, 81, Springer-Verlag, Berlin, 1987.
[9] A.G. Lee, Interactions between anaesthetics and lipid

mixtures amines, Biochim. Biophys. Acta 448 (1976) 34–44.
[10] P. Schlieper, L. Michaelis, Interaction of local anesthetics with small phospholipid vesicles investigated by proton NMR spectroscopy, Biophys. Struct. Mech. 10 (1983) 1–9.
[11] S. Desai, T. Hadlock, C. Messam, R. Chafetz, G. Strichartz, Ionization and adsoption of a series of local anesthetics in detergent micelles: studies of drug fluorescence, J. Pharmacol. Exp. Ther. 271 (1994) 220–228.
[12] G.R. Strichartz, V. Sanchez, R. Arthur, R. Chafetz, D. Martin, Fundamental properties of local anesthetics. II. Measured octanol:buffer partition coefficient and pKa values of clinically used drugs, Anesth. Analg. 71 (1990) 158–170.
[13] R.J.E. Grouls, E.W. Ackerman, H.H.M. Korsten, L.J. Hellebrekers, D.D. Breimer, Partition coefficients (*n*-octanol/water) of N-butyl-p-aminobenzoate and other local anesthetics measured by reversed-phase high-performance liquid chromatography, J. Chromatogr. B 694 (1997) 421–425.
[14] H. Matsuki, K. Shimada, S. Kaneshima, H. Kamaya, I. Ueda, Difference in surface activities between uncharged and charged local anesthetics: correlation with their anesthetic potencies, Coll. Surf. B-Biointerf. 11 (1998) 287–295.
[15] J.T. Dodge, C. Mitchell, D.J. Hanahan, The preparation and chemical characteristics of hemoglobin-free ghosts of human erythrocytes, Arch. Biochem. Biophys. 100 (1963) 131–139.
[16] S. Schreier, W.A. Frezzatti Jr., P.S. Araujo, H. Chaimovich, I.M. Cuccovia, Effect of lipid membranes on the apparent pK of the local anesthetic tetracaine. Spin label and titration studies, Biochim. Biophys. Acta 769 (1984) 231–237.
[17] E. de Paula, S. Schreier, Use of a novel method for determination of partition coefficient to compare the effect of local anesthetics on membrane structure, Biochim. Biophys. Acta 1240 (1995) 25–33.
[18] E. Lissi, M.L. Bianconi, A.T. AmaraL, E. de Paula, L.E.B Blanch, S. Schreier, Methods for the determination of partition coefficients based on the effect of solutes upon membrane structure, Biochim. Biophys. Acta 1021 (1990) 46–50.
[19] S.V.P. Malheiros, E. de Paula, N.C. Meirelles, Contribution of trifluoperazine/lipid ratio and drug ionization to hemolysis, Biochim. Biophys. Acta 1373 (1998) 332–340.
[20] D. Lichtenberg, Characterization of the solubilization of lipid bilayers by surfactants, Biochim. Biophys. Acta 821 (1985) 470–478.
[21] S.V.P. Malheiros, N.C. Meirelles, E. de Paula, Pathways involved in trifluoperazine-, dibucaine- and praziquantel-induced hemolysis, Biophys. Chem. 83 (2000) 89–1000.
[22] S. Roth, P. Seeman, The membrane concentrations of neutral and positive anesthetics (alcohols, chlorpromazine, morphine) fit the Meyer-Overton rule of anesthesia; negative narcotics do not, Biochim. Biophys. Acta 255 (1972) 207–219.
[23] F.A.P.C. Gobas, J.M. Lahittete, G. Garofalo, W.Y. Shiu, D. Mackay, A novel method for measuring membrane-water partition coefficients of hydrophobic organic chemicals: comparison with 1-octanol-water partitioning, J. Pharm. Sci. 77 (1988) 265–272.
[24] H.P Duwe, E. Sackmann, Bending, elasticity and thermal excitations of lipid bilayer vesicles — modulation by solutes, Phys. Acta 163 (1990) 410–428.
[25] Y.–M. Li, D.E. Wingrove, H.P. Too, M. Marnerakis, E.R. Stimson, G.R. Strichartz, J.E. Maggio, Local anesthetics inhibit substance P binding and evoked increases in intracellular Ca^{2+}, Anesthesiology 82 (1995) 166–173.
[26] S.N. Shashkov, M.A. Kiselev, S.N. Tioutiounnikov, A.M. Kiselev, P. Lesieur, The study of DMSO/water and DPPC/DMSO/water systems by means of the X-ray, neutron small angle scattering, calorimetry and IR spectroscopy, Phys. B 271 (1999) 184–191.
[27] Z.-W. Yu, P.J. Quin, Solvation effects of dimethyl sulphoxide on the structure of phospholipid bilayers, Biophys. Chem. 70 (1998) 35–39.
[28] A. Brosowski, F. Müller, Temperature-dependance of the pH-value and effects on the kinetics of the hydrolytic decomposition of benzocaine, Eur. J. Pharm. Biopharm. 40 (1994) 96–100.
[29] P.E. Godici, F.R. Landsberger, The dynamic structure of lipid membranes. A ^{13}C nuclear magnetic resonance study using spin labels, Biochemistry 13 (1974) 362–368.
[30] Y. Boulanger, S. Schreier, I.C.P. Smith, Molecular details of anesthetic-lipid interaction as seen by deuterium and phosphorus-31 nuclear magnetic resonance, Biochemistry 20 (1981) 6824–6830.
[31] Y. Kuroda, K. Kitamura, Intra- and intermolecular ^{1}H-^{1}H nuclear overhauser effect studies on the interactions of chlorpromazine with lecithin vesicles, J. Am. Chem. Soc. 106 (1984) 1–6.
[32] J.F. Ellena, S.J. Archer, R.N. Dominey, B.D. Hill, D.S. Cafiso, Localizing the nitroxide group of fatty acid and voltage-sensitive spin-labels in phospholipid bilayers, Biochim. Biophys. Acta 940 (1988) 63–70.
[33] A. Seelig, J. Seelig, Bilayers of dipalmitoyl-3-sn-phosphatidylcholine conformational difference between the fatty acyl chains, Biochim. Biophys. Acta 406 (1975) 1–5.
[34] D.A. Driscoll, S. Samarasinghe, S. Adamy, J. Jonas, A. Jonas, Pressure effects on dipalmitoylphosphatidylcholine bilayers measured by ^{2}H nuclear magnetic resonance, Biochemistry 30 (1991) 3322–3327.
[35] R.F. Flewelling, W.L. Hubbell, Hydrophobic ion interactions with membranes. Thermodynamic analysis of tetraphenylphosphonium binding to vesicles, Biophys. J. 49 (1986) 531–540.
[36] P. Seeman, The membrane actions of anesthetics and tranquilizers, Pharmacol. Rev. 24 (1972) 583–655.
[37] P. Seeman, Erythrocyte membrane stabilization by local anesthetics and tranquilizers, Biochem. Pharmacol. 15 (1966) 1753–1766.

[38] H. Matsuki, S. Hashimoto, S. Kaneshima, Surface adsorption and volume behavior of Local Anesthetics, Langmuir 102 (1994) 1882–1887.
[39] A.G Lee, S. Schreier, in Entrapment of drugs and other materials (Liposome Technology, Vol. II), C.R.C. Press, Boca Raton, 1993.
[40] A.T. Guertler, W.A. Pearce, A prospective evaluation of benzocaine-associated methemoglobinemia in human beings, Ann. Emerg. Med. 24 (1994) 626–630.
[41] F.D. Ellis, J.G. Seiler, M.M. Palmore, Jr., Methemoglobinemia: a complication after fiberoptic orotracheal intubation with benzocaine spray, J. Bone Jt. Surg. Amer. 77 (1995) 937–939.
[42] D.G. Martin, C.E. Watson, M.B. Gold, C.L. Woodard Jr., S.I. Baskin, Topical anesthetic-induced methemoglobinemia and sulfhemoglobinemia in macaques: a comparison of benzocaine and lidocaine, J. Appl. Toxicol. 15 (1995) 153–158.
[43] S. Schreier, S.V.P. Malheiros, E. de Paula, Surface active drugs: self-association and interaction with membranes and surfactants. Physicochemical and biological aspects, Biochim. Biophys. Acta (in press).
[44] D.S. Ragsdale, J.C. McPhee, R. Scheuer, W.A. Catterall, Molecular determinants of state-dependent block of Na^+ channels by local anesthetics, Science 265 (1994) 1724–1728.
[45] D.S. Ragsdale, J.C. McPhee, R. Scheuer, W.A. Catterall, Common molecular determinants of local anesthetic, antiarrhytmic, and anticonvulsant block of voltage-gated Na^+ channels, Proc. Natl. Acad. Sci. USA 93 (1996) 9270–9275.

3.2 – SPECTROSCOPIC EVIDENCE FOR A PREFERENTIAL LOCATION OF LIDOCAINE INSIDE PHOSPHOLIPID BILAYERS

ELSEVIER

Biophysical Chemistry 99 (2002) 229–243

Biophysical Chemistry

www.elsevier.com/locate/bpc

Spectroscopic evidence for a preferential location of lidocaine inside phospholipid bilayers

Leonardo Fernandes Fraceto[a,d], Luciana de Matos Alves Pinto[a], Lorella Franzoni[b], Ataualpa Albert Carmo Braga[c], Alberto Spisni[b,d], Shirley Schreier[e], Eneida de Paula[a,*]

[a]*Departamento de Bioquímica, Instituto de Biologia/Unicamp, Instituto de Biologia, Universidade Estadual de Campinas, CP 6109, CEP 13083-970, Campinas, SP, Brazil*

[b]*Dipartimento di Medicina Sperimentale Sez. 'Chimica e Strutturistica Biochimica', Universita di Parma, Via Volturno, 39, 43100 Parma, Italy*

[c]*Instituto de Química/Universidade Estadual de Campinas, Campinas, SP, Brazil*

[d]*Centro de Biologia Molecular e Estrutural, Lab. Nacional Luz Síncrotron, Campinas, SP, Brazil*

[e]*Departamento de Bioquímica, Instituto de Química/Universidade de São Paulo, São Paulo, Brazil*

Received 1 May 2002; received in revised form 13 June 2002; accepted 13 June 2002

Abstract

We examined the effect of uncharged lidocaine on the structure and dynamics of egg phosphatidylcholine (EPC) membranes at pH 10.5 in order to assess the location of this local anesthetic in the bilayer. Changes in the organization of small unilamellar vesicles were monitored either by electron paramagnetic resonance (EPR)—in the spectra of doxyl derivatives of stearic acid methyl esters labeled at different positions in the acyl chain (5-, 7-, 12- and 16-MeSL)—or by fluorescence, with pyrene fatty-acid (4-, 6-, 10- and 16-Py) probes. The largest effects were observed with labels located at the upper positions of the fatty-acid acyl-chain. Dynamic information was obtained by ^{1}H-NMR. Lidocaine protons presented shorter longitudinal relaxation times (T_1) values due to their binding, and consequent immobilization to the membrane. In the presence of lidocaine the mobility of all glycerol protons of EPC decreased, while the choline protons revealed a higher degree of mobility, indicating a reduced participation in lipid–lipid interactions. Two-dimensional Nuclear Overhauser Effect experiments detected contacts between aromatic lidocaine protons and the phospholipid-choline methyl group. Fourier-transform infrared spectroscopy spectra revealed that lidocaine changes the access of water to the glycerol region of the bilayer. A 'transient site' model for lidocaine preferential location in EPC bilayers is proposed. The model is based on the consideration that insertion of the bulky aromatic ring of the anesthetic into the glycerol backbone region causes a decrease in the mobility of that EPC region (T_1 data) and an increased mobility of the acyl chains (EPR and fluorescence data).

Keywords: Lidocaine; Membrane; Nuclear magnetic resonance

Abbreviations: EPC, egg phosphatidylcholine; EPR, electron paramagnetic resonance; FTIR, Fourier-transform infrared spectroscopy; LA, Local anesthetics; LDC, lidocaine; MeSL, methyl ester of doxyl-stearic acid spin label; LMV, large multilamellar vesicles; *P*, partition coefficient; Py, pyrene-derivative fluorescent probe; NMR, nuclear magnetic resonance; T_1, longitudinal relaxation times; ROESY, Rotational nuclear Overhauser Effect SpectroscopY; SUV, small unilamellar vesicles

*Corresponding author. Tel.: +55-19-37886-143; fax: +55-19-37886-129.

E-mail address: depaula@unicamp.br (E. de Paula).

0301-4622/02/$ - see front matter © 2002 Elsevier Science B.V. All rights reserved.
PII: S0301-4622(02)00202-8

1. Introduction

Local anesthetics (LA) are known to exert their anesthetic effect by blocking inward sodium transport and therefore, the action potential of axons [1]. In addition to binding to the voltage-gated sodium channel, these molecules are known to bind to other membrane proteins affecting their function [2]. Local anesthetic also interact with and alter the organizational properties of lipid membranes [3–13]. In biological membranes such changes could interfere with lipid–protein interactions, leading to protein conformational changes with a reflection on their activity [1,2,14,15]. Moreover, according to the so called Meyer–Overton rule—that the more hydrophobic, the more potent is the anesthetic [16–18]—partitioning into the lipid bilayer can modulate the access of local anesthetic to their binding sites in Na^+ channels [16,19–21].

In spite of their different structures, the majority of local anesthetic share common chemical features that are relevant for their biological function: an aromatic ring, a polar group and an ionizable amine with pK around physiological pH [2,18,22].

Although evidence for a specific binding of charged local anesthetic to Na^+ channels has been reported [19,22–24] and studies conducted at physiological pH have indicated that local anesthetic activity is related to the protonated form, the importance of the uncharged species has been increasingly recognized in view of: (i) the postulated existence, in voltage-gated Na^+ channels, of a binding site for the uncharged local anesthetic form located deep inside the hydrophobic membrane core [20,21]; (ii) more pronounced partitioning and perturbation of lipid bilayer organization for uncharged local anesthetic species [5,12]; and (iii) a recognized correlation between local anesthetic hydrophobicity, potency and toxicity [16–18,25,26].

The advantages of the uncharged species might be related to their stronger binding to the membrane. In fact, their dispersion into the bilayer could provide a way to protect the molecule from metabolic processes that would produce their elimination [2]. As a result, one would expect delayed clearance in time, justifying long-lasting anesthesia. Indeed, good evidence for this hypothesis is given by the observation that hydrophobic anesthetics show longer half-lives than hydrophilic ones [17,24].

However, we have shown that while the uncharged forms of nine local anesthetic bind to egg phosphatidylcholine (EPC) model membranes, decreasing membrane organization as detected by EPR [12], their perturbing effect does not correlate with local anesthetic hydrophobicity or class (esters vs. amides). In fact, lidocaine (Fig. 1), one of the less hydrophobic anesthetics [26] studied, has been found to decrease membrane organization to a greater extent than the more hydrophobic local anesthetic such as etidocaine, bupivacaine, dibucaine or tetracaine. These results therefore suggest that binding to the membrane is not regulated only by hydrophobicity. Indeed, polar interactions or other steric parameters might determine a specific or preferential location for each local anesthetic molecule inside the membrane.

Here, we present a study on lidocaine (LDC) binding to EPC liposomes where, by measuring the anesthetic's effect on lipid organization, we collected strong evidence for the existence of a preferential location for lidocaine insertion into the bilayer. The detection of a preferential location for each different local anesthetic molecule in the bilayer—determined by its own physicochemical properties—opens a new perspective for the understanding of local anesthetic activity at the molecular level. Even considering the fast movement of local anesthetic molecules across the membrane, this 'transient site' in the bilayer could modulate the access of these molecules to their site(s) in the voltage-gated sodium channel.

2. Materials and methods

Egg phosphatidyl choline, deuterated water (D_2O, 99.9%), Chelex resin and spin labels, methyl esters of doxyl stearic acid (MeSL) labeled at carbons 5, 7, 12 and 16 were obtained from Sigma Chemical Co. (St. Louis, MO, USA). The fluorescent fatty acid probes *n*-pyrene butanoic, hexanoic, decanoic and hexadecanoic acid (4-, 6-, 10- and 16-Py, respectively) were purchased from Molecular Probes Inc. (Eugene, OR, USA). Lidocaine

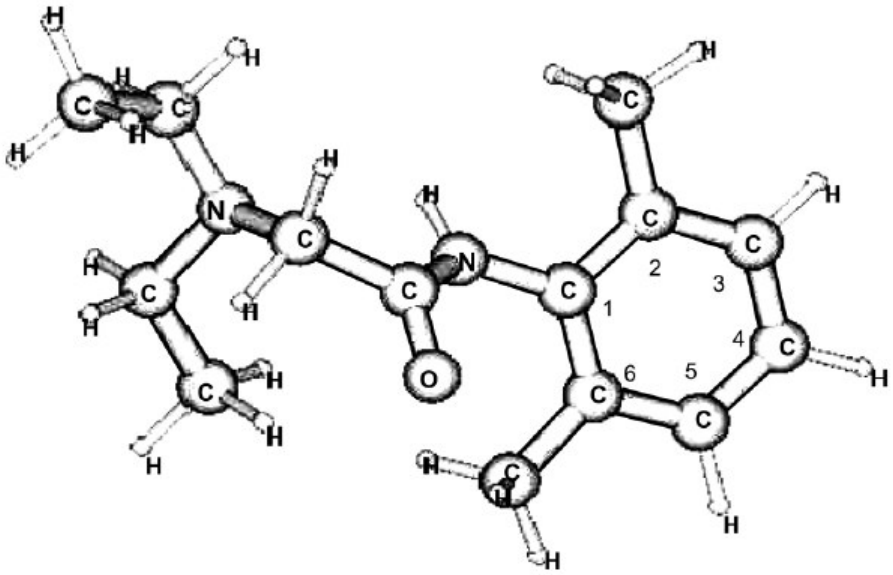

Fig. 1. Lidocaine molecular modeling, in vacuum.

hydrochloride was a gift from Apsen Brasil, Ind. Quim. Farm. Ltda, São Paulo, Brazil. All other reagents were of analytical grade.

2.1. Membrane preparation

Liposomes were obtained by evaporating stock chloroform solutions of EPC under a stream of nitrogen. The samples were left under vacuum for no less than 2 h to remove residual solvent. The lipids were then suspended in 0.02 M carbonate/bicarbonate buffer solution, pH 10.5. Large multilamellar vesicles (LMV) were obtained by vortexing for 3 min. For EPR and fluorescence experiments the labels were dissolved in chloroform and added at a concentration of 1 mole% with respect to lipid.

Small unilamellar vesicles (SUV), were obtained from freeze-dried LMV suspended in D_2O (pD 10.5). The samples were sonicated until clear (approx. 15 min) using a Sonics and Materials (Newtown, CT, USA) equipment. During sonication, the temperature was kept at 0–4 °C by intermittent (1 min) apparatus agitation cycles in an ice water bath. The sonicated samples were centrifuged with Chelex resin at $1000\times g$ for approximately 20 min to remove residual large particles and any titanium from the sonicator tip.

2.2. Partition coefficient determination

The LDC/EPC molar ratios inside the membrane were calculated by the membrane–water partition coefficient, P, of lidocaine determined by phase-separation between SUV/water at pH 10.5, according to the Eq. (1):

$$P=\frac{n_m/V_m}{n_w/V_w} \quad (1)$$

where n denotes the number of moles of lidocaine, V is the volume, and the subscripts m and w refer to the membrane and aqueous phase, respectively. The amount of lidocaine bound to the lipid phase was optically determined at 262 nm ($\varepsilon_M=420$) after ultra-centrifugation at $120\,000\times g$ for 2 h, by subtracting the supernatant concentration from the total drug concentration measured before phase mixing.

Phospholipid concentration was determined according to [27].

2.3. Electron paramagnetic resonance (EPR) experiments

The spectra were obtained with a Bruker ER-200 SRC spectrometer operating at 9 GHz (3.4 kG). Flat cells for aqueous solutions (Wilmad Co., USA) were used and the experiments were conducted at room temperature (22 °C). From the spin label spectra we calculated the h_{+1}/h_0 parameter, the height ratio of low-field to mid-field resonance, after lidocaine addition to the membranes. h_{+1}/h_0 is an empirical parameter that measures changes in overall membrane organization and is expressed as a percent 'effect' relative to the control [12], according to Eq. (2):

$$\%\ \text{Effect} = \frac{(h_{+1}/h_0)\ \text{sample} - (h_{+1}/h_0)\ \text{control}}{(h_{+1}/h_0)\ \text{control}} \times 100 \quad (2)$$

This empirical parameter comprises the effect of both molecular mobility and order in the bilayer: the slower and the more anisotropic the motion of the probe, the greater the difference between the low-field (h_{+1}) and the mid-field (h_0) peak heights. As membrane organization decreases h_{+1}/h_0 approaches 1, as for the probe in an isotropic environment [6,28].

2.4. Fluorescence experiments

The experiments were conducted using a Hitachi F4500 fluorimeter (Tokyo, Japan) at room temperature (22 °C). Pyrene probes were excited at 345 nm and the emission spectra collected in the 350–500 nm range. Quenching titrations were carried out by adding aliquots of lidocaine stock solution directly to the fluorescence cuvette containing the labeled SUV. Quenching (I_0/I, %) was obtained by the ratio between the emission intensity with (I) and without (I_0) lidocaine.

2.5. Nuclear magnetic resonance (NMR) experiments

The spectra were collected either with a Bruker AMX 400 (University of Parma, Parma, Italy) or Bruker DRX 500 (Universidade de São Paulo, Brazil) apparatus. The samples were degassed to avoid interference of dissolved O_2 with the T_1 and/or NOE measurements. For ^{1}H-NMR, a 90° pulse was typically 10–15 μs and the recycling time was set to five times the largest T_1 (those of the aromatic protons), typically 6 s. Longitudinal relaxation times (T_1) were obtained by the conventional inversion recovery method at temperature between 20 and 40 °C. The Rotational nuclear Overhauser Effect SpectroscopY (ROESY) experiments [29] were carried out using 50 ms mixing times, for the detection of build-up NOEs [30,31]. ^{31}P-NMR decoupled spectra were recorded at 202 MHz using a single pulse sequence [d_1-π/6-τ_1(acquisition)]; pulse length was 7 μs and the recycling time was 3 s. Eighty-five percent H_3PO_4 was used as standard.

2.6. Fourier transform infrared (FTIR) determinations

The experiments were carried out using the CaF_2 cell of a BOMEM-MB Series FTIR spectrometer, at Instituto de Química/Unicamp. Spectra were deconvoluted using different Gaussians/Lorentzians rates. Each spectrum of 64 scans was averaged with the detector at 2 cm^{-1} resolution. The samples were prepared in D_2O buffered solution to avoid the strong water absorption band at 1650 cm^{-1}.

2.7. Molecular modeling

The molecules were built with the Molden software and processed/visualized with the GAMESS (General Atomic and Molecular Electronic Structure System) program that uses a semi-empirical AM1 approach and MNDO approximation. The programs were licensed to Centro Nac. Processamento de Alto Desempenho em São Paulo (CENAPAD) that allowed us to calculate the molecules in a parallel process.

3. Results and discussion

In a previous study we demonstrated that lidocaine, an amino–amide local anesthetic (Fig. 1), was the most efficient among the nine local anes-

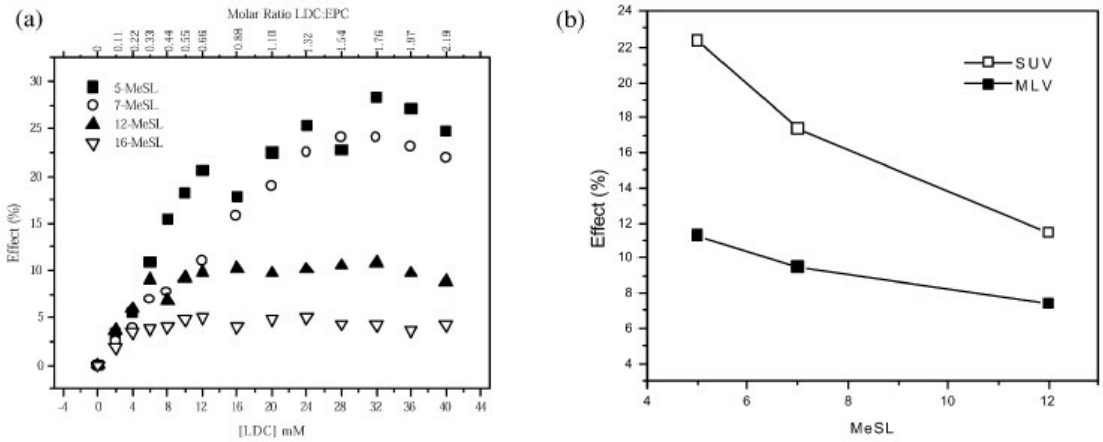

Fig. 2. (a) Effect of lidocaine on membrane organization detected by the EPR spectra of spin probes at different depths (5-,7-,12- and 16-MeSL) in large multilamellar EPC (8 mM) vesicles in 0.02 M carbonate buffer, pH 10.5, at 22 °C. (b) Comparative effect for a 0.33:1, LDC/EPC molar ratio in the membrane on small unilamellar (□) and large multilamellar (■) vesicles.

thetic tested in decreasing the membrane organization of EPC multilamellar vesicles at pH 10.5 [12]. This finding was quite intriguing if we consider the Meyer–Overton rule and the relatively low hydrophobicity of lidocaine.

3.1. Electron paramagnetic resonance experiments

The effect of lidocaine on egg phosphatidylcholine membrane organization was followed by methyl ester derivatives of stearic acid (MeSL) spin labels. These probes carry paramagnetic doxyl groups at carbons 5, 7, 12 or 16, monitoring different depths of the bilayer [32]. In LMV (Fig. 2a) the decrease in membrane organization induced by lidocaine was observed with all the spin-labels used. The hyperbolic curves were indicative of membrane saturation, in agreement with our previous observation using the 5-MeSL probe [12]. The maximum decrease in membrane organization reached 26% with 5-MeSL. Using the partition coefficient of lidocaine between LMV/water ($P=144$ at pH 10.5 [12]), we calculated that membrane saturation in the curves illustrated in Fig. 2a occurred when the anesthetic reached a 0.4:1 molar ratio (LDC/lipid, in the membrane).

According to the curves in Fig. 2a, the sensitivity of the MeSL probes to the effect of lidocaine decreased as the nitroxide assumed deeper positions in the acyl chain (5>7>12≥16 MeSL), as predicted by the profile of the acyl chain order [33,34] and dynamics [30,32,35] inside the phospholipid bilayers.

We determined the partition coefficient for Lidocaine between SUV/water ($P=74\pm24$ at pH 10.5) and carried out experiments like those in Fig. 2a using unilamellar vesicles. While membrane saturation was reached at the same molar ratio (approx. 0.4:1, LDC/lipid) in the membrane as for LMV, the maximum effect reached 36.5% in the curve for 5-MeSL. Knowledge of P values allowed us to carry out the analysis of EPR data at a fixed lidocaine/lipid molar ratio in the membrane. Fig. 2b compares the effect of lidocaine, at a 0.33:1 LDC/lipid molar ratio in the membrane—in the different membrane regions monitored by the MeSL probes—both for LMV and SUV. Data from 16-MeSL were not included because changes were quite small, within the error of the experiment. The profile for LMV and SUV was similar: the effect of lidocaine on membrane organization was stronger at positions near the membrane/water interface (5 and 7 MeSL), although the decrease in membrane organization was much more evident in the unilamellar vesicles, probably due to the

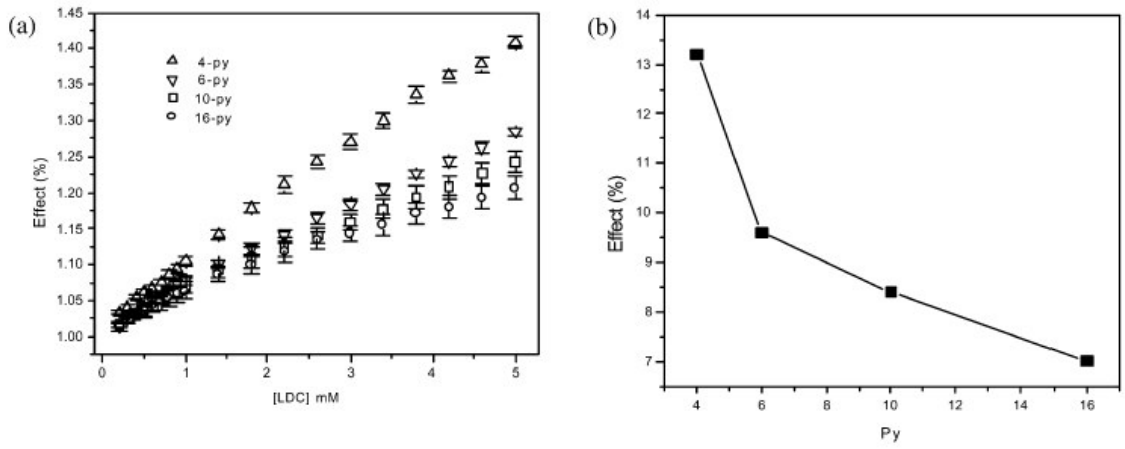

Fig. 3. Effect of lidocaine on membrane organization detected by the spectra of fluorescence probes at different depths (4-,6-,10- and 16-Py) on small unilamellar EPC (0.7 mM) vesicles, pH 10.5, 22 °C. (b) Comparative effect for a 0.07:1 (LDC/EPC, molar ratio in the membrane).

looser packing of the lipids in these vesicles [36,37].

Differences in the acyl chain order and dynamics could not explain the profiles observed in Fig. 2b. Moreover, the effect of lidocaine on membrane organization detected by EPR (5>7>12 MeSL) differs from that of tetracaine (5≈7>12 MeSL) and benzocaine (5<7>12), as we have shown before [13].

These data suggest that lidocaine penetrates the lipid bilayer in the region comprised between the glycerol backbone and the 2–5 carbons of the acyl chain, acting as a spacer between lipid molecules. Lidocaine is rather spherical, and the presence of two *o*-methyl groups in its aromatic ring creates a significant steric hindrance for its insertion between the lipids. This extra volume in the aromatic ring could explain the higher effect of lidocaine on membrane organization in comparison to tetracaine [12], an amino-ester local anesthetic that does not have *o*-methyl groups. Tetracaine is essentially cylindrical in shape and has a long amino-butyl tail in the *para* position of the benzoic acid ring that is expected to favor the orientation of the molecule parallel to the acyl chains of the phospholipids [2]. Previous results from our laboratory have shown that in LMV monitored by 5-MeSL probes, tetracaine was not able to decrease membrane organization by more than 15% [12].

Local anesthetic disturb the packing of the lipids since they are shorter (lidocaine length=9.4 Å) than the lipid molecules (approx. 25 Å). Local anesthetic is believed to create inter-lipid spaces that would permit an increase in the probability of Gauche–CH_2 bonds, decreasing the acyl chain order [2]. This disturbing effect can be more pronounced if the local anesthetic occupies more restricted portions of the bilayer such as the glycerol backbone and first carbons of the acyl chain [32–35]. In fact, etidocaine and bupivacaine—hydrophobic analogs of lidocaine—did not have the pronounced effect of lidocaine on membrane organization [12] and we have evidence for a deeper insertion of both local anesthetics inside EPC bilayers (Fraceto and de Paula, in preparation).

3.2. Fluorescence experiments

The effect of local anesthetic on membrane organization has been studied also by fluorescence using fatty-acid pyrene derivatives as probes; like the spin labels, these fluorescent molecules were able to monitor different depths of the acyl chain [38], but light scattering limited the studies in SUV up to 1 mM concentration.

In Fig. 3 the quenching of the pyrene probes is located at different membrane depths and was

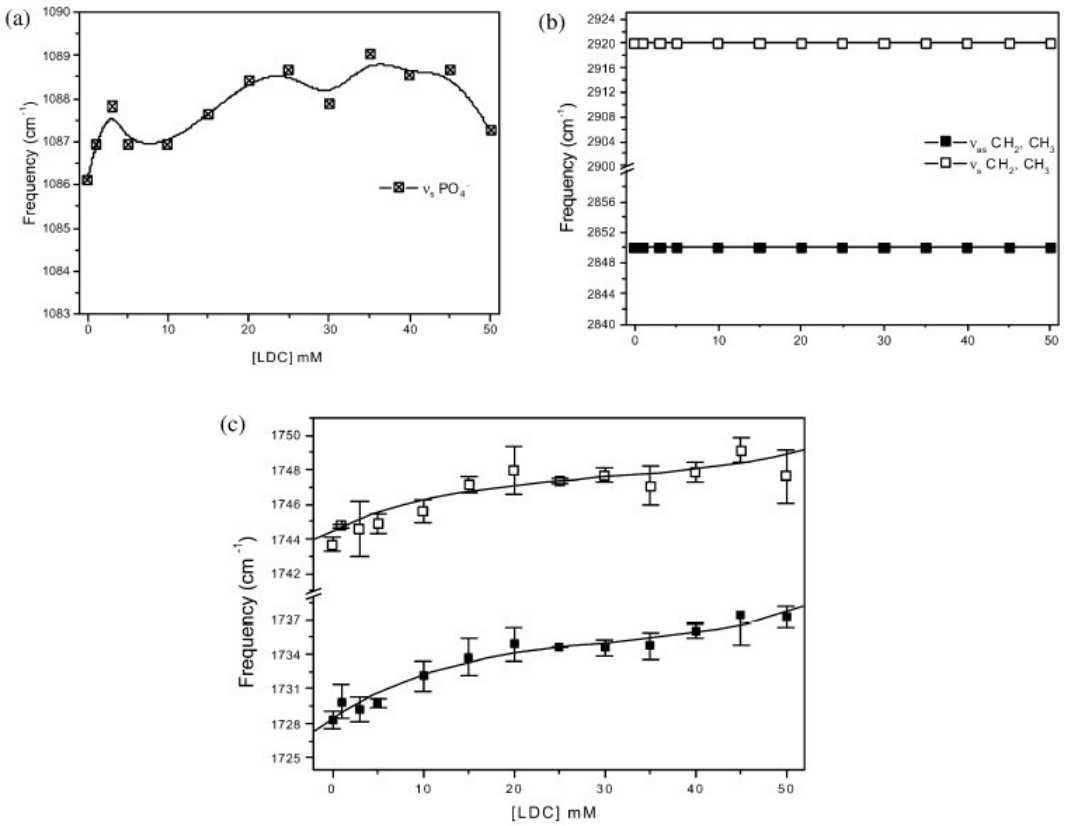

Fig. 4. Changes in the FTIR absorption of the phosphate stretching band, ν_s (a); acyl chain stretching bands $-CH_2-CH_3$ ν_s, and ν_{as} (b), and carbonyl stretching bands (c) of EPC small unilamellar vesicles in the presence of increasing lidocaine concentration. [EPC] = 65 mM, CaF_2 cell, 22 °C, pH 10.5.

considered to be the *effect* resulting from decreased order or increased molecular mobility inside the bilayer [39] caused by lidocaine. Partitioning of the anesthetic into the membrane decreased its organization in a concentration-dependent manner, in agreement with the EPR results. Since lipid concentration was limited to 1 mM to avoid scattering, lidocaine could not reach an adequate concentration (0.4:1, mole%) in the membrane to induce saturation (as in Fig. 2b).

As evidenced by the pyrene probes in Fig. 3b, for a fixed molar ratio (0.07:1, LDC/EPC) in the membrane, the *effect* of Lidocaine on membrane organization was stronger for the probes near the membrane surface and weakened towards the bilayer core (4 > 6 > 10 > 16 Py-fatty acid), in a profile similar to that observed for spin-label probes.

3.3. ^{31}P-NMR and FTIR experiments

Since EPR and fluorescence data indicated that Lidocaine affected mainly the more superficial portions of the bilayer, we decided to verify the degree of perturbation that could be induced at the polar head-group of phosphatidylcholine.

Boulanger et al. reported an 8% change in the ^{31}P-NMR chemical shift anisotropy of EPC mul-

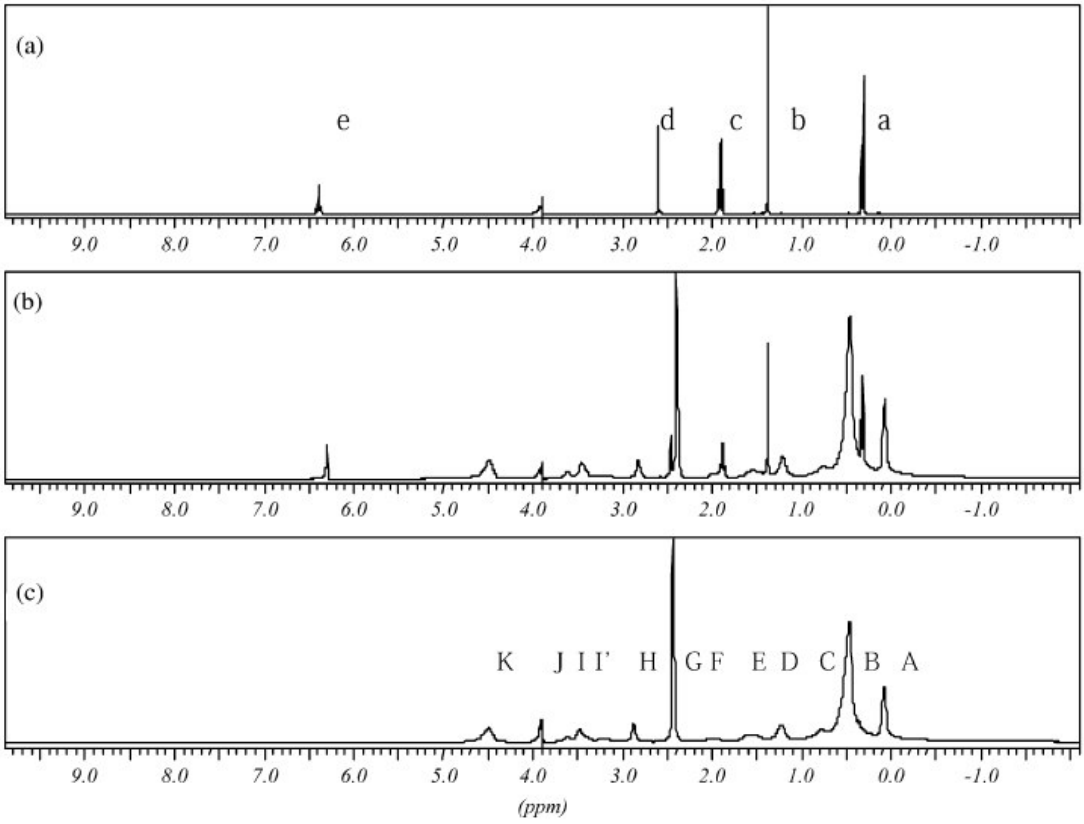

Fig. 5. Four hundred megaHertz ^{1}H-NMR spectra of lidocaine (a), lidocaine/EPC 0.33:1, molar ratio in the membrane (b), and 65 mM small unilamellar EPC vesicles (c); pH 10.5, 30 °C. Assignment as in Table 1.

tilamellar vesicles in the presence of charged tetracaine and no changes with the uncharged form, which penetrates deeper into the membrane [2]. Indeed, we could not detect any significant effect in the phosphate NMR spectra of EPC multilamellar vesicles (de Paula et al., in preparation) after the addition of lidocaine or other local anesthetic, at pH 10.5.

In sonicated vesicles Kuroda and Fujiwara reported discrete shifts in the ^{31}P resonance of EPC induced by the charged tetracaine, dibucaine and procaine [40]. Here, we detected no significant changes in the ^{31}P-NMR spectra of SUV after the addition of uncharged lidocaine.

Analysis of the phosphate stretching band in FTIR experiments (Fig. 4a) with sonicated EPC vesicles did not demonstrate any specific effect of lidocaine in the neighborhood of the PO_4^- group. The PO_4^- stretching band (ν_{as}) and acyl chain-CH_2 and CH_3-stretching bands (ν_{as} and ν_s) were equally insensitive to the presence of lidocaine (Fig. 4b).

Interestingly, the carbonyl stretching bands were changed in the presence of lidocaine (Fig. 4c). Lidocaine shifted the band position of both ester groups of EPC, i.e. the more (1728 cm^{-1}) and the less hydrated (1741 cm^{-1}), to higher wave numbers—1738 and 1748, respectively. This effect was interpreted in terms of a decrease in hydrogen bonding for both ester C=O. Data from the literature have shown that anesthetics disturb membrane organization in such a way that they improve the access of water molecules to the carbonyl bands [41]. However, this is not the case

Table 1
Chemical Shifts in the ^{1}H-NMR spectra of lidocaine, EPC and lidocaine/EPC (0.33:1 mole% in the membrane)

Peak	Assignment[a]	Chemical shift (ppm)		
		LDC in D_2O	EPC	LDC/EPC
A	ω-CH_3		0.00	0.00
a	**Ethyl–CH_3**	**0.16**		**0.25**
B	$(CH_2)_n$		0.40	0.38
C	β–CH_2		0.70	0.69
D	$CH_2C{=}C$		1.15	1.15
b	**Aromatic–CH_3**	**1.25**		**1.30**
E	α–CH_2		1.50	1.50
c	**Ethyl–CH_2**	**1.86**		**1.80**
F	$=C–CH_2–C=$		1.90	1.90
G	$N^+(CH_3)_3$		2.39	2.30
d	**CO–CH_2–N:**	**2.54**		**2.39**
H	$CH_2–N^+$		2.80	2.70
I	$O_3PO–CH_2$ (choline)		3.20	3.20
I'	$O_3PO–CH_2$ (glycerol)		3.40	3.40
J	CH_2–OCO		3.55	3.50
	HDO	3.90	3.90	3.90
K	CH=CH, CH–OCO		4.40	4.40
e	**Aromatic -3,4,5**	**6.34**		**6.20**

[a] Capital letters refer to EPC; lower-case letters refer to lidocaine peaks.

for lidocaine. The upshift in the C=O stretching band frequencies supports the hypothesis that the presence of the lidocaine molecule in the glycerol neighborhood creates a more hydrophobic environment in which lipids are less hydrogen-bonded to water. No changes in the proportion of the bands were detected after lidocaine addition, excluding the possibility of conformational changes in the polar head-group bending angle relatively to the acyl chain [42,43].

These FTIR data suggest that lipid molecules directly adjacent to a hydrophobic group of lidocaine (probably the aromatic ring) may experience a transition from a stronger to a weaker hydrogen-bonding environment caused by the displacement of water molecules from the carbonyl region.

3.4. ^{1}H magnetic resonance experiments

Fig. 5 shows the ^{1}H-NMR spectra of lidocaine in D_2O (a), EPC unilamellar vesicles (c) and EPC plus Lidocaine, at a 0.33:1 molar ratio (LDC/lipid) in the membrane (b). The assignment of EPC and lidocaine protons is reported in Table 1, where capital letters refer to the phospholipid [40], and lower-case letters identify the local anesthetic resonances. Upon mixing, all lidocaine protons were broadened, confirming their insertion into the lipid membrane; and their chemical shifts were slightly changed to up-field (peaks c, d and e) or to low-field (methyl protons, peaks a and b) frequencies. No significant changes in the line-width or chemical shifts of EPC resonance peaks were observed, except for the up-field shifts of peaks (g) and (h) (0.1 ppm choline protons) and of peak (j) (0.05 ppm), in the glycerol backbone. Overall, these results suggest that just a few protons, at the polar head-group of EPC unilamellar vesicles, are affected by the presence of lidocaine. Since the literature reports that aromatic molecules in the bilayer can shift resonances by the short-range ring current effect [44] this result indicates a superficial insertion of lidocaine into this bilayer.

3.5. Nuclear Overhauser experiments

ROESY experiments were carried out in SUV of egg phosphatidylcholine with the addition of Lidocaine (0.33:1, LDC/EPC, molar ratio in the membrane) in order to identify lidocaine/EPC contacts. To reduce artifacts due to spin diffusion the ROESY spectra were run at short mixing times, i.e. up to 50 ms [30,40,45–48]. Only two intermolecular dipolar interactions were detected between protons from lidocaine and the lipid molecules (Fig. 6) and we have checked that these cross-peaks were not due to magnetization transfer between lidocaine protons [i.e. (b)–(d); (d)–(e)]. The cross-peaks were assigned to protons e-G and b-G, indicating interactions between the local anesthetic aromatic ring and the choline methyl protons of EPC.

3.6. T_1 measurements

Longitudinal relaxation time (T_1) measurements provided complementary information about the dynamics of the LDC/EPC system. Fig. 7 reports the T_1 values for lidocaine protons in water and when incorporated into the anisotropic membrane

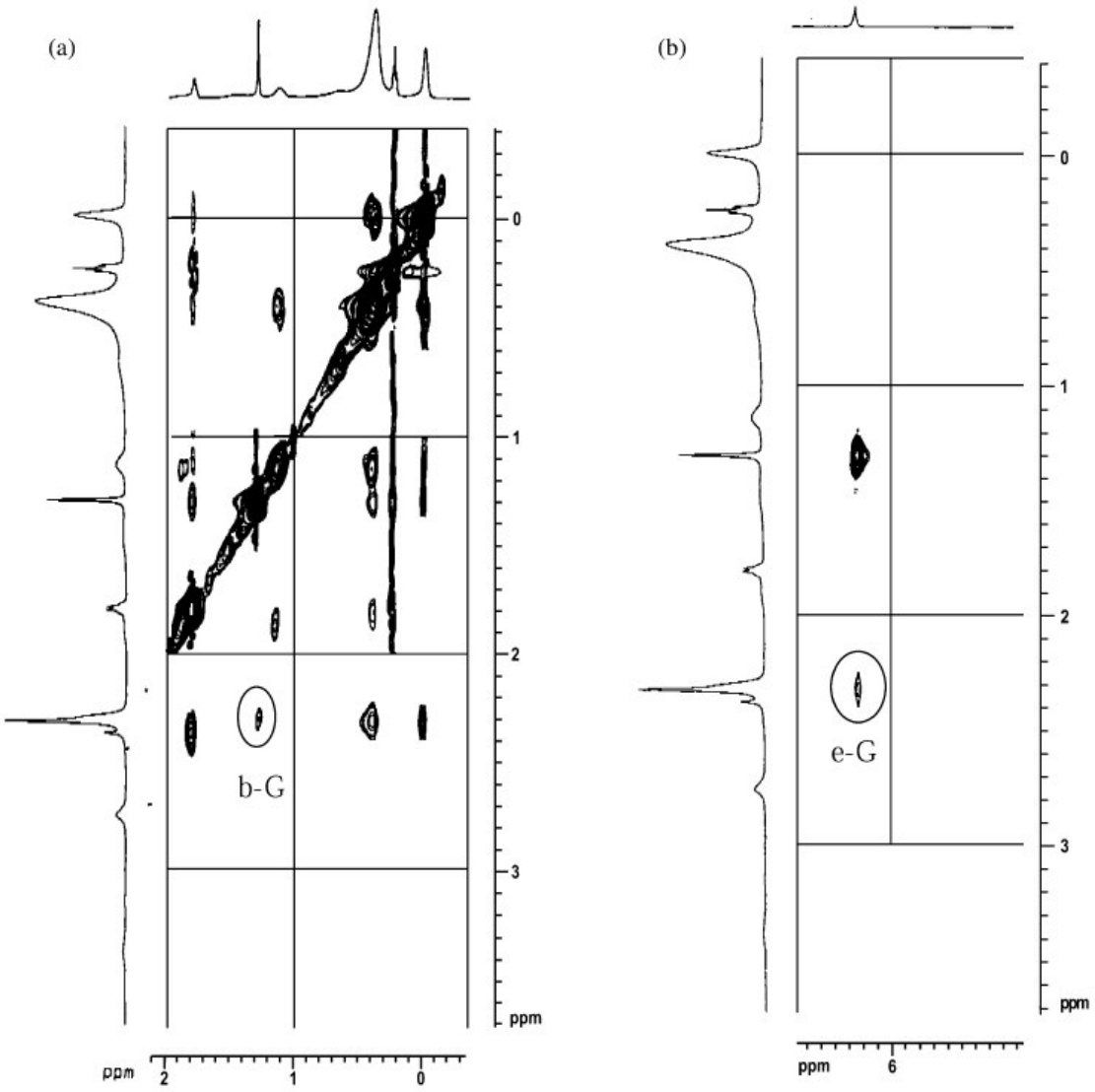

Fig. 6. Detail of a ROESY spectrum of lidocaine/EPC (0.33:1, molar ratio in the membrane) system, revealing intramolecular (lidocaine-EPC) cross-peaks. 65 mM EPC, pH adjusted to 10.5, spectra run at 500 MHz, 30 °C.

environment. In the presence of EPC vesicles we observed a clear reduction of the T_1 values of all lidocaine protons. This observation, in agreement with the observed broadening of their resonance peaks (Fig. 5), is indicative of a restriction in the mobility of the lidocaine protons, confirming that the molecule is fully inserted into the membrane.

Analysis of the T_1 values for the EPC protons (Fig. 8a) revealed the bilayer regions that were more affected by the presence of lidocaine. The

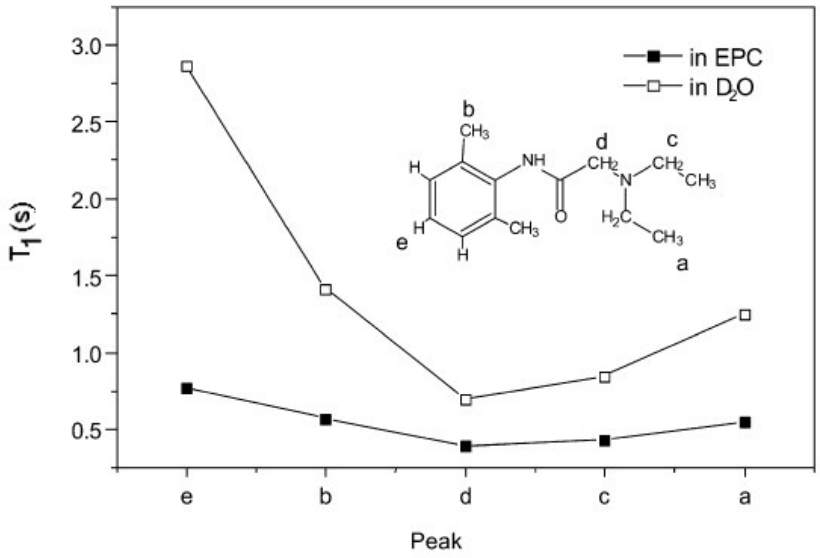

Fig. 7. Longitudinal relaxation times (T_1) of Lidocaine protons in D_2O and in EPC small unilamellar vesicles (0.33:1, LDC/lipid, molar ratio in the membrane). Peak assignment as in Table 1; experimental condition as in Fig. 6.

T_1 values for EPC protons are in good agreement with those reported in the literature [30,49]; the polar head group protons show shorter T_1 values, reflecting the increased relaxation caused by the electrostatic interaction between the choline $-N^+(CH_3)_3$ and phosphate groups of adjacent lipids [50]. The small acyl chain dynamics in the first 2–8 carbons-peak C in Fig. 8a—increases towards the hydrophobic core-peaks B, D, K and A—in agreement with the profile of phospholipid dynamics in lipid membranes reported in ^{13}C, ^{2}H, ^{1}H-NMR [30,32,35] and EPR [51] studies.

Upon addition of Lidocaine the T_1 values changed mainly for the protons in the polar headgroup region of EPC. Protons bound to the choline amine group—the methyl (G) and methylene (H) peaks—presented longer T_1 values, indicating that they lacked lipid–lipid inter-molecular interaction in the presence of lidocaine. In contrast, peaks I—corresponding to the choline CH_2 adjacent to the phosphate group—I′ and J, at the glycerol backbone, became more restricted allowing us to conclude that the lidocaine molecule stays there, increasing the relaxation of these protons. The effect of lidocaine on the choline and phosphate protons of EPC is highlighted in Fig. 8b, with experiments run between 20 and 40 °C.

4. Conclusion

Clinically used local anesthetics are small amphiphiles containing an ionizable amino group with a pK between 7 and 9. It is believed that the stronger binding of the uncharged species to the membrane would protect local anesthetic from blood clearance, thus justifying long lasting anesthesia. If this hypothesis is accepted, uncharged local anesthetic clearly acquire a crucial role in anesthesia.

The interaction of uncharged lidocaine with small unilamellar and multilamellar EPC vesicles resulted in a decrease of the overall membrane organization, as revealed by EPR and fluorescence data. Lidocaine induced a less tightly packing of the lipids in the vesicles, possibly by creating inter-lipid spaces. This effect was more evident in the glycerol region and also in the small unilamellar vesicles.

To describe the lidocaine/lipid interaction we employed a variety of spectroscopic techniques.

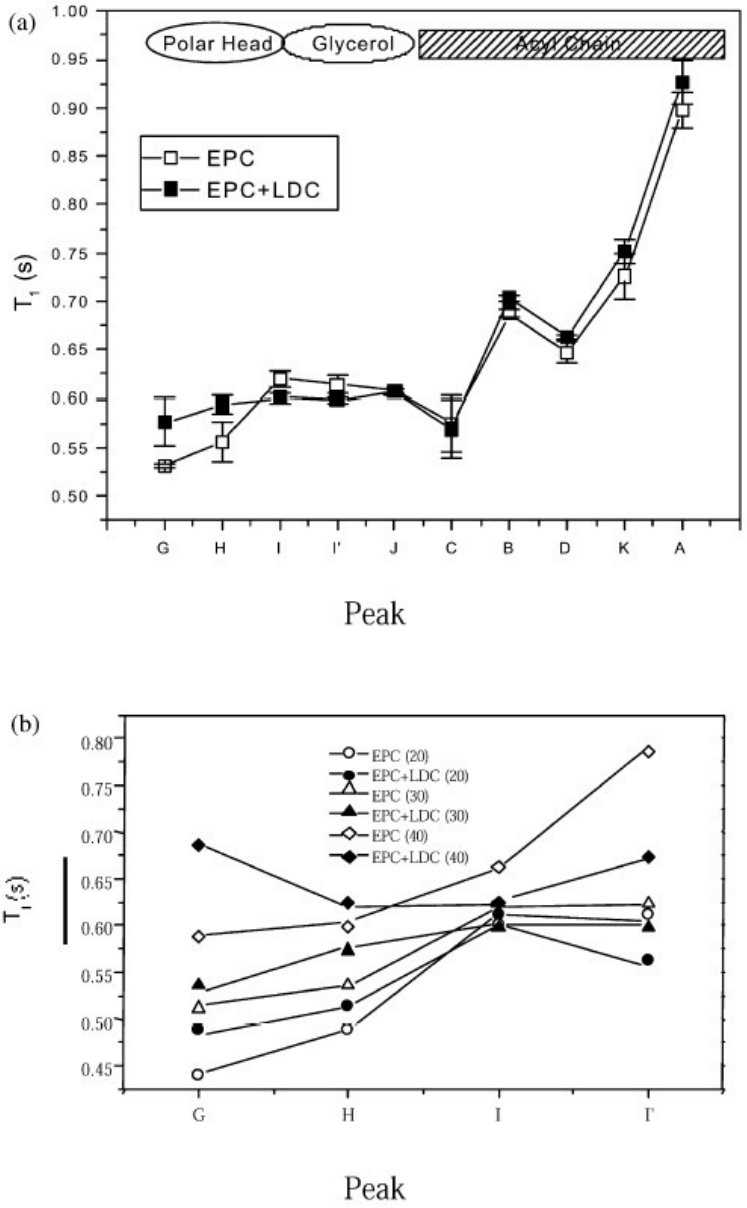

Fig. 8. Effect of Lidocaine (0.33:1 LDC/lipid, molar ratio in the membrane) on the relaxation times of EPC protons at 30 °C (a). Detail of the effect on the polar head group and glycerol region at variable temperatures of 20, 30 and 40 °C (b). T_1 values were determined by the inversion-recovery technique. Assignment as in Table 1.

For the unilamellar EPC vesicles in particular, our data suggest that lidocaine possesses a preferential location inside the EPC vesicle, with its aromatic ring (the bulky part of the molecule) in the vicinity of the glycerol backbone. This positioning affects atoms at the choline, glycerol (NMR), carbonyl

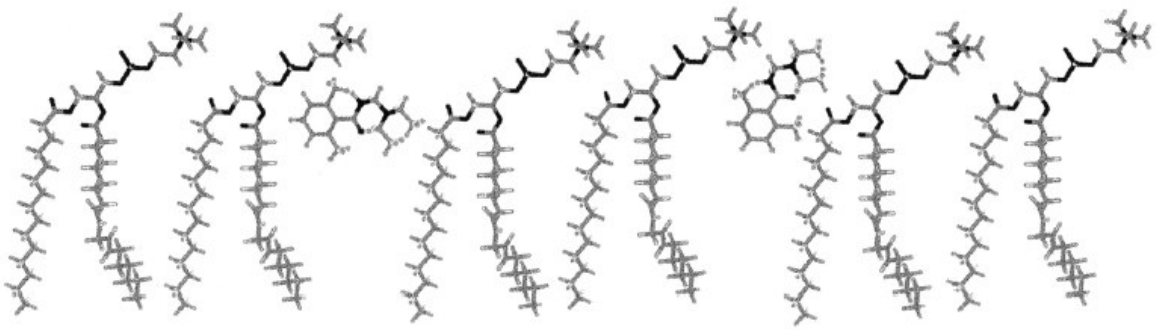

Fig. 9. Proposed model for lidocaine insertion into EPC small unilamellar vesicles.

(FTIR) and at the first portion of the acyl chain (EPR and fluorescence data). Although up to now no realistic models are available for phospholipid bilayer [52] representation at atomic resolution, the cartoon in Fig. 9 is useful to outline the depth of insertion of lidocaine, while its conformation and orientation can probably change. In fact, it is quite probable that lidocaine diffuses laterally at the level of the glycerol backbone.

It is important to point out that the existence of a preferential membrane location for the local anesthetic does not mean that these molecules remain steadily at that site. In fact, anesthesia requires a rapid equilibrium of local anesthetic between adjacent membrane and water compartments, implying that they have to move quickly across membrane and water. EPR experiments have demonstrated the existence of such a fast steady-state equilibrium since it is not possible to detect distinct populations of spin-labeled local anesthetic [53,54] upon local anesthetic addition to liposomes. Therefore, we suggest that while local anesthetic are able to cross the membrane, they occupy a 'transient site' at a specific bilayer depth, determined by their hydrophobicity, polarity and steric features.

In a previous report [12] we demonstrated the importance of steric properties and location in determining the degree of membrane perturbation caused by local anesthetic. Indeed, the location and orientation of anesthetics in the membrane could play a crucial role in the mechanism of anesthesia, since they can modulate LA-Na^+ channel binding by directing the molecule to access the proper site at the channel and/or by enhancing LA concentration in the surroundings of the binding site(s) [19,20].

Lidocaine provides good evidence for this hypothesis because even though it is not a highly hydrophobic anesthetic, it decreases membrane organization to a greater extent than other anesthetics with a higher hydrophobic character, such as tetracaine. The van der Waals volume of lidocaine (228.5 $Å^3$) is smaller than that of tetracaine (251.4 $Å^3$) [18]; nevertheless, because of its spherical shape, the spacing created by lidocaine inserted into the bilayer is greater than that of tetracaine [2].

The features of the specific bilayer region (polarity, fluidity, etc.) where the anesthetic stays most of the time could then determine its orientation and conformation, directing the molecule to the hydrophobic site(s) of action [20,21] of the voltage-gated sodium channel.

Acknowledgments

This work was partly supported by FAPESP (Grant 96/1451-9), CNPq (Grant 520539-8), CAPES and FAEP/Unicamp Brazil (EP, SS) and MURST, Italy (A.S.). We acknowledge the C.I.M. (Centro Interdipartimentale di Misure) Universitá degli Studi di Parma, Italy, for the use of the NMR facility, and CENAPAD for the use of molecular modeling programs. L.M.A.P. and L.F.F. were the recipients of fellowships from FAPESP (Proc. 96/

9786-0 and 00/0362-0). S.S. and E.P. are the recipients of research fellowships from CNPq.

References

[1] J.F. Butterworth, G.R. Strichartz, Molecular mechanisms of local-anesthesia—a review, Anesthesiology 72 (1990) 711–734.

[2] E. de Paula, S. Schreier, Molecular and physicochemical aspects of local anesthetic–membrane interaction, Braz. J. Med. Biol. Res. 29 (1996) 877–894.

[3] D. Papahadjoupoulos, K. Jacobson, G. Poste, G. Shepherd, Effects of local-anesthetics on membrane properties. 1. Changes in fluidity of phospholipids bilayers, Biochim. Biophys. Acta 394 (1975) 504–519.

[4] A.G. Lee, Interactions between anesthetics and lipid mixtures amines, Biochim. Biophys. Acta 448 (1976) 34–44.

[5] Y. Boulanger, S. Schreier, I.C.P. Smith, Molecular details of anesthetic–lipid interaction as seen by deuterium and P-31 nuclear magnetic resonance, Biochemistry 20 (1981) 6824–6830.

[6] S. Schreier, W. Frezzatti Jr., P.S. Araujo, H. Chaimovich, I.M. Cuccovia, Effect of lipid-membranes on the apparent pK of local-anesthetic tetracaine—spin label and titration studies, Biochim. Biophys. Acta 769 (1984) 231–237.

[7] S. Schreier, W. Frezzatti Jr., P.S. Araujo, I.M. Cuccovia, in: K.L. Mittal, B. Lindmam (Eds.), Surfactants in Solution, 3, Plenum Press, New York, London, 1984.

[8] E.C. Kelusky, Y. Boulanger, S. Schreier, I.C.P. Smith, A 2H-NMR study on the interactions of the local anesthetic tetracaine with membranes containing phosphatidylserine, Biochim. Biophys. Acta 856 (1986) 85–90.

[9] Y. Kaminoh, T. Inone, S.M. Ma, I. Ueda, S.H. Lin, Membrane–buffer partition-coeficients of tetracaine for liquid–crystal and solid–gel membranes estimated by direct ultraviolet spectrophotometry, Biochim. Biophys. Acta 946 (1988) 337–344.

[10] M.L. Bianconi, A.T. Amaral, S. Schreier, Use of membrane spin label spectra to monitor rates of reaction of partitioning compounds—hydrolysis of a local-anesthetic analog, Biochem. Biophys. Res. Commun. 152 (1988) 344–350.

[11] M. Auger, I.C.P. Smith, H. Mantsch, P.T.T. Wong, High-pressure infrared study of phosphatidylserine bilayers and their interactions with the local-anesthetic tetracaine, Biochemistry 29 (1990) 2008–2015.

[12] E. de Paula, S. Schreier, Use of a novel method for determination of partition-coeficients to compare the effect of local-anesthetics on membrane-structure, Biochim. Biophys. Acta 1240 (1995) 25–33.

[13] L.M.A. Pinto, D.K. Yokaichiya, L.F. Fraceto, E. de Paula, Interaction of benzocaine with model membranes, Biophys. Chem. 87 (2000) 213–223.

[14] B. Hille, K. Courtney, R. Dunn, in: B.R. Fink (Ed.), Molecular Mechanisms of Anesthesia, Progress in Anesthesiology, 1, Raven Press, New York, 1975, pp. 13.

[15] A.G. Lee, Model for action of local-anesthetics, Nature 262 (1976) 545–548.

[16] K.R. Courtney, Structure–activity relations for frequency-dependent sodium-channel block in nerve by local-anesthetics, J. Pharmacol. Exp. Ther. 213 (1980) 114–119.

[17] B.G. Covino, H.G. Vassalo, Local Anesthetics: Mechanisms of Action and Clinical Use, Chapter 3, Grune and Stratton, New York, 1976.

[18] S.P. Gupta, Quantitative structure–activity relationship studies on local-anesthetics, Chem. Rev. 91 (1991) 1109–1119.

[19] B. Hille, pH-dependent rate of action of local-anesthetics on node of ranvier, J. Gen. Physiol. 69 (1977) 497–515.

[20] D.S. Ragsdale, J.C. McPhee, R. Scheuer, W.A. Catterall, Molecular determinants of state-dependent block of Na^+ channels by local-anesthetics, Science 265 (1994) 1724–1728.

[21] D.S. Ragsdale, J.C. McPhee, R. Scheuer, W.A. Catterall, Common molecular determinants of local anesthetic, antiarrhythmic, and anticonvulsant block of voltage-gated Na^+ channels, Proc. Natl. Acad. Sci. USA 93 (1996) 9270–9275.

[22] J.M. Ritchie, B.R. Ritchie, P. Greengard, Active structure of local anesthetics, J. Pharmacol. Exp. Ther. 150 (1965) 152–159.

[23] T. Narahashi, M. Yamada, D.T. Frazier, Cationic forms of local anaesthetics block action potentials from inside nerve membrane, Nature 223 (1969) 748–749.

[24] T. Narahashi, D.T. Frazier, M. Yamada, Site of action and active form of local anesthetics. 1. Theory and pH experiments with tertiary compounds, J. Pharmacol. Exp. Ther. 171 (1970) 32–44.

[25] R.H. de Jong, Local Anesthetics, Mosby, St. Louis, 1994.

[26] B.G. Covino, in: G.R. Strichartz (Ed.), Local Anesthetics. Handbook of Experimental Pharmacology, 81, Springer-Verlag, Berlin, 1987, pp. 187–212.

[27] G. Rouser, S. Fleicher, A. Yamamoto, Two dimensional thin layer chromatographic separation of polar lipids and determination of phospholipids by phosphorus analysis of spots, Lipids 5 (1970) 494–496.

[28] W. Frezzatti Jr., W.R. Toselli, S. Schreier, Spin label study of local anesthetic–lipid membrane interactions—phase-separation of the uncharged form and bilayer micellization by the charged form of tetracaine, Biochim. Biophys. Acta 860 (1986) 531–538.

[29] A. Bax, D.G. Davis, Pratical aspects of two-dimensional transverse NOE spectroscopy, J. Magn. Res. 63 (1985) 207–213.

[30] Y. Kuroda, K. Kitamura, Intramolecular and intermolecular H1–H1 nuclear Overhauser effect studies on the

interactions of chlorpromazine with lecithin vesicles, J. Am. Chem. Soc. 106 (1984) 1–6.
[31] J. Baber, J.F. Ellena, D.S. Cafiso, Distribution of general-anesthetics in phospholipids-bilayers determined using H-2 NMR and H1–H1 NOE spectroscopy, Biochemistry 34 (1995) 6533–6539.
[32] P.E. Godici, F.R. Landsberger, Dynamics structure of lipid-membranes—C13 nuclear magnetic resonance study using spin labels, Biochemistry 13 (1974) 362–368.
[33] A. Seelig, J. Seelig, Bilayers of dipalmitoyl-3-*sn*-phosphatidylcholine—conformational differences between fatty acyl chains, Biochim. Biophys. Acta 406 (1975) 1–5.
[34] D.A. Driscoll, S. Samarasinghe, S. Adamy, J. Jonas, A. Jonas, Pressure effects on dipalmitoylphosphatidylcholine bilayers measured by H-2 nuclear-magnetic-resonance, Biochemistry 30 (1991) 3322–3327.
[35] J.F. Ellena, S.J. Archer, R.N. Dominey, B.D. Hill, D.S. Cafiso, Localizing the nitroxide group of fatty-acid and voltage-sensitive spin-labels in phopholipid-bilayers, Biochim. Biophys. Acta 940 (1988) 63–70.
[36] S.I. Chan, M.P. Sheetz, C.H.A. Seiter, et al., Nuclear magnetic resonance studies of structure of model membranes systems—effect of surface curvature, Ann. NY Acad. Sci. 222 (1973) 499–522.
[37] M.A. Swairjo, B.A. Seaton, M.F. Roberts, Effect of vesicle composition and curvature on the dissociation of phosphatidic-acid in small unilamellar vesicles—a ^{31}P-NMR study, Biochim. Biophys. Acta 1191 (1994) 354–361.
[38] K.A. Sikaris, W.H. Sawyer, The interaction of local-anesthetic with synthetic phospholipids-bilayers, Biochem. Pharmacol. 31 (1982) 2625–2631.
[39] E. Lissi, M.L. Bianconi, A.T. Amaral, E. de Paula, L.E.B. Blanch, S. Schreier, Methods for the determination of partition-coefficients based on the effect of solutes upon membrane-structure, Biochim. Biophys. Acta 1021 (1990) 46–50.
[40] Y. Kuroda, Y. Fujiwara, Locations and dynamic perturbations for lipids of cationic forms of procaine, tetracaine and dibucaine in small unilamellar phosphatidylcholine vesicles as studied by nuclear Overhauser effects in H-1 nuclear magnetic resonance spectroscopy, Biochim. Biophys. Acta 903 (1987) 395–410.
[41] I. Ueda, J.S. Chiou, P.R. Krishma, H. Kamaya, Local-anesthetics destabilize lipid-membranes by breaking hydration shell—infrared and calorimetry studies, Biochim. Biophys. Acta 1190 (1994) 421–429.
[42] A. Blume, W. Hübner, G. Messner, Fourier-transform infrared-spectroscopy of C–13=O-labeled phospholipids hydrogen-bonding to carbonyl groups, Biochemistry 27 (1988) 8239–8249.
[43] M. Beck, F. Siebert, T.P. Sakmar, Evidence for the specific interaction of a lipid molecule with rhodopsin which is altered in the transition to the active state metarhodopsin II, FEBS Lett. 436 (1998) 304–308.
[44] W.M. Yau, W.C. Wimley, K. Gawrisch, S.H. White, The preference of tryptophan for membrane interfaces, Biochemistry 37 (1998) 14713–14718.
[45] M. Wakita, Y. Kuroda, Y. Fujiwara, T. Nakagawa, Conformations of dibucaine and tetracaine in small unilamellar phosphatidylcholine vesicles as studied by nuclear Overhauser effects in H-1 nuclear magnetic resonance spectroscopy, Chem. Phys. Lipids 62 (1992) 45–54.
[46] J.A. Barry, K. Gawrisch, Direct NMR evidence for ethanol binding to the lipid–water interface of phospholipids-bilayers, Biochemistry 33 (1994) 8082–8088.
[47] L.L. Holte, K. Gawrisch, Determining ethanol distribution in phospholipid multilayers with MAS-NOESY spectra, Biochemistry 36 (1997) 4669–4674.
[48] D. Huster, K. Gawrish, NOESY NMR crosspeaks between lipid headgroups and hydrocarbon chains: spin diffusion or molecular disorder?, J. Am. Chem. Soc. 121 (1999) 1992–1992.
[49] D. Huster, K. Gawrish, Investigation of lipid organization in biological membranes by two-dimensional nuclear overhauser enhancement spectroscopy, J. Phys. Chem. B 103 (1999) 243–251.
[50] G. Büldt, R. Wohlgemuth, The headgroup conformation of phospholipids in membranes, J. Membr. Biol. 58 (1981) 81–100.
[51] B.J. Gaffney, H.M. McConnell, Paramagnetic-resonance spectra of spin labels in phospholipids membranes, J. Magn. Res. 16 (1974) 1–30.
[52] K.M. Merz Jr., Molecular dynamics simulations of lipid bilayers, Curr. Opin. Struct. Biol. 7 (1997) 511–517.
[53] R.J. Gargiulo, G.J. Giotta, H.H. Wang, Spin-labeled analogs of local anesthetics, J. Med. Chem. 16 (1973) 707–708.
[54] G.J. Giotta, D.S. Chan, H.H. Wang, Binding of spin-labeled local-anesthetics to phosphatidylcholine and phosphatidylserine liposomes, Arch. Biochim. Biophys. 163 (1974) 453–458.

3.3 - ANESTÉSICOS LOCAIS: INTERAÇÃO COM MEMBRANAS DE ERITRÓCITOS DE SANGUE HUMANO, ESTUDADA POR RESSONÂNCIA MAGNÉTICA NUCLEAR DE ^{1}H E ^{31}P

ANESTÉSICOS LOCAIS: INTERAÇÃO COM MEMBRANAS DE ERITRÓCITOS DE SANGUE HUMANO, ESTUDADA POR RESSONÂNCIA MAGNÉTICA NUCLEAR DE ^{1}H E ^{31}P

Leonardo Fernandes Fraceto e Eneida de Paula*

Departamento de Bioquímica, Instituto de Biologia, Universidade Estadual de Campinas, CP 6109, 13083-970 Campinas – SP

e-mail: depaula@unicamp.br

LOCAL ANESTHETIC: INTERACTION WITH HUMAN ERYTHROCYTE MEMBRANES, AS STUDIED BY ^{1}H AND ^{31}P NUCLEAR MAGNETIC RESONANCE

Literature carries many theories about the mechanism of action of local anesthetics (LA). We can highlight those focusing the direct effect of LA on the sodium channel protein and the ones that consider the interaction of anesthetic molecules with the lipid membrane phase. The interaction between local anesthetics and human erythrocyte membranes has been studied by ^{1}H and ^{31}P nuclear magnetic resonance spectroscopy. It was found that lidocaine (LDC) and benzocaine (BZC) bind to the membranes, increase the mobility of the phospholipid's acyl chains protons, decrease the mobility and/or change the structure of the polar head groups. The results indicate that lidocaine molecules are inserted across the polar and liquid interface of the membrane, establishing both electrostatic (charged form) and hydrophobic (neutral form) interactions. Benzocaine locates itself a little deeper in the bilayer, between the interfacial glycerol region and the hydrophobic core. These changes in mobility or conformation of membrane lipids could affect the Na^{+-}channel protein insertion in the bilayer, stabilizing its to the inactivated state, thus causing anesthesia.

Keywords: local anesthetic; Nuclear Magnetic Resonance; erythrocyte membrane.

* e-mail: depaula@unicamp.br

INTRODUÇÃO

Anestésicos locais (AL) compreendem um grande número de moléculas, de diferentes estruturas químicas: amino-ésteres, amino-amidas, amino-cetonas, amidas, álcoois, tio-ésteres, tio-amidas, derivados de uréia, poliéteres, etc[1], capazes de bloquear a condução do estímulo nervoso. Na clínica, amino-amidas como a lidocaína e a bupivacaína são os mais usados. Embora os amino-ésteres sejam, em geral, mais potentes que as amino-amidas[2] e a tendência atual é a de desenvolver-se amino-amidas mais potentes, pelo fato de serem menos tóxicas e mais resistentes à hidrólise quando comparadas aos amino-ésteres[3].

Por serem moléculas anfifílicas, os anestésicos locais têm grande afinidade pela membrana celular[2]. Podemos classificar as teorias propostas para explicar os mecanismos de ação destes compostos em duas categorias: a que atribui o efeito anestésico à ligação na proteína canal de sódio voltagem-dependente de axônios e a que considera a interação dos anestésicos locais com os lipídios da membrana (conhecida como "hipótese do lipídio") como o mecanismo responsável pelas alterações na proteína canal de sódio, levando ao bloqueio da condução do estímulo nervoso.

Em nosso laboratório temos estudado a interação de anestésicos locais com membranas modelo, tendo em vista as alterações estruturais e dinâmicas provocadas pelos anestésicos na fase lipídica[4-8].

A literatura traz relatos da ação de anestésicos locais na diminuição da temperatura de transição de fases de lipídios, estudada por diferentes técnicas. Lee[9,10], utilizando calorimetria diferencial de varredura, registrou diminuição da T_C de vesículas de fosfatidilcolina causada pela partição da benzocaína, procaína, tetracaína, lidocaína e dibucaína, em concentrações iguais as necessárias para 50% de bloqueio na condução do estímulo nervoso.

O fato dos AL perturbarem o empacotamento dos fosfolipídios em membranas modelo e biológicas foi bastante estudado por experimentos de ressonância paramagnética eletrônica (RPE) e outras técnicas espectroscópicas

como ressonância magnética nuclear (RMN), infravermelho e fluorescência[5], trazendo enorme contribuição para o entendimento da interação AL / membrana.

Através da técnica de absorção no infravermelho Schöpflin e colaboradores[11] demonstraram a incorporação da dibucaína, procaína e dois outros AL em monocamadas de palmitoiloleil fosfatidilcolina, estudando as bandas de absorção dos compostos, entre 1400 e 1800 cm^{-1}. A combinação de estudos de infravermelho com pressão possibilitou a Auger e colaboradores demonstrarem que a tetracaína, incorporada em membranas de fosfatidilcolina, fosfatidil serina e biológicas, é expulsa da bicamada por aumento da pressão[12].

Os primeiros experimentos com RMN de hidrogênio (^{1}H-RMN) detectaram imobilização da molécula do anestésico local, quando intercalada na bicamada lipídica[13-17], efeito semelhante ao observado por RPE com análogos paramagnéticos dos AL[18,19] .

Ainda com ^{1}H-RMN vários trabalhos mostraram a interação da forma protonada e da forma neutra dos anestésicos locais[20-27] com membranas fosfolipídicas.

Em nosso laboratório temos estudado a interação de anestésicos locais com membranas lipídicas, através de técnicas de RMN, RPE e fluorescência[4,5,8]. Para os anestésicos locais do tipo amino-amida, lidocaína, mepivacaína, bupivacaína e etidocaína, o efeito diferencial dos anestésicos locais sobre regiões da bicamada monitoradas por diferentes sondas paramagnéticas, alterações nos tempos de relaxação longitudinal dos lipídios em presença de anestésicos locais e interações intermoleculares específicas entre hidrogênios dos AL e dos lipídios forneceram evidências sobre a localização destes no interior da bicamada[7,28].

Nakagawa e colaboradores[29,30] estudaram a interação de dibucaína com "ghosts" de eritrócito de porco utilizando ^{1}H-RMN e ^{31}P-RMN. Naquele trabalho observaram que a dibucaína interage com as membranas aumentando a mobilidade das cadeias acila e alterando a conformação da cabeça polar dos lipídios. Os autores mostraram assim, que a dibucaína se localiza entre a cabeça polar e as cadeias acila dos lipídios, sendo tal localização mantida por interações

eletrostáticas e hidrofóbicas. Segundo esses autores, essas mudanças na mobilidade ou conformação dos lipídios seriam de grande importância no efeito causado pelo AL ao redor da proteína canal de sódio, levando-a ao estado inativado.

Neste trabalho comparamos os efeitos causados por dois anestésicos locais (**Figura 1**): lidocaína - uma amino-amida - e benzocaína - um éster - em membranas de eritrócito humano, utilizando técnicas de ^{1}H-RMN e ^{31}P-RMN.

PARTE EXPERIMENTAL

Materiais e métodos

A água deuterada, o cloridrato de Lidocaína e a benzocaína usados nos experimentos foram adquiridos da Sigma Chem. Co. Todos os outros reagentes utilizados apresentavam grau analítico.

Preparo das membranas de "ghosts"

Bolsas com papa de hemácias foram obtidos do Hemocentro da Unicamp. As bolsas eram recentes - até 3 dias da data de coleta - e possuíam sorologia negativa para Chagas, Sífilis, AIDS e hepatite B. As hemácias foram ressuspensas em solução hipotônica (tampão fosfato 5mM, pH 8,0) e levadas à centrifugação (900 *x* g por 20 min., procedimento repetido por várias vezes até se observar a precipitação de membranas esbranquiçadas, os *"*ghosts*"* de eritrócitos, obtidas pela lise das células e extravasamento do seu conteúdo interno[31]. Essas membranas esbranquiçadas foram lavadas com tampão fosfato 50mM, pH 7,4 e estocadas em biofreezer (a –80 ^{o}C). Para os experimentos com RMN de fósforo o tampão fosfato 5mM foi substituído por tampão Tris.HCl 50mM, pH 7.4.

A determinação da concentração proteica foi feita utilizando o método de Lowry[32].

Determinação do coeficiente de partição dos AL entres "ghosts"/Tampão, por separação de fases

As membranas de eritrócito foram preparadas como descrito anteriormente. Alíquotas de solução estoque dos AL, 1mM de benzocaína e 3mM de lidocaína, em tampão fosfato, foram adicionadas à suspensão de membranas, de modo a

atingir leitura de absorção adequada a 284 nm (ε_M=15850) e 262 nm (ε_M=480), respectivamente para a BZC[8] e LDC[4]. Após ultracentrifugação (120.000 *x* g por 2h), determinou-se a concentração de anestésico livre no sobrenadante. A concentração de benzocaína e lidocaína na membrana foi calculada pela diferença entre a concentração do AL livre no sobrenadante e concentração inicial. Conhecendo os volumes da fase aquosa lipídica, o coeficiente de partição (P) foi calculado conforme a Equação 1.

$$P = (nm / Vm)/(na / Va) \quad (1)$$

Os valores de n*m* e n*a* representam o número de moles de soluto na fase membranar e aquosa, respectivamente; V representa volume. O volume da fase lipídica (Va) foi calculado assumindo-se uma densidade de 1g/mL para a fosfatidilcolina de ovo[4,33] .

Experimentos de ^{1}H-RMN e ^{31}P-RMN

As medidas foram realizadas em espectrômetro Bruker DRX500 (500 MHz para ^{1}H e 202 MHz para ^{31}P), no Instituto de Química da Universidade de São Paulo. Os espectros de hidrogênio e fósforo foram obtidos com janelas de 12 ppm e 100 ppm, respectivamente, em sondas de 5 mm. O número de aquisições no espectro de hidrogênio foi de 128 e no espectro de fósforo 6000.

Para medidas de ^{1}H-RMN os *"*ghosts*"*, preparados como descrito acima, foram ressuspensos em tampão fosfato 50mM pH 7,4, preparado em D_2O. A concentração de fosfolipídios utilizada nos experimentos foi 5mM, calculada a partir da relação molar proteína/lipídio de 1,1/1[34,35], assumindo que a porcentagem de fosfolipídios nos lipídios totais é de 56%[36] e tomando a massa molar média dos fosfolipídios (750) pela média ponderada da distribuição percentual dos mesmos na membrana de eritrócito[30].

Nas amostras de ^{31}P-RMN usamos concentrações de *"*ghosts*"* maiores (12mM) dada à baixa sensibilidade deste núcleo e tampão TRIS-HCl 50mM,

preparado em água desionizada. Utilizou-se um capilar de D_2O, selado, para sintonia do equipamento de RMN.

Para os experimentos de hidrogênio, adicionou-se o anestésico local ao *"*ghosts*"* na concentração de 3mM, enquanto nos experimentos de fósforo adicionou-se AL na concentração de 10mM. As medidas foram feitas à 30^{o}C.

RESULTADOS E DISCUSSÃO

Medidas do coeficiente de partição por separação de fases

Os valores de coeficiente de partição, determinados por separação de fases à temperatura ambiente, para o sistema *"*ghosts*"*/tampão foram de 303±105 (n=7) para a LDC e 287 ± 76 (n=7) para a BZC, em pH 7,4 .

Entre lipossomas multilamelares de fosfatidilcolina de ovo e água, os valores de P para a lidocaína e para benzocaína, em pH 7,4, são, respectivamente 76 [37] e 253[8].

Não foi encontrada na literatura descrição de valores de P entre membranas *"*ghosts*"*/água para os anestésicos estudados. Para o anestésico DBC o valor de P em *"*ghosts*"* de eritrócitos é de 375 ± 62[6], bem menor que o valor encontrado em lipossomas multilamelares de fosfatidilcolina (2240 ±1050)[4], mostrando que não é possível predizer o valor de P em membranas biológicas, pela simples comparação com os valores obtidos em membranas lipídicas. Enquanto a presença de proteínas faz diminuir consideravelmente a partição da dibucaína nas membranas de eritrócito, a lidocaína parece aumentar sua ligação a membrana e a benzocaína tem partição semelhante aquela observada em lipossomos. A maior partição da LDC entre *"*ghosts*"*/água indica haver interação entre o anestésico protonado e resíduos de aminoácidos das proteínas e/ou com lipídios carregados negativamente, da membrana do eritrócito. Já para a BZC, um

AL que não se protona em pH fisiológico[8], isto não aconteceu, levando a valores de coeficiente de Partição muito semelhantes, nos dois tipos de membrana, *"*ghosts*"* e vesículas de fosfatidilcolina de ovo.

^{1}H e ^{31}P RMN dos anestésicos e "ghosts"

Os espectros de ^{1}H-RMN dos AL e das membranas de *"*ghosts*"* podem ser vistos na Figura 2 e Figura 3. A Tabela 1 mostra as atribuições e deslocamentos químicos dos hidrogênios desses AL, cuja estrutura química encontra-se na Figura 1. Os espectros foram referenciados ao pico da água residual - em 4,8ppm - de forma a serem comparados com os experimentos em que se usou *"*ghosts*"*.

O espectro das membranas de *"*ghosts*"* apresenta grande similaridade aos descritos na literatura[29] e corresponde aos hidrogênios de lipídios e proteínas da membrana, além de uma pequena fração de proteínas residuais, dissolvidas no tampão mesmo após as repetidas lavagens das suspensões de *"*ghosts*"*. A contribuição dessas proteínas contaminantes ao espectro da suspensão de *"*ghosts*"* é muito pequena e pode ser desconsiderada[29]. No espectro existem picos bastante alargados, quando comparados com os espectros de anestésicos, dados a grande sobreposição de sinais (haja vista o grande número de núcleos de hidrogênios diferentes), aliada à pouca mobilidade dos núcleos em sistemas membranares[23,38]. Se compararmos os espectros da Figura 2A e 2C, observamos que nos espectros dos anestésicos (A) pode-se observar o acoplamento entre os hidrogênios vizinhos, que é perdido no espectro da suspensão de *"*ghosts*"* (C), justamente pela maior imobilização dos hidrogênios, neste último.

A atribuição de picos do espectro da suspensão de *"*ghosts*"* está de acordo com o descrito na literatura[29] e está mostrada na Tabela 2.

O espectro do sistema *"*ghosts*"*:LDC pode ser visto na Figura 2B. Através deste experimento concluímos que a molécula de lidocaína está inserida no interior das membranas, onde interage com lipídios e/ou com proteínas, visto que os picos observáveis de sua molécula estão alargados, isto é, imobilizados pela inserção

entre os componentes da bicamada. Com relação ao deslocamento químico, não foram encontradas variações maiores que 0,05 ppm nos picos atribuídos ao anestésico ou aos componentes da membrana.

O espectro obtido para o sistema *"*ghosts*"*:BZC pode ser visto na Figura 3B. O alargamento dos picos atribuídos à benzocaína, em relação aos do anestésico em água, mais uma vez indica a inserção do anestésico na bicamada. Com relação ao deslocamento químico, com a benzocaína ocorreram algumas alterações: de 0,17 ppm para o pico **a** (CH_3-et), 0,86 ppm para o pico **b** (CH_2-et) e 0,30 ppm para o pico **d** (Ar 2,6), indicando que houve uma grande mudança no ambiente químico dos núcleos da porção linear (CH_2-CH_3) e próximos ao grupamento éster da molécula do anestésico (Tabela 1).

As alterações no deslocamento químico dos hidrogênios da benzocaina, não observadas para a lidocaína, podem indicar uma inserção mais profunda da benzocaína no interior da bicamada lipídica (mudança no ambiente químico). De fato estudos em vesículas multilamelares de fosfatidilcolina de ovo, mostraram que a BZC se insere mais profundamente que a LDC na bicamada, distribuindo-se entre a região do glicerol e primeiros carbonos da cadeia acila dos fosfolipídios, diferentemente da LDC que estaria ancorada na cabeça polar dos lipídios[7,8]. Por medidas de tempo de relaxação longitudinal (T_1) em vesículas unilamelares de fosfatidilcolina de ovo mostramos que a LDC altera a mobilidade dos hidrogênios da cabeça polar dos lipídios, não tendo efeito pronunciado sobre aqueles do glicerol e primeiros carbonos da cadeia acila, onde a ordem da bicamada é máxima[7]. A maior liberdade de rotação dos hidrogênios da cabeça polar (região de maior mobilidade) poderia explicar a não observação de alterações no deslocamento químico dos hidrogênios da LDC (Tabela 1) inserida nesta porção da bicamada. Nestes sistema devida a não resolução e alargamento dos sinais do espectro de ^{1}H-RMN de "ghosts" nao se pode aplicar tal abordagem (medidas de T_1) nesse sistema, o mesmo acontecendo para medidas de efeito nuclear Overhauser (NOE) não são eficientes pois a relaxação dos hidrogênios leva a valores de NOE próximos a zero.

A partir dos valores de coeficiente de partição determinados para esses anestésicos no sistema *"*ghosts*"*/água calculamos a concentração destas no interior dos "ghosts", usando a Equação 1. Nas condições de ensaio (5 mM de "ghosts") 53% da LDC e 52% da BZC total adicionadas foram incorporadas à bicamada.

Tais dados mostram que as quantidades de anestésicos na membrana são praticamente as mesmas, ou seja, o efeito diferencial existente entre os dois anestésicos não se deve a quantidades diferentes na membrana e sim a diferenças na interação destes com as membranas.

Considerando a carga positiva parcial da LDC em pH 7,4, podemos imaginar que as moléculas de LDC apresentam interação em uma região mais superficial da bicamada (Figura 2B), devido ao alargamento espectral provocado pela imobilização dos hidrogênios não acompanhado de mudanças no deslocamento químico de seus hidrogênios. Já para a BZC ocorreu tanto uma mudança na mobilidade de seus hidrogênios (alargamento) ao inserir-se nos *"*ghosts*"*, quanto no deslocamento químico (ambiente químico), o que, aliado à sua carga neutra em pH fisiológico, justificaria uma inserção um pouco mais profunda no interior das bicamadas (Figura 3B).

Possivelmente a inserção mais superficial da LDC deva-se à grande fração de moléculas carregadas em pH 7,4[4] que podem ser estabilizadas por cargas de proteínas e/ou lipídios carregados negativamente como a fosfatidilserina, fosfatidilinositol e ácido fosfatídico; tal estabilização justificaria uma imobilização da molécula o que causaria um alargamento dos sinais dos picos da LDC.

Tais resultados estão de acordo com o perfil de inserção em vesículas multilamelares de fosfatidilcolina de ovo proposto por Pinto e colaboradores[8], onde a BZC se insere mais profundamente (região entre glicerol e primeiros carbonos da cadeia acila) que a LDC. A inserção preferencial da LDC, em região próxima ao grupamento fosfato e cabeça polar encaixa-se perfeitamente bem com as evidências de localização deste AL em lipossomas de fosfatidilcolina de ovo[7].

Para uma análise da região de interface entre a cabeça polar e o núcleo hidrofóbico da bicamada, foram realizados experimentos de ^{31}P-RMN. A Figura 4 mostra o espectro de ^{31}P dos fosfolipídios presentes na suspensão de *"ghosts"* em ausência (A) e presença dos anestésicos: lidocaína (B) e benzocaína (C).

No espectro dos *"ghosts"*, podemos verificar um perfil para o pico do fosfato que é típico de fases lamelares (bicamadas)[39,40], isto é, com um pico direito de alta intensidade e um "ombro" alargado em campo baixo. Este sinal anisotrópico reflete a orientação dos grupamentos fosfato dos fosfolipídios na bicamada. A medida do deslocamento químico anisotrópico, D.Q.A. (distância entre o pico de alta intensidade e o de campo baixo)[39] neste espectro foi de 35 ppm, o que está de acordo com os valores obtidos, em *"ghosts"*, por Wakita e colaboradores[29]. Na Figura 4, o pico isotrópico observado em 0 ppm reflete os fosfatos livres em solução (fosfolipídios e/ou fosfato inorgânico) ou grupamentos fosfatos presentes em proteínas fosforiladas da membrana dos *"ghosts"* [41] .

Os experimentos em presença de anestésicos locais foram realizados para observar possíveis mudanças no D.Q.A., que refletiriam mudanças na ambiência química dos grupamentos fosfato (mobilidade ou estrutura da cabeça polar dos lipídios) causadas pela inserção dessas moléculas na vizinhança do grupamento fosfato.

Os espectros de *"ghosts"* com LDC apresentam o mesmo perfil espectral mostrado na Figura 4A, indicando que a lidocaína não altera a organização lamelar dos lipídios para outro tipo de fase. No entanto, a medida de deslocamento químico anisotrópico na Figura 4B foi de 40 ppm, mostrando que as moléculas de lidocaína diminuem a mobilidade dos grupamentos fosfato, causando mudanças conformacionais na cabeça polar dos fosfolipídios o que, como nos dados de ^{1}H-RMN, indica que a LDC tem localização preferencial nas regiões mais superficiais das bicamadas. Este efeito pode estar ocorrendo devido à perda de interações eletrostáticas entre as cabeças polares de fosfolipídios adjacentes e aumento da ordem local (região do grupamento fosfato) pela inserção da lidocaína com conseqüente aumento no deslocamento químico anisotrópico. Efeito parecido foi descrito na literatura pela interação de dibucaína em vesículas multilamelares de

fosfatidilserina[42] e *"ghosts"*[29], onde a interação eletrostática entre as moléculas de dibucaína carregadas e os grupamentos fosfato, causaram diminuição na interação entre os fosfolipídios, gerando uma mudança conformacional na cabeça polar dos lipídios e aumento na ordem local, observada através de um aumento no deslocamento químico anisotrópico ^{31}P-RMN.

Em vesículas multilamelares de fosfatidilcolina de ovo, Boulanger e colaboradores[20] mostraram que a tetracaína, em sua forma protonada, causa uma alteração de até 8% o deslocamento químico anisotrópico do grupamento fosfato; segundo esses autores as cargas positivas das moléculas de tetracaína estabilizariam as cargas negativas dos grupamentos fosfatos dos lipídios, justificando o efeito no sinal do grupamento fosfato.

A variação de 14% no deslocamento químico anisotrópico provocado pela adição de lidocaína em pH 7,4, indica a ligação das moléculas de LDC protonadas aos grupamentos fosfato, levando a estabilização de cargas e causando alterações conformacionais na cabeça polar dos fosfolipídios[7] presentes na membrana de *"ghosts"*.

A medida de deslocamento químico anisotrópico para os *"ghosts"* em presença de benzocaína foi de 33 ppm, variação não significativa e que indica que este anestésico não causa alteração na cabeça polar dos lipídios, provavelmente por inserir-se em região mais profunda da bicamada, como evidenciado pelos dados de ^{1}H-RMN e resultados anteriores de RPE[8].

Um fato interessante é que houve um aumento no sinal isotrópico do fosfato na presença dos dois anestésicos (Figura 4). Este aumento pode ter sido causado, por ação de fosfolipases presentes no meio e que devido ao longo tempo dos experimentos, causariam o aparecimento de lisofosfolipídios e ácidos graxos livres, aumentando o sinal isotrópico do grupamento fosfato[41,43].

Wakita e colaboradores[29] encontraram, em membranas de *"ghosts"*, um aumento de 11ppm, ou seja, 32% no deslocamento químico anisotrópico dos grupamentos fosfato, em presença de dibucaína. Esse efeito da dibucaína, bem maior que o encontrado para a LDC (14%) reflete o volumoso anel quinolínico da dibucaína, que deve causar um maior espaçamento entre os fosfolipídios

adjacentes na cabeça polar ao inserir-se naquela região da bicamada, como a lidocaína[29]. Estudos de modelagem molecular mostram que a LDC apresenta uma área de 433 $Å^2$ enquanto para a DBC este valor é de 617 $Å^2$ [1].

Um fato que deve ser levado em consideração é que grupos fosfato apresentam cargas negativas que podem estabilizar cargas positivas dos anestésicos locais. Há na literatura, vários relatos da competição de AL com íons cálcio, pela interação com grupamentos fosfato de vesículas lipídicas[40, 44]. Desta forma, sabendo que a BZC não apresenta carga líquida em pH 7,4 justifica-se o fato deste AL não ter efeito sobre a cabeça polar, pois não tem como realizar interação eletrostática. Já a LDC (pKa 7,9)[4], que em pH fisiológico apresenta mais da metade das moléculas com carga positiva, possui efeito no sinal do grupamento fosfato. Se considerarmos que a dibucaína (pKa 8,3)[4] tem, em pH 7,4, ainda maior proporção de moléculas na forma protonada que a LDC, encontramos outro fator que justifica seu maior efeito sobre os grupamentos fosfato, visto que os coeficientes de partição destes três anestésicos tem valores muitos próximos, nos "ghosts": 303±101 (LDC), 287±76 (BZC) e 375±62 (dibucaína)[6].

Um estudo anterior de nosso laboratório utilizando vesículas unilamelares de fosfatidilcolina de ovo e utilizando técnica de ^{1}H-RMN mostrou, por determinação dos tempos de relaxação longitudinal que a lidocaína desprotonada localiza-se em uma região próxima ao grupamento fosfato da cabeça polar dos fosfolipídios[7]. Este fato reforça ainda mais a idéia de que moléculas de LDC com carga encontram-se na região próximas aos grupamentos fosfato dos fosfolipídios, estabelecendo interações eletrostáticas que causam um grande efeito nesta região.

É importante destacar que esta localização é a preferencial, isto é, onde ela deve se encontrar, na maior parte do tempo. No entanto não podemos esquecer que estas moléculas anfifílicas, distribuem-se rapidamente entre a membrana biológica e a fase aquosa[5], ou seja, apresentam um equilíbrio dinâmico, além da inserção preferencial no interior das bicamadas. Esta localização, determinada pelas interações do AL com os fosfolipídios deve ser determinante

para a ação específica do AL em sítio (s) de ligação, na proteína canal de sódio[45,46].

CONCLUSÃO

Os resultados aqui relatados mostram que lidocaína e benzocaína interagem em regiões diferentes das membranas de eritrócitos humanos, e que estes dados estão de acordo com experimentos prévios, com lipossomos de fosfatidilcolina de ovo[7,8], em que a LDC insere-se próximo a cabeça polar, enquanto a BZC interage com regiões mais profundas da membrana de *"ghosts"*. A localização destes anestésicos no interior das membranas biológicas pode ser um fator determinante para a interação destes com sítios hidrofóbicos na proteína canal de sódio[45 ,46].

AGRADECIMENTOS

Os autores agradecem à FAPESP pelo auxílio financeiro (Proc. 96/01451-9) e bolsa de doutorado (L. F. Fraceto, Proc. 00/00362-0); ao CNPq pela bolsa de produtividade em pesquisa (E. de Paula, Proc. 300197/95-0) e a Dra S. Schreier e Instituto de Química/USP pelo uso do equipamento de RMN.

REFERÊNCIAS

1. Gupta, S. P.; *Chem. Rev.* **1991**, *91*, 1109.
2. Covino, B. G.; Vassalo, H. G. Em *Local Anesthetics: mechanisms of action and clinical use***;** Grune and Stratton: New York, 1976, cap. 3.
3. De Jong, R. H. Em *Local Anesthetics;* Thomas, C.C.,ed., Springfield: Illinois, 1994, cap. 2.
4. de Paula, E.; Schreier, S.; *Biochim. Biophys. Acta* **1995,** *1240*,25.
5. de Paula, E.; Schreier, S.; *Braz. J. Med. Res*. **1996**, *29***,** 877.
6 . Malheiros, S. V. P.; Meirelles, N. C.; de Paula, E. ; *Biophys. Chem.* **2000**, *83*, 89.
7. Fraceto, L. F.; Pinto, L. M. A.; Franzoni, L.; Braga, A. A. C.; Spisni, A.; Schreier, S.; de Paula, E.; *Biophys. Chem*. **2002**, *99*, 229.
8. Pinto, L. M. A.; Yokaichiya, D. K.; Fraceto, L. F.; de Paula, E.; *Biophys. Chem.* **2000**, *87*, 213.
9. Lee, A. G.; *Biochim. Biophys. Acta* **1976,** *448***,** 34.
10. Lee, A. G.; *Biochim. Biophys. Acta* **1978,** *514*, 95.
11. Schopflin, M.; Fingeli, U. P.; Perlia, X.; *J. Am. Chem. Soc.* **1987**, *109*, 2375.
12. Auger, M.; Jarrel, H. C.; Smith, I. C. P.; Wong, P. T. T.; Siminovitch, D. J.; Mantsch, H. H.; *Biochemistry* **1987**, *26*, 8513.
13. Hauser, H.; Dawson, R.M.C.; *Biochem. J.* **1968**, *109*, 909.
14. Cerbon, J.; *Biochim. Biophys. Acta* **1972**, *290*, 57.
15. Darke, A.; Finer, E. G.; Flook, A. G.; Phillips, M. C.; *J. Mol. Biol.* **1972,** *63*, 265.
16. Finer, E. G.; Flook, A. G.; Hauser, H.; *Biochim. Biophys. Acta* **1972**, *260*, 49.
17. Lee, A. G.; Birdsall, J. M.; Levine, Y. K.; Metcalfe, J. C.; *Biochim. Biophys. Acta* **1972**, *255*, 43.
18. Gargiulo, R. J.; Giotta, G. J.; Wang, H. H.; *J. Med. Chem.* **1973**, *16*, 707.
19. Giotta, G. J.; Chan, D. S.; Wang, H. H.; *Arch. Biochim. Biophys.* **1974**, *163*, 453.
20. Boulanger, Y.; Schreier, S.; Leitch, L. C.; Smith, I. C. P.; *Can. J. Biochem.* **1980**, *58* 986.

21. Boulanger, Y.; Schreier, S.; Smith, I. C. P.; *Biochemistry* **1981**, *20*, 6824.
22. Westman, J.; Boulanger, Y.; Ehrenberg, A.; Smith, I. C. P.; *Biochim. Biophys. Acta* **1982**, *685***,** 315.
23. Kuroda, Y. ; Kitamura, K.; *J. Am. Chem. Soc.* **1984**, *106*, 1.
24. Kelusky, E. C.; Smith, I. C. P.; *Can. J. Biochem. Cell. Biol.* **1984**, *62*, 178.
25. Kuroda, Y.; Fujiwara, Y.; *Biochim. Biophys. Acta* **1987**, *903***,** 395.
26. Yokono, S.; Ogli, K.; Miura, S.; Ueda, I.; *Biochim. Biophys. Acta* **1989**, *982*, 300.
27. Wakita, M.; Kuroda, Y.; Fujiwara, Y.; Nakagawa, T.; *Chem. Phys. Lipids* **1992**, *62*, 45.
28. Fraceto, L. F.; *Tese de Mestrado*, Universidade Estadual de Campinas, Campinas/SP, **2000**.
29. Wakita, M.; Kuroda, Y.; Nakagawa, T.; *Chem. Pharm. Bull.* **1992**, *40*, 1361.
30. Kuroda , Y.; Wakita, M.; Nakagawa, T.; *Chem. Pharm. Bull.* **1994**, *42*, 2418.
31. Dodge, J. R. C.; Mitchell, R. H.; Hanaban, D. J.; *Arch. Biochem. Biophys.* **1963**, *100*, 119.
32. Lowry, O. H.; Rosenberg, N. J.; Farr, A. L.; Randall, R. J.; *J. Biol. Chem.* **1951**, *193*, 265.
33. Lissi, E.; Bianconi, M. L.; Amaral, A. T.; de Paula, E.; Blanch, L. E. B.; Schreier, S.; *Biochim. Biophys. Acta* **1990**, *1021*, 46.
34. Dodge, J. R. C.; Mitchell, R. H.; Hanaban, D. J. *Arch. Biochem. Biophys.* **1963**, *100*, 119.
35. Warren, R. C. *Physics and achitecture of cell membranes;* Adam-Hilger: Bristol, 1987.
36. Sato, T.; Fujii, T.; *Chem. Pharm. Bull.* **1971**, *19*, 377.
37. Malheiros, S. V. P, Comunicação pessoal.
38. Holte, L. L.; Gawrisch, K.; *Biochemistry* 1997, *36*, 4669.
39. Seelig, J.; *Biochim. Biophys. Acta* **1978**, *515*, 105.
40. De Kruijff, B.; van den Besselaar, A. M. H. P.; Cullis, P. R.; van den Bosch, H.; van Deenen, L. L. M.; *Biochim. Biophys. Acta* **1978**, *514*, 1.
41. van Meer, G.; De Krujiff, B.; Op den Kamp, J. A. F.; van Deenen, L. L. M.; *Biochim. Biophys. Acta* **1980**, *596*, 1.

42. Cullis, P. R.; Verkleij, A. J.; Ververgaert, P. H. J. Th.; *Biochim. Biophys. Acta* **1978**, *513*, 11.

43. Verkleij, A. J.; Zwasl, R. F. A.; Roelofsen, B.; Comfurius, P.; kastelijn, D.; van Deenen, L. L. M.; *Biochim. Biophys. Acta* **1973**, *323*, 178.

44. Cullis, P. R.; Verkleij, A. J.; *Biochim. Biophys. Acta* **1979**, *552*, 546.

45. Ragsdale, D. S.; McPhee, J. C.; Scheuer, R.; Catterall, W. A.; *Science* **1994**, *265*, 1724.

46. Ragsdale D. S.; McPhee J. C.; Scheuer, R.; Catterall, W. A.; *Proc.Natl.Acad.Sci.USA* **1996**, *93*, 9270.

Tabela 1**: Atribuição e deslocamentos químicos dos hidrogênios das moléculas de LDC e BZC. Os valores com asteriscos não foram obtidos por motivo de sobreposição espectral**

Pico	Deslocamento químico em água (ppm)		Deslocamento químico em presença de "ghost" (ppm)	
	LDC	BZC	LDC	BZC
a	1,38	1,40	**1,38**	**1,23**
b	2,26	4,38	*	**3,52**
c	3,40	6,89	**3,41**	*
d	4,30	7,93	*	**7,63**
e	7,28	-	**7,27**	-

Tabela 2**: Atribuição e deslocamento químicos dos hidrogênios das membranas de *"ghosts"***

Deslocamento químico (ppm)	**Característica do pico**	Atribuição
0,9	Alargado	hidrogênios CH_3 dos lipídios, colesterol e proteínas.
1,3	Alargado	hidrogênios $(CH_2)_n$ da cadeia acila dos lipídios
2,2	Alargado	hidrogênios N-acetil, dos resíduos de açúcares e proteínas.
3,3	Estreito	hidrogênios dos grupos colina $(N^+(CH_3)_3)$ da cabeça polar dos lipídios
6,8 a 8,4	Alargado	hidrogênios aromáticos, dos aminoácidos das proteínas de membranas

Legenda das Figuras

Figura 1: Estrutura química dos anestésicos locais

Figura 2: Espectro de ^{1}H-RMN da: A) LDC (3mM); B) "ghosts":LDC (5mM:3mM); C) suspensão de membranas de *ghosts* (5mM), em pH 7,4 e 30^{o}C. Espectro referenciado ao sinal da HDO residual (4,8ppm), 500MHz. Os picos da LDC estão identificados por letras, os picos marcados com asteriscos estão sobrepostos aos picos das membranas

Figura 3: Espectro de ^{1}H-RMN da: A) BZC (3mM); B) "ghosts":BZC (5mM:3mM); C) suspensão de membranas de "ghosts" (5mM), em pH 7,4 e 30^{o}C. Espectro referenciado ao sinal da HDO residual (4,8ppm), 500MHz. Os picos da BZC estão identificados por letras, os picos marcados com asteriscos estão sobrepostos aos picos das membranas

Figura 4: Espectro de ^{31}P-RMN de suspensão de: A) "ghosts" (12mM); B) "ghosts" em presença de LDC; C) "ghosts" em presença de BZC. Tampão TRIS-HCl 50mM, pH 7,4. 202 MHz e 30^{0}C

	Estrutura
LDC	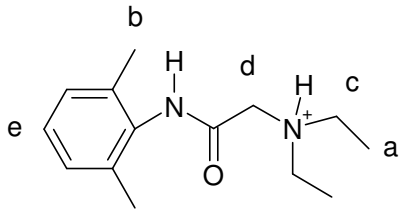
BZC	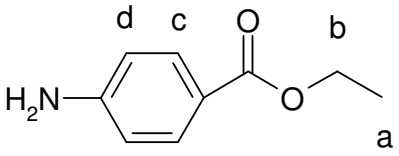

Figura 1

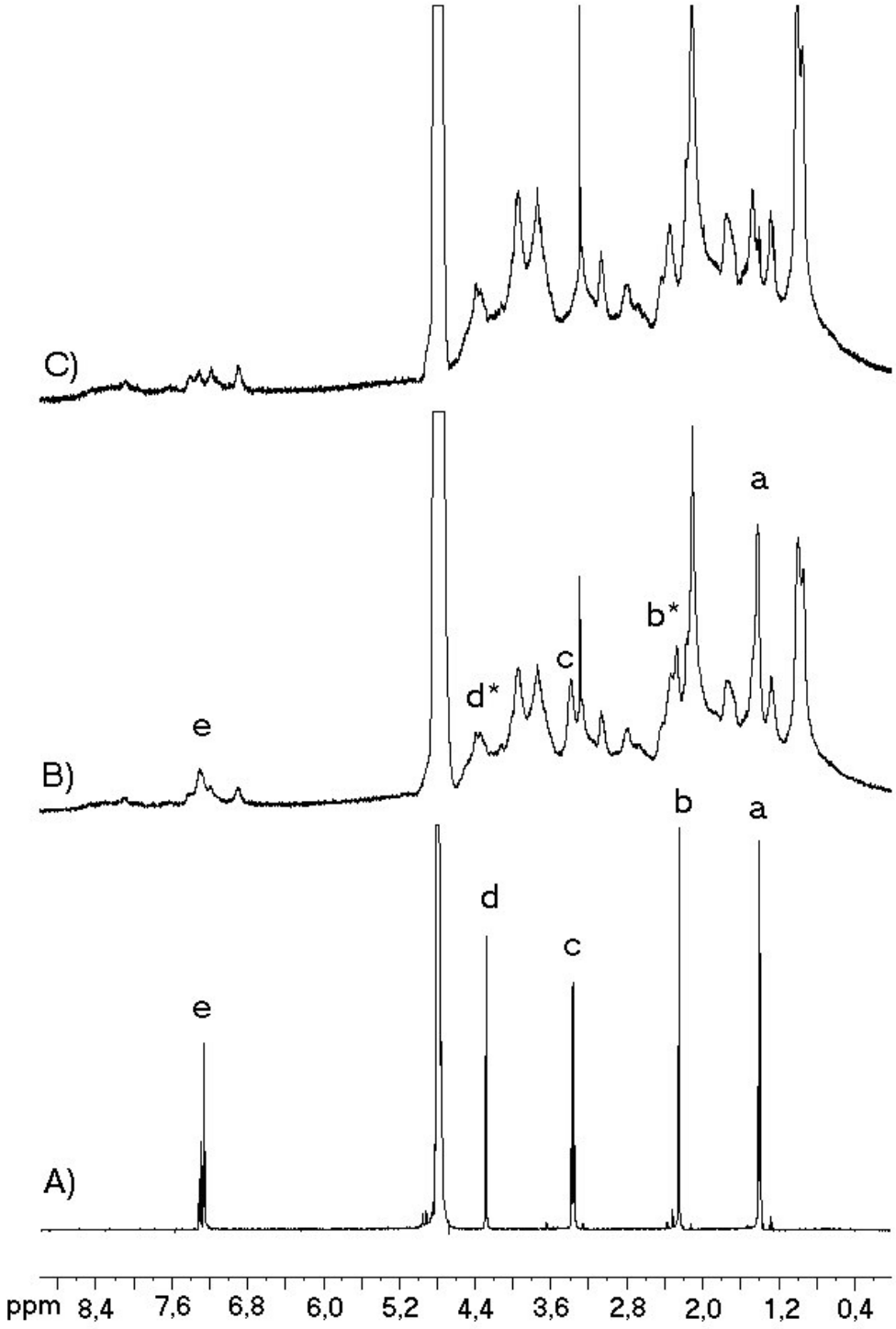

Figura 2

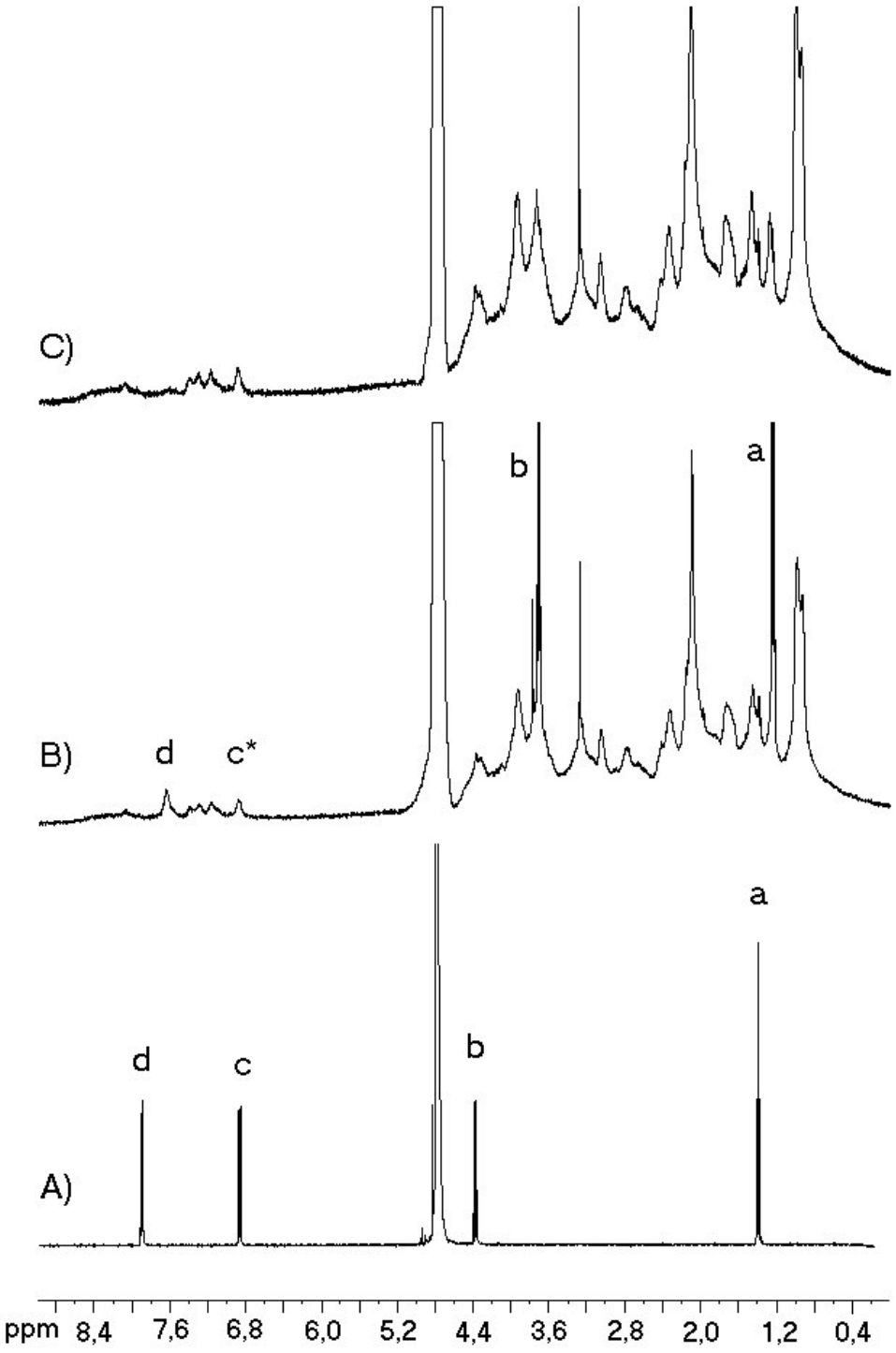

Figura 3

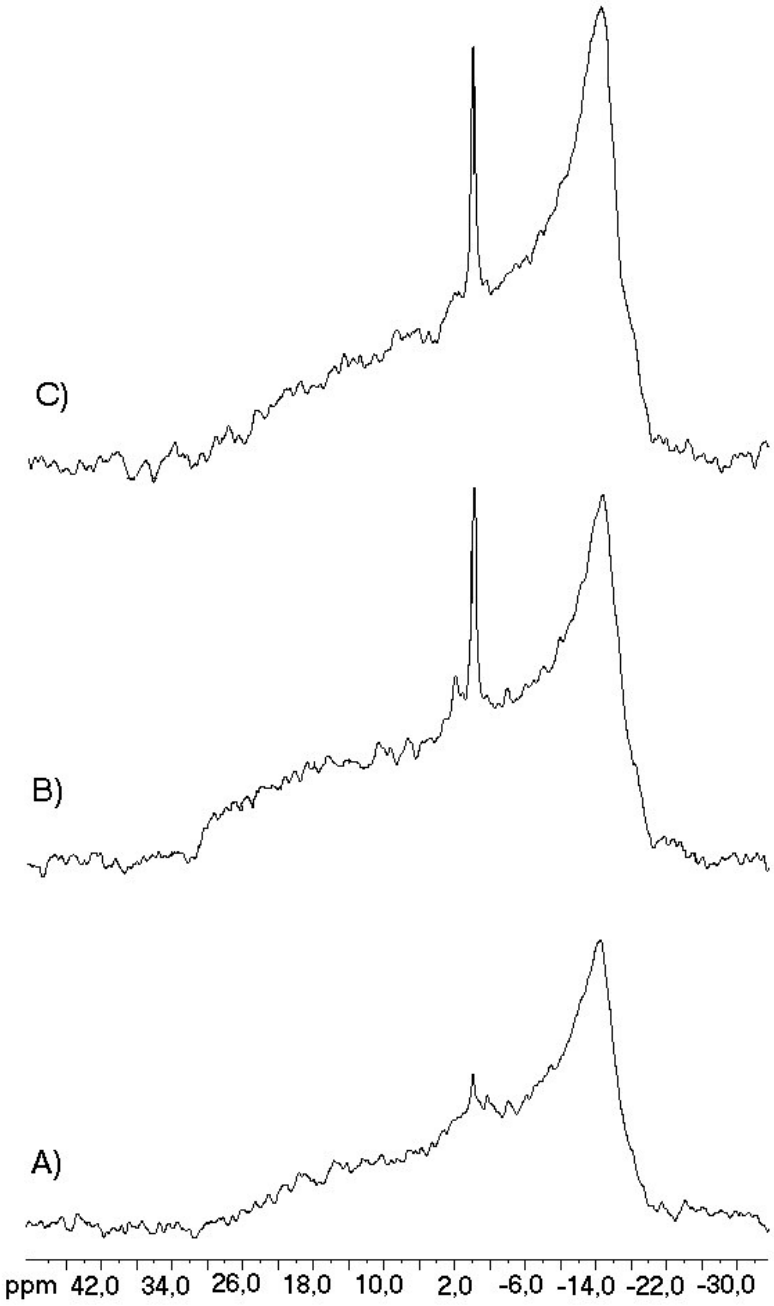

Figura 4

3.4 – SELECTIVE INTERACTION OF LOCAL ANESTHETICS WITH A PEPTIDE DERIVED FROM THE VOLTAGE-GATED Na^+ CHANNEL. A NMR STUDY

SELECTIVE INTERACTION OF LOCAL ANESTHETICS WITH A PEPTIDE DERIVED FROM THE VOLTAGE-GATED Na^+ CHANNEL. A NMR STUDY.

Leonardo Fernandes Fraceto [1,2], Clóvis R. Nakaie [3], Alberto Spisni [2,4], Eneida de Paula[1] & Thelma A. Pertinhez [2 *]

[1] Department of Biochemistry, Institute of Biology, State University of Campinas, Campinas, Brazil

[2] BioNMR Lab, Center of Molecular and Structural Biology, LNLS, Campinas, Brazil.

[3] Departament of Biophysics, Federal University of São Paulo, Brazil.

[4] Sect. Chemistry and Structural Biochemistry, Department of Experimental Medicine, University of Parma, Parma, Italy.

***** To whom correspondence should be addressed: National Synchrotron Light Laboratory (LNLS), PO Box 6192, 13084-971, Campinas, São Paulo, Brazil. Phone: +55 (19) 3287-4520; Fax: +55 (19) 3287-7110; e-mail: thelma@lnls.br

ABSTRACT

The solution structure of the peptide *p*IV/S4-S5, KGIRTLLFALMMSLPALFNIG-NH_2, 1644-1664, encompassing the cytoplasmic linker that connects the S4-S5 helices in domain IV of the human brain voltage-gated Na^+ channel, has been studied by circular dichroism (CD) and nuclear magnetic resonance (NMR) spectroscopy. Its interaction with two local anesthetics (LA): lidocaine (LDC), an amine-amide that ionizes at physiologic pH and benzocaine (BZC), a non ionizable local anesthetic, has been evaluated by Diffusion Ordered Spectroscopy (DOSY) and heteronuclear ^{15}N-HSQC experiments. The peptide exhibits an α-helical structure extending over most of its length with a bend at the proline position. In the central part of the α-helix it is evident it possesses an amphypathic nature. The DOSY experiments indicate that the LA interact with the peptide and that BZC displays a higher affinity than LDC. As judged by the chemical shift variations, while BZC affects residues L^{1653}, M^{1655} and S^{1656}, LDC perturbs primarily the hydrophobic residues close to the N-terminus (I^{1646}, L^{1649}) and to the C-terminus (A^{1659}, L^{1660}). These differences in affinity and site of interaction can be explained on the basis of the physico-chemical properties of the two local anesthetics. In fact, BZC, being smaller and more hydrophobic is expected to access more efficiently some of the side chains packed in the peptide α-helical structure. Overall we suggest that the ability of LA to bind to selected residues in the IV/S4-S5 linker may explain their local anesthesia effect. In fact, those specific interactions might stabilize the Na^+ channel inactivated state by interfering with the membrane internalization of the S4 helix, necessary to switch back to the open state.

Keywords: Voltage-gated Sodium Channel, Peptide, Local Anesthetics, Benzocaine, Lidocaine, Nuclear Magnetic Resonance.

INTRODUCTION

Voltage-gated Na^+ channels are responsible for the initiation and propagation of action potentials in a variety of excitable cells (Catterall, 1992; Fozzard, 1996; Marban et al., 1998). In response to membrane depolarization the Na^+ channels open and allow the influx of sodium ions into the cells. Sodium channels are concentrated in axons and muscle and they have an architecture similar to the K^+ and Ca^{2+} channels consisting of α and β subunits. The α-subunit (260 kDa) is composed of four homologous domains (I-IV), each containing six transmembrane segments (S1-S6) (Catterall, 1992; Fozzard, 1996; Marban et al., 1998). During maintained depolarization, the channels switch, on a millisecond time scale, to an inactivated non-conducting state and re-polarization of the membrane is required for recovery from this inactivation (Armstrong, 1977). The fast inactivation gating of the Na^+ channel has been resolved in some detail. The Ile, Phe, Met sequence, forming the IFM motif in the intracellular linker between domain III and domain IV, is thought to be a part of the "inactivation particle" (West et al., 1992) and to interact with the S4-S5 linker within domains III and IV (Smith, 1997; McPhee et al., 1998).

LA act by binding to the Na^+ channel, inhibiting Na^+ uptake and blocking the nervous impulse. Many LA are ionizable amines and both the charged and uncharged forms are thought to be relevant for the mechanism of anesthesia. In fact, it has been proposed that while the uncharged form is the main species, being ideal to cross the cell membrane, the binding to a specific site on the channel, that triggers the anesthetic effect, would be achieved by the protonated form (Ritchie, 1966; Narahashi & Yamada, 1969; Frazier, 1970). Nevertheless, some local anesthetics are non-ionizable compounds (e.g. benzocaine, benzyl alcohol), thus suggesting that a more accurate mechanistic model is required to explain their effectiveness.

Along the years, much work has been devoted to describe the molecular mechanism associated to LA pharmacological activity (Patton et al., 1992; Zamponi, 1994; Ragsdale et al., 1994; Ragsdale et al., 1996; Yarov-Yarovoy, 2002). The first mapping of LA binding sites on Na^+ channels revealed that four residues, in the middle of segment IV/S6, are critical (Ragsdale et al., 1994). Further studies suggested that, particularly when

Na^+ channels are in their inactivated state, two additional residues in the middle of segment I/S6 are aligned in close proximity with the tertiary amine moiety of the LA (Wang, 1998; Nau et al., 1999). Interestingly, the binding of LA is channel state dependent, being favored preferentially when the channel is in its inactivated state (Hille, 1977). In addition, the residues in the Pro region, located in the S5-S6 linker of both IV/S6 and I/S6 which control the ion selectivity of Na^+ channels, may be involved in the LA binding as well (Sunami et al., 1997).

Recently, Miyamoto and coworkers (Kuroda et al., 1996; Kuroda et al., 2000; Miyamoto et al., 2001a; Miyamoto et al, 2001b) have determined the structure, in sodium dodecylsufate (SDS) micelles, of a peptide encompassing portion of the cytoplasmic linker IV/S4-S5 from human brain Na^+ channels: Ac-TLLFALMMSLPALFNIGLL-NH_2; 1648-1666. The study shows that the peptide presents mainly a hydrophobic α-helical region between residues L^{1650}-S^{1656} and a β-turn starting at P^{1658}. In addition, the authors suggest that the inactivation gate is partly controlled by the interaction between the hydrophobic cluster on IV/S4-S5, formed by residues F^{1651}, $MM^{1654-1655}$, L^{1657} and A^{1659}, and the III-IV linker, specifically residues $IFM^{1488-1490}$, $YY^{1497-1498}$ and M^{1501}, probably through the interaction of antiparallel α-helices.

To obtain more insights on this molecular model, we have determined the NMR-derived 3D solution structure of the peptide *p*IV/S4-S5: KGIRTLLFALMMSLPALFNIG-NH_2, 1644-1664. The peptide encompasses the entire linker between helices S4 and S5 in domain IV of the human brain Na^+ channel (Figure 1). In addition, using Diffusion Ordered Spectroscopy (DOSY) and heteronuclear ^{15}N-^1H NMR we have studied its interaction with two local anesthetics: lidocaine (LDC), an amine-amide LA ionizable at physiologic pH, and benzocaine (BZC) an uncharged local anesthetic (Figure 2).

MATERIALS AND METHODS

The LA LDC and BZC nave been obtained from Sigma Chemical Co (St. Louis, MO). All other reagents were of analytical grade.

Peptide Synthesis Purification and Characterization

The peptide: KGIRTLLFALMMSLPALFNIG-NH_2 (*p*IV/S4-S5) was synthesized manually accordingly to the standard t-Boc/Bzl strategy (Barany, 1980; Atherton, 1989). *p*-methylbenzhydrylamine-resin (0.79 mmol/g) was used as the solid support and the following side-chain protecting groups were used: 2-Cl-benzyloxycarbonyl (Lys), p-toluenosulphonyl (Arg) and benzyl (Thr and Ser). The α-amine group deprotection and neutralization steps were performed in 30% (v/v) trifluoroacetic acid/dichoromethane for 30 min and in 10% (v/v) *N*,*N* -diisopropylethylamine/dichoromethane for 10 min. The coupling reaction was carried out with the acylating agents 2-(benzotriazol-1-yl)-1,1,3,3-tetramethyluronium tetrafluoroborate/N_1-hydroxybenzotriazole/*N*,*N* -diisopropylethylamine in a three fold excess condition over the amount of resin-bound amine groups. Cleavage of peptide from the resin was done in fluoridric acid:*o*-cresol:dimethylsulfide (9:0.5:0.5) at 0ºC, for 90 min. The resin was rinsed with ethyl acetate and peptide was extracted with 5% acetic acid and lyophilized.

The peptide purification was carried out on a Waters 510 HPLC instrument with a Vydac C_{18} semi-preparative column, using 0.1% trifluoroacetic acid /H_2O as solvent A and 0.08%TFA/60% acetonitrile (ACN)/H_2O, as solvent B.

Linear gradient ranging from 25 to 65% of B was applied over a period of 2h. The homogeneity of the purified peptide was characterized by analytical HPLC (Waters), electrospray LC/MS mass spectrometry (Micromass), m/z 2307 (average) and amino acid analysis (Biochrom 20 Plus, Amersham-Biosciences).

Circular Dichroism experiments

Circular Dichroism (CD) measurements were carried out on a Jasco J-810 spectropolarimeter equipped with a Peltier unit. The Far UV CD spectra were acquired using quartz cells of 0.01 and 0.02 cm path length. The wavelength range 190-250 nm and

all measurements were carried out at 20°C. Four scans were averaged for each sample and the blank spectra were subtracted. The observed optical activity is reported as the mean residue molar ellipticity, [θ] (deg.cm^2.dmol^{-1}).

The samples were prepared by dissolving the lyophilized peptide either in pure water or in the SDS or TFE water mixtures, at variable molar ratio, to a final peptide concentration of 50 μM. The pH was adjusted to 7.4 with small aliquots of NaOH and HCl throughout all measurements.

NMR experiments

Sample for NMR experiments were prepared by dissolving the peptide in H_2O:TFE-d_3 (70:30 %) to yield a concentration of 1.0 mM, pH 4.1. LDC or BZC were added directly to the NMR sample to reach a final LA:*p*IV/S4-S5 molar ratio of 1:1. The ^{1}H-NMR experiments were carried out on a Varian Inova 600AS spectrometer operating at 599.683 MHz for ^{1}H, at 20 °C. The proton chemical shifts were referenced to 4,4-dimethyl-4-silapentane-1-sulfonate, DSS (0.00 ppm). Sequential assignments were achieved by standard procedures (Wüthrich, 1986) using COSY (Nagayama et al., 1980), TOCSY (Griesinger, 1988) with 85 ms mixing time and spin-lock field of 10 kHz, NOESY (Bodenhausen et al., 1984) with 200 and 400 ms mixing times (States et al., 1982). The spectra width was typically 8000 Hz and, 648 τ_1 increments were recorded with 64 transients of 2K complex points for each free induction decay. The ^{15}N-HSQC (heteronuclear single quantum correlation) spectra were acquired using 128 increments and 32 transients with 1K of complex points. The spectra width was 2200 Hz and 6000 Hz for ^{15}N e ^{1}H dimensions, respectively.

Data were processed on a Silicon Graphics Octane2 workstation, using the FELIX NMR 2000 Software (Accelrys Inc., San Diego, CA.). Prior to Fourier transformation, the time domain data were zero-filled in both dimensions, to yield a 8K x 2K data matrix. When necessary, a fifth-order polynomial baseline correction was applied after transformation and phasing.

To obtain the inter-proton distances, cross-peaks volumes from the 200 ms NOESY spectrum were calibrated with respect to the cross-peak volume of the well-defined

geminal β-protons that correspond to the distance of 1.8 Å. The resulting inter-proton distance constraints were classified as strong (1.8-2.5 Å), medium (1.8-3.5 Å) and weak (1.8-5.0 Å). In all cases the lower bounds were taken to be the sum of the van der Waals radii (1.8 Å) for the interacting protons. Upper distance restraints involving non stereo-specific assigned methylenes, aromatic and methyl protons were replaced by appropriated pseudo-atoms (Wüthrich, 1986). The *p*IV/S4-S5 ^{1}H resonance assignment has been deposited to BioMagResBank (access number 5837).

To investigate the interaction between LA and the *p*IV/S4-S5 peptide, ^{15}N-HSQC and DOSY have been used. In this case, the NMR experiments were carried out on a Varian Inova 500AS spectrometer operating at 499.783 MHz for ^{1}H, 128 transients, at 20 ^{o}C. ^{15}N-HSQC spectra were collected as described above with increasing anesthetic concentrations: 0.00, 0.25, 0.50, 0.75 and 1.0 mM of local anesthetic.

The DOSY experiments were run with the BPPSTE (bipolar pulse pairs stimulated echo) (Johnson Jr, 1999). The duration of the total diffusion-phase encoding gradient pulse was 0.002 sec, diffusion delay 0.05 sec and the minimum gradient strength was set to 0.3 Gauss/cm. The diffusion coefficients were measured in the absence and in the presence of local anesthetic, at a 1:1 LA:*p*IV/S4-S5 molar ratio.

DOSY data analysis

For both LA the fraction bound to the peptide was measured as described in the literatute (Waldeck et al., 1997; Wimmer et al., 2002) where the bound and free LA undergo fast exchange on the diffusion time scale, and therefore, the observed LA diffusion coefficient, $D_{free+bound}$, is the weighted average of the free solution, D_{free}, and *p*IV/S4-S5 bound, D_{bound}, values (Eqn. 1).

$$D_{free+bound} = (1-f_{bound}).D_{free} + f_{bound}.D_{bound} \qquad \text{(Eqn.1)}$$

where $f_{free} + f_{bound} = 1$. Rearranging Eqn. 1 we got:

$$f_{bound} = (D_{free} - D_{free+bound}).(D_{free} - D_{bound})^{-1} \quad \text{(Eqn. 2)}$$

where f_{free} and f_{bound} are, respectively, the fractions of free LA and LA bound to *p*IV/S4-S5; D_{bound} is the diffusion coefficient of the complex and D_{free} that of the free LA.

The *p*IV/S4-S5 diffusion coefficient was almost unaffected upon complexation. D_{free} of LA was measured, in the absence of *p*IV/S4-S5. It was assumed that the diffusion coefficient of the LA bound to the peptide is the same of *p*IV/S4-S5 measured for the LA/*p*IV/S4-S5 solution.

Molecular Modeling

The 3D structure was determined using the DYANA software (Güntert et al., 1998). Each round of refinement started with 20 random conformers, and the 10 models with the lowest target function were used to analyze constraint violations and to assign additional NOE constraints, to be included in the subsequent calculation. This process was repeated until all violations were eliminated. In the final round of refinement, a total of 100 structures were calculated and the 40 conformers with the lowest target function were considered for further analysis. After simulated annealing, the 40 structures, characterized by a target function smaller than 1 $Å^2$, and by distance violation not larger than 0.2 Å, were energy minimized with the Consistent Valence Force Field (Morse and Lennard-Jones potentials, coulombic term) by steepest descents and conjugated gradients, using several thousands interactions, until the maximum derivative was less than 0.001 Kcal/mol.Å. All calculations were carried out on a Silicon Graphics Octane2 Workstation, using the DISCOVER (Accelrys, Inc., San Diego, CA.) software implemented in the INSIGHT II package.

The quality of the final structures was analyzed on the basis of the root mean square deviation (r.m.s.d.) of the backbone and by the PROCHECK-NMR program (Laskowski et al., 1996).

RESULTS AND DISCUSSION

pIV/S4-S5 structure analysis

Figure 3 shows the CD spectrum of the peptide *p*IV/S4-S5 in water, pH 7.4. The negative band at 203 nm is indicative of a predominant random conformation. Nonetheless, the weak negative band in the 220-225 nm region may suggest the presence of some helical elements. In fact, the analysis of the spectra using according to Chen and coworkers (Chen et al., 1974) indicates that the helix content in these experimental conditions is 14 %. When the peptide is in the presence of TFE or of SDS micelles, the shift of the negative band at 203 nm to 208 nm and the concomitant increase of intensity of both the negative band at 222 nm and the positive band at 196 nm, clearly indicate an increase of α-helix secondary structure. The TFE titration, as evidenced by the variation of the intensity of the 220 nm band, Figure 3 – *inset*, shows that the increase of helical content stabilizes above 15% TFE. The analysis of these spectra indicates that, in TFE, the peptide acquire a maximum α-helix content of 43%. A similar behavior is observed in the presence of SDS micelles (data not shown). In this case, in 20 mM SDS the α-helical content is 47%.

The conformational plasticity of this region of the Na^+ channel has been reported recently by studies on peptides encompassing shorter fragments of that linker. In fact, Helluin and coworkers (Helluin et al., 1996) have shown that the peptide Ac-IRTLLFALMMS-NH_2 (1646-1656) in 15% TFE is 96% β-strand while its conformation in 75% TFE exhibits 40% of α-helix. Miyamoto and coworkers (Miyamoto et al., 2001a) have shown that the peptide Ac-TLLFALMMSLPALFNIGLL-NH_2 (1648-1666), in the presence of SDS micelles, acquires a mixed conformation consisting of α-helix and β-strand elements, with a 28% of helical content.

The solution structure of the pIV/S4-S5 peptide

Having verified by CD spectroscopy that both in TFE and in the presence of SDS micelles the peptide possesses a similar secondary structure, we have determined its 3D solution structure in 30% TFE by homonuclear multidimensional NMR. The NMR

resonance assignment was performed based on the combined use of two dimensional TOCSY and NOESY spectra (Wüthrich, 1986).

The residual chemical shifts of the $C_\alpha H$ protons (Wishart et al., 1992) of *p*IV/S4-S5 indicate the presence of a α-helical structure in the region R^{1647}-M^{1655} (data not shown). Figure 4, summarizes the short and medium range NOEs. The dense pattern of $d_{\alpha N}(i,i+3)$, $d_{\alpha N}(i,i+4)$ and $d_{\alpha\beta}(i,i+3)$ indicate that the helix extends between G^{1645} and I^{1663}.

Figure 5a displays the superposition of the best 20 models, selected on the base of their minimum energy and of the residual distance violation less than 0.2 Å. The quality of the structures has been evaluated by using PROCHECK-NMR (Laskowski et al., 1996) and it is reported in Table 1. It can be seen that more than 95% of the ϕ and ψ angles are in the most favored region while the remaining ones in the favored region (Table 1).

In the region I^{1646}-L^{1657} the peptide acquires a well defined helical structure (backbone r.m.s.d. 0.12 ± 0.04 Å, and heavy atoms r.m.s.d. 0.70 ± 0.02 Å) followed by a bend at residue P^{1658}.

It is worth noting that our structure differs from the one reported by Miyamoto et al. (Miyamoto et al., 2001b), obtained in SDS micelles. In fact, they observed a β-turn subsequent to the bend induced by the Pro residue. This apparent discrepancy may be justified by the fact that in SDS micelles the C-terminal portion of the peptide might be located near the negatively charged micelles surface, an environment less favorable to α-helix conformation. At any rate, in spite of this difference, also in our case the helix shows a certain amphypathic nature, (Figure 5b,c), a structural feature considered important for the channel functionality (Lerche et al., 1997; Filatov et al., 1998). In fact, it has been suggested that the hydrophobic surface of the helix interacts with residues in the III-IV linker (Miyamoto et al., 2001b), thus favoring the stabilization of the inactivation state of the Na^+ channel (Miyamoto et al., 2001c).

Interaction of pIV/S4-S5 with local anesthetics

LA are chemicals that reversibly block the action potential in excitable membranes (Strichartz, 1987) and, in particular, they tend to stabilize the channel inactivated state (Hille, 1977; Postma, 1984). Evidence have been reported that the linker between S4 and S5

in domain IV can be a possible site of action for local anesthetic (Tang et al., 1996; Lerche et al., 1997; McPhee et al., 1998). To substantiate this possibility we have used DOSY and ^{15}N-^{1}H HSQC experiments to verify if the peptide *p*IV/S4-S5 is able to interact with LA.

The results obtained from DOSY experiments are shown in Table 2. From the analysis of the diffusion coefficients we conclude that both LA are able to interact with *p*IV/S4-S5. Nonetheless, BZC displays a stronger binding capability. In fact, we observe a 35% of the peptide bound to BZC and only 13% when LDC is used. A possible explanation of this higher affinity exhibited by BZC might reside in its higher hydrophobic character (Covino, 1976).

In order to verify the existence of specific contacts between each LA and *p*IV/S4-S5, we carried out a series of ^{15}N-^{1}H HSQC experiments where the peptide was dissolved in a solution containing increasing concentrations of LA corresponding to: 0.25, 0.50, 0.75 and 1.0 LA:*p*IV/S4-S5 molar ratio. The results indicate that only few residues are affected by the presence of the LA (data not shown). Figure 6 reports the most significant ^{15}N chemical shift variations, normalized with respect to the maximum variation, for the two more representative residues. It is interesting to observe that each LA interacts specifically with one of the two residues. Other nearby residues are affected but at a smaller extent (data not shown). Overall these results suggest the existence of preferential binding sites for the two LA.

Various authors (Shuker et al., 1996, Stockman, 1998; Pellechia et al., 2002)[47-49] have proposed the use of the $\Delta\delta(^{1}H,^{15}N)$ parameter as a more effective way to identify the sites of interaction between a protein and a ligand. In our case the data clearly confirm that the two LA have distinct sites of interaction with *p*IV/S4-S5, Figure 7. In the case of LDC the bigger effect is observed in two regions close to the N- and C- terminus and involving the hydrophobic residues I^{1646}, L^{1649} and A^{1659}, L^{1660}, respectively. As for BZC, instead, it affects the residues L^{1653}, M^{1655} and S^{1656} located in the central part of the main helical stretch of the peptide. Considering that the size of the $\Delta\delta(^{1}H,^{15}N)$ perturbation observed with BZC is of the same order of magnitude of the ones observed by other authors studying enzyme/substrate systems (Fesik, 1991; Shuker et al., 1996; Hadjuk et al., 1997), we may conclude that between BZC and the peptide there must be significant interaction. As for LDC, Figure 7 reports reduced values of the $\Delta\delta(^{1}H,^{15}N)$ chemical shift perturbation

thus supporting the hypothesis, suggested by the DOSY experiments, of a weaker affinity of this LA for the peptide.

CONCLUSION

Various authors (Lerche et al., 1997; Miyamoto et al., 2001b; Filatov et al., 1998) have proposed that the stabilization of the inactivation state of the Na^+ channel implies an initial hydrophobic interaction between the S4-S5 linker of domain IV and a portion of the linker between domains III and IV, probably via the interaction of anti-parallel α-helices. In particular, they indicate as key residues, F^{1651}, $MM^{11654-1655}$, L^{1657} and A^{1659} in IV/S4-S5 and $YY^{1497-1498}$, M^{1501} in the III-IV linker. It is worthwhile to point out that this initial important step is controlled by the interaction between methionines and aromatic residues, a process that has been shown to be energetically favorable (Stapley et al., 1995).

Another important step associated to the transition from the inactivated to the open state is a movement of the signal helix S4 that leads to the internalization in the lipid membrane of a number of residues of the IV/S4-S5 linker (Ragsdale, 1998).

Since our data show that LA interact specifically with some of the residues in the IV/S4-S5 linker, we suggest that their binding, while it is not perturbing the interactions necessary to maintain the inactivated state, it interferes with the internalization process necessary to switch the channel into the open state thus producing their pharmacological effect. The higher affinity for *p*IV/S4-S5 exhibited by BZC might be due not only to its higher hydrophobic nature, but also to its smaller molecular size that should facilitate its access to some of the side chains packed in the peptide α-helical structure.

In conclusion, we believe these data, besides contributing to the understanding of the Na^+ channels functionality, provide important clues, at atomic level, on the mechanisms that define LA affinity and activity and may help to design more effective anesthetics.

ACKNOWLEDGMENTS

This work has been supported by Fundação de Amparo à Pesquisa do Estado de São Paulo (FAPESP) Grant (99/11030-9 and 99/07574-3). L.F.F had fellowship from FAPESP (#00/0362-0). T.A.P. has a fellowship from FAPESP (#00/02026-7).

REFERENCES

Armstrong, C.M., and F. Bezanilla. 1977. Inactivation of the sodium channel. II Gating current experiments. *J. Gen. Physiol.* 70:567-590

Atherton, E., and R.C. Sheppard. 1989. In Solid Phase Peptide Synthesis: A pratical Approach. I.L.R. Press, Oxford

Barany, G., and R.B. Merrifield. 1980. The Peptides: Analysis, Synthesis and Biology. E. Gross, and J. Meienhofer, editors. Academic Press, New York

BioMagResBank (BMRB), a NIH funded bioinformatics resource, Departament of Biochemistry, University of Wisconsin-Madison, Madison, WI USA (URL: http://www.bmrb.wisc.edu) Grant: LM05799-02.

Bodenhausen, G., H. Kogler, and R.R. Ernst. 1984. Selection of coherence-transfer pathways in NMR pulse experiments. *J. Magn. Reson.* 58: 370-388

Catterall, W.A. 1992. Cellular and molecular biology of voltage-gated sodium channels. *Physiol. Rev.* 72:S15-S18

Chen, Y-H., J.T. Yang, and K.H. Chau. 1974. Determination of the helix and beta form of proteins in aqueous solution by circular dichroism. *Biochemistry* 13:3350-3359

Covino, B.G., and H.G. Vassalo. 1976. Local Anesthetics: mechanisms of action and clinical use. Grune and Stratton, New York

Fesik, S.W. 1991. NMR studies of molecular complexes as a tool in drug design. *J. Med. Chem.* 34:2937-2945

Filatov G.N., T.P. Nguyen, S.D. Kraner, and R.L. Barch. 1998. Inactivation and secondary structure in the D4/S4-5 region of the SkM1 sodium channel. *J. Gen. Physiol.* 111:703-715.

Fozzard, H.A., and D.A. Hanck. 1996. Structure and function of voltage-dependent sodium channels: comparison of brain II and cardiac isoforms. *Physiol. Rev.* 76:887-926

Frazier, D.T., T. Narahashi, and M. Yamada. 1970. The site of action and active form of local anesthetics. II. Experiments with quaternary compounds. *J. Pharmacol. Exp. Ther.* 171:45-51

Griesinger, C., G. Otting, K. Wüthrich, and R.R. Ernst.1988. Clean TOCSY for ^{1}H spin system identification in macromolecules. *J. Am. Chem. Soc*.110:7870-7872

Güntert, P., C. Mumenthaler, and T. Herrmann. 1998. DYANA User's Manual, Institut für Molekularbiologie und Biophysik, Zürich, Switzerland

Hajduk, P.J., R.P. Meadows, and S.W. Fesik. 1997. Discovering high-affinity ligands for proteins. *Science* 278:497-499

Helluin, O., J. Breed, and H. Duclohier. 1996. Polarity-dependent conformational switching of a peptide mimicking the S4-S5 linker of the voltage-sensitive sodium channel. *Biochim. Biophys. Acta* 1279:1-4

Hille, B. 1977. Local anesthetics: hydrophilic and hydrophobic pathways for the drug-receptor reaction. *J. Gen. Physiol.* 69:497-515

Johnson Jr, C.S. 1999. Diffusion ordered nuclear magnetic resonance spectroscopy: principles and applications. *Prog. Nucl. Magn. Reson. Spectrosc.* 34:203-256

Kuroda Y., M. Ogawa, H. Nasu, M. Terashima, M. Kasahara, Y. Kiyama, M. Wakita, Y. Fujiwara, N. Fujii, and T. Nakagawa. 1996. Locations of local anesthetic dibucaine in model membranes and interaction between dibucaine and a Na^{+} channel inactivation gate peptide as studied by ^{2}H- and ^{1}H-NMR Spectroscopies, *Biophys. J.* 71:1191-1207

Kuroda, Y., K. Miyamoto, M. Matsumoto, Y. Maeda, K. Kanaori, A. Otaka, N. Fujii, and T. Nakagawa. 2000. Structural study of the sodium channel inactivation gate peptide including an isoleucine-phenylalanine-methionine motif and its analogous peptide

(phenylalanine/glutamine) in trifluoroethanol solutions and SDS micelles. *J. Peptide Res*. 56:172-184

Laskowski, R. A., J. A. C. Rullmann, M.W. MacArthur, R. Kaptein, and J.M. Thornton. 1996. AQUA and PROCHECK-NMR: Programs for checking the quality of protein structures solved by NMR. *Journal of Biomolecular NMR.* 8:477-486

Lerche, H., W. Peter, R. Fleischhauser, U. Pika-Hartlaub, T. Malina, N. Mitrovic, and F. Lehmann-Horn. 1997. Role in fast inactivation of the IV/S4-S5 loop of the human muscle Na^+ channel probed by cysteine mutagenesis. *J. Physiol.* 505:345-352

Marban, E., T. Yamagishi, and G.F. Tomaselli. 1998. Structure and function of voltage-gated sodium channels. *J. Physiol*. 508:647-657

McPhee, J.C., D.S. Ragsdale, T. Scheuer, and W.A. Catterall. 1998. A critical role for the S4-S5 intracellular loop in domain IV of the sodium channel alpha-subunit in fast inactivation. *J. Biol. Chem.* 273:1121-1129

Miyamoto K., T. Nakagawa, and Y. Kuroda. 2001. Solution structure of the cytoplasmic linker between domain III-S6 and domain IV-S1 (III-IV linker) of the rat brain sodium channel in SDS micelles. *Biopolymers* 59:380-393

Miyamoto, K., Kanaori, K., Nakagawa, T. & Kuroda, Y. Solution structures of the inactivation gate particle peptides of rat brain type-IIA and human heart sodium channels in SDS micelles. *J. Peptide Res.* **2001**, 57, 203-214

Miyamoto, K., T. Nakagawa, and Y. Kuroda. 2001. Solution structures of the cytoplasmic linkers between segments S4 and S5 (S4-S5) in domains III and IV of human brain sodium channels in SDS micelles. *J. Peptide Res.* 58:193-203

Nagayama, K., A. Kumar, K. Wüthrich, and R.R. Ernst.1980. Experimental techniques of two-dimensional correlated spectroscopy. *J. Magn. Reson*. 40:321-334

Narahashi, T., D.T. Frazier, and M. Yamada. 1970. The site of action and active form of local anesthetics. I. Theory and pH experiments with tertiary compounds. *J. Pharmacol. Exp. Ther.* 171:32-44

Nau,C., S.-Y. Wang, G.R. Strichartz, and K.G. Wang. 1999. Point mutations at N434 in DI-S6 of a Na^+ channels modulate potency and stereoselectivity of local anesthetic enantiomers. *Mol. Pharmacol*. 56:404-413

Patton, D.E., J.W. West, W.A. Catterall, and A.L. Goldin. 1992. Amino acid residues required for fast Na^+ channel inactivation: charge neutralization and deletions in the III-IV linker. *Proc. Natl. Acad. Sci.* USA, 89:10905-10909

Pellechia, M., D.S. Sem, and K. Wüthrich. 2002. NMR in drug discovery. *Nature review/Drug discovery* 1:211-219

Postma S.W., and W.A. Catterall. 1984. Inhibition of binding of [^{3}H]batrachotoxinin A 20-alpha-benzoate to sodium channels by local anesthetics. *Mol. Pharmacol*. 25:219-227

Ragsdale D.S., J.C. McPhee, T. Scheuer, and W.A. Catterall. 1994. Molecular determinants of state-dependent block of Na^+ channels by local anesthetics. *Scienc*e 265:1724-1728

Ragsdale D.S., J.C. McPhee, T. Scheuer, and W.A. Catterall. 1996. Common molecular determinants of local anesthetic, antiarrhythmic, and anticonvulsant block of voltage-gated Na+ channels. *Proc. Natl. Acad. Sci.* USA 93:9270-9275

Ragsdale, D.S., and M. Avoli. 1998. Brain Sodium channels as molecular targets for antiepileptic drugs. *Res. Brain. Res. Rev*. 26:16-28

Ritchie, J.M, and P. Greengard. 1966. On the mode of action of local anesthetics. *Annu. Rev. Pharmacol.* 6: 405-430

Shuker, S.B., P.J. Hajduk, R.P. Meadows, and S.W. Fesik. 1996. Discovering high-affinity ligands for proteins: SAR by NMR. *Science* 274:1531-1534

Smith, M.R., and A.L. Goldin. 1997. Interaction between the sodium channel inactivation linker and domain III S4-S5. *Biophys. J.* 73:1885-1895

Stapley, B.J., C.A. Rohl, and A.J. Doig. 1995. Addition of side chain interactions to modified Lifson-Roig helix coil theory: application to energetics of phenylalanine-methionine interactions. *Protein Sci.* 4:2383-2391

States, D. J., R.A. Haberkorn, and D.J. Ruben. 1982. A Two-Dimensional Nuclear Overhauser Experiment with Pure Absorption Phase in Four Quadrants. *J. Magn. Reson.* 48:286-292.

Stockman B.J. 1998. NMR spectroscopy as a tool for structure-based drug design. *Prog. Nucl. Magn. Reson. Spectrosc.* 33:109-151

Strichartz, G.R., and J.M. Ritchie. 1987. Local Anesthetics. Handbook of Experimental Pharmacology. G.R. Strichartz, editor. Springer-Verlag, Berlin

Sunami, A., S.C. Dudley, and H.A. Fozzard. 1997. Sodium channel selectivity filter regulates antiarrhythmic drug binding. *Proc. Natl. Acad. Sci.* USA 94: 14126-14131.

Tang, L., R.G. Kallen, and R. Horn. 1996. Role of an S4-S5 linker in sodium channel inactivation probed by mutagenesis and a peptide blocker. *J.Gen. Physiol.* 108:89-104

Waldeck, A.R., P.W. Kuchel, A.J. Lennon, and B.E. Chapman. 1997. NMR diffusion measurements to characterize membrane transport and solute binding. *Prog. Nucl. Magn. Reson. Spectrosc.* 30:39-68

Wang, S.-Y., and G.K. Wang. 1998. Point mutations in segment I-S6 render voltage-gated Na^+ channels resistant to batrachotoxin. *Proc. Natl. Acad. Sci.* USA 95:2653-2658

West, J.W., D.E. Patton, T. Scheuer, Y. Wang, A.L. Goldin, and W.A. Catterall. 1992. A cluster of hydrophobic amino acids residues required for fast Na^+ channel inactivation. *Proc. Natl. Acad. Sci.* USA 89:10910-10914

Wimmer, R., F.L. Aachamann, K.L. Larsen, and S.B. Petersen. 2002. NMR diffusion as a novel tool for measuring the association constant between cyclodextrin and guest molecules. *Carbohydrate Res.* 337:841-849

Wishart, D.S., B.D. Sykes, and F.M. Richard. 1992. The chemical shift index: a fast and simple method for the assignment of protein secondary structure through NMR spectroscopy. *Biochemistry* 31:1647-1651

Wüthrich, K. 1986. NMR of Proteins and Nucleic Acids. John Wiley & Sons, New York

Yarov-Yarovoy, V., J.C. McPhee, D. Idsvoog, C. Pate, T. Scheuer, and W.A. Catterall. 2002. Role of amino acid residues in transmembrane segments IS6 and IIS6 of the Na+ channel alpha subunit in voltage-dependent gating and drug block. *J. Biol. Chem*. 277:35393-35401

Zamponi G.W., and R.J. French. 1994. Open-channel block by internally applied amines inhibits activation gate closure in batrachotoxin-activated sodium channels. *Biophys J.* 67:1040-1051

Table 1: Structure statistics for the ensemble of 20 structures of *p*IV/S4-S5.

Constrains	*p*IV/S4-S5
Intraresidue	102
Sequential	32
Medium range	65
Total	199
PROCHECK – Ramachandran plot analysis	
Most favoured region (%)	95%
Additionally allowed region (%)	5%
Generously allowed region (%)	0
Disallowed region (%)	0
RMSD[a]	
Backbone (residues 1646-1662)	0.12 ± 0.04
Heavy atoms (residues 1646-1662)	0.70 ± 0.02

[a]Root mean square deviation from pairwise comparison between all the structures (Å).

Table 2: LA and *p*IV/S4-S5 diffusion constants (10^{-10} $m^2.s^{-1}$) and percentage of each LA bound to the peptide. D*free* = diffusion coefficient of the free LA; D*bound* = diffusion coefficient of the complex (diffusion of peptide); D *free+bound* = diffusion coefficient of both bound and free LA, 1:1 LA:*p*IV/S4-S5, molar ratio, 20°C. The percentage of LA bound is calculated as described by references [33, 34].

LA	$\mathbf{D}_{free}$	$\mathbf{D}_{bound}$	$\mathbf{D}_{free+bound}$	f_{bound} **(%)**
LDC	2.92±0.138	1.08±0.192	2.68±0.174	13
BZC	2.87±0.199	1.08±0.165	2.24±0.129	35

Figures Legends

Figure 1 Model of segments S4-S5 and the cytoplasmic connecting loop of the domain IV of the α-subunit of the adult human brain Na^+ channel. The peptide sequence studied in this work, named *p*IV/S4-S5 is colored in gray.

Figure 2 Chemical structure of local anesthetics, a) lidocaine (LDC) and b) benzocaine (BZC).

Figure 3 Far-UV CD spectra of *p*IV/S4-S5 (50 μM) in water, pH 7.4 (solid line), in the presence of: 30% TFE (dash-line) and 20 mM SDS (dot line). The inset shows TFE-induced conformation transition of *p*IV/S4-S5, 20°C.

Figure 4 Summary of the sequential and medium-range NOE connectivities for *p*IV/S4-S5 (1.0 mM) in 30% of TFE, at 20°C. The intensities of the observed NOE are represented by the thickness of lines and were classified as strong, medium and weak, corresponding to upper bound constraints of 2.5, 3.5 and 5 Å, respectively. The stars indicate potential NOE connectivities that could not be obtained due to resonance overlap.

Figure 5 a) Ensemble of the 20 final structures of pIV/S4-S5 with superposition over residues I^{1646} to N^{1662} gives a r.m.s.d. of 0.70 ± 0.02 Å for the heavy atomos, pairwise comparison, b) Helical-wheel diagram of peptide *p*IV/S4-S5 from residues I^{1646} to P^{1658}, the hydrophobic aminoacid are coloured in gray, c) Hydrophobic potentials surface calculated from *p*IV/S4-S5 with InsightII at the Connoly surface. Hydrophobic and hydrophilic surfaces are shown in red and blue, respectively, whereas white represents an intermediary hydrophobicity.

Figure 6 Effect of BZC (full symbol) and LDC (open symbol) on the chemical shift of ^{15}N from *p*IV/S4-S5 for I^{1646} (square) and M^{1655} (circle) residues. The data are normalized for BZC and LDC.

Figure 7 Chemical shift changes of *p*IV/S4-S5 in the presence of BZC(■) and LDC(□). *p*IV/S4-S5:LA, 1:1 molar ratio. Weighted averaged chemical shifts were used ($\Delta\delta(^1H,^{15}N) = |\Delta\delta(^1H)| + 0.2*|\Delta\delta(^{15}N)|$), as described by Shuker and coworkers [49].

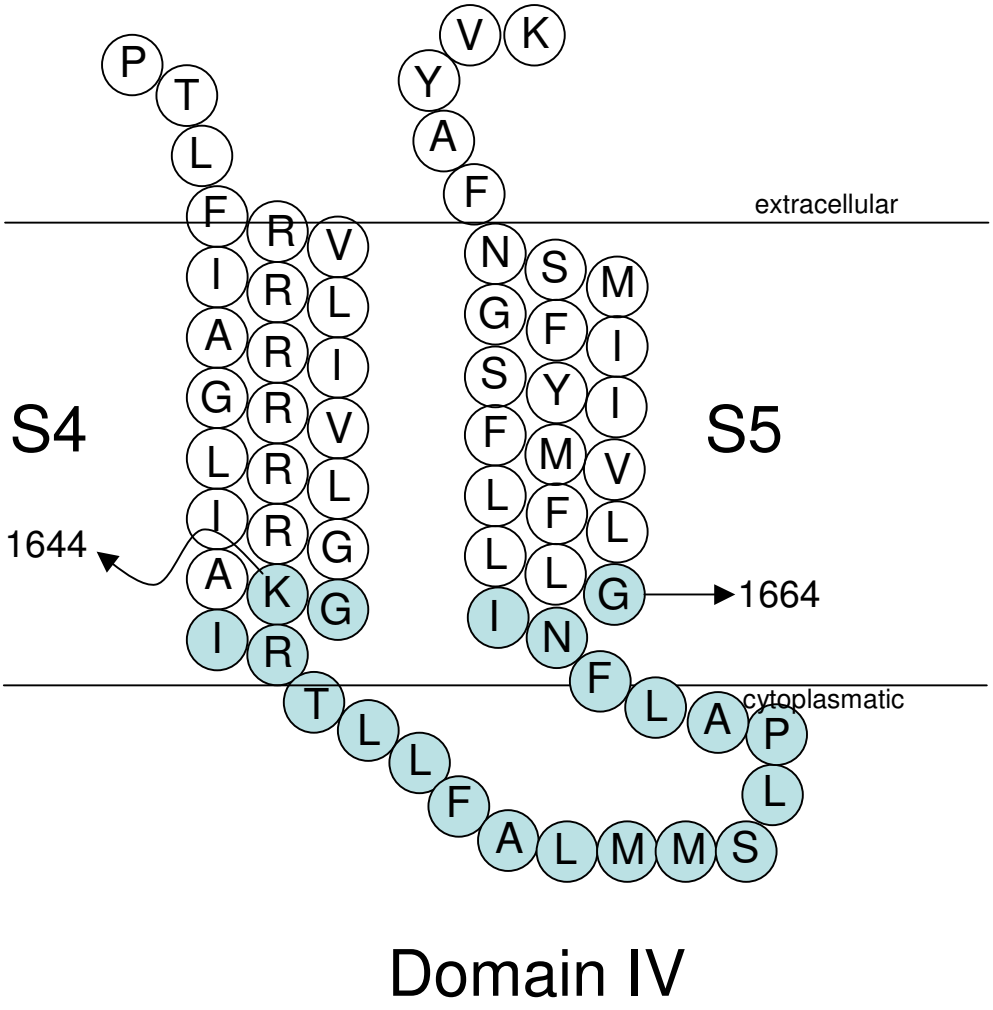

Figure 1

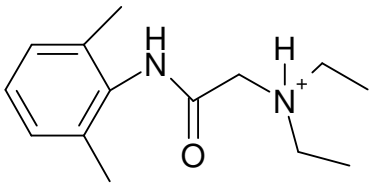

a)

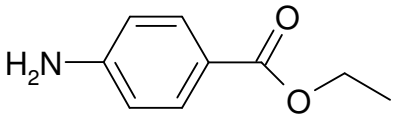

b)

Figure 2

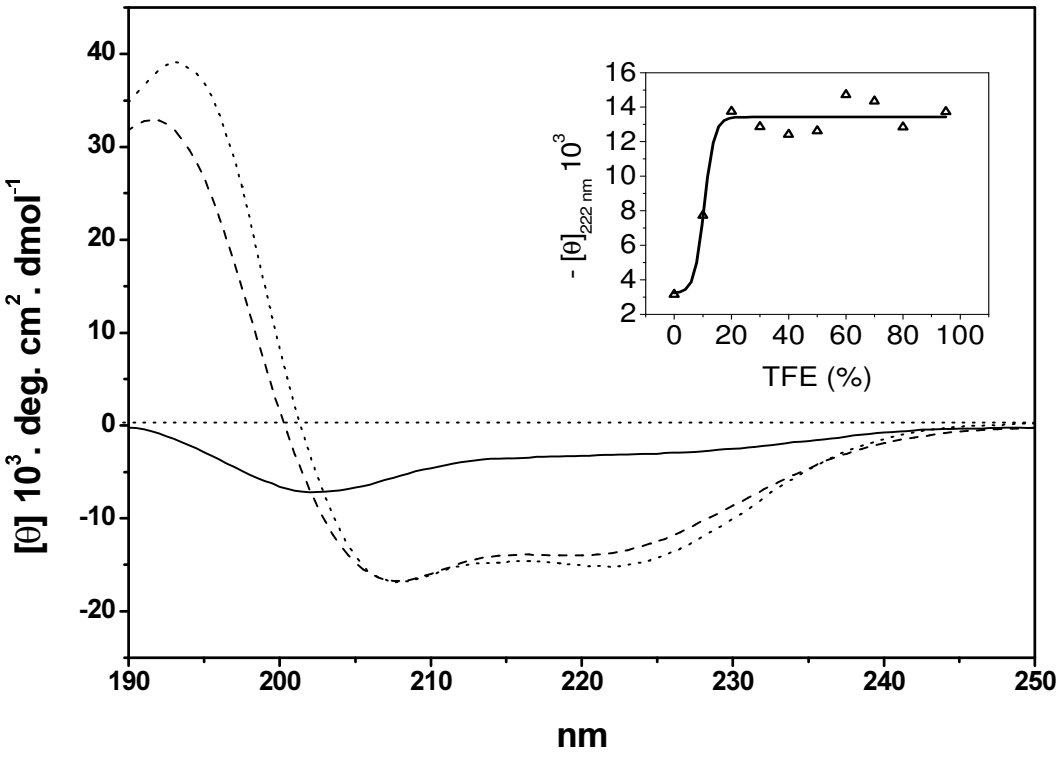

Figure 3

Figure 4

a)

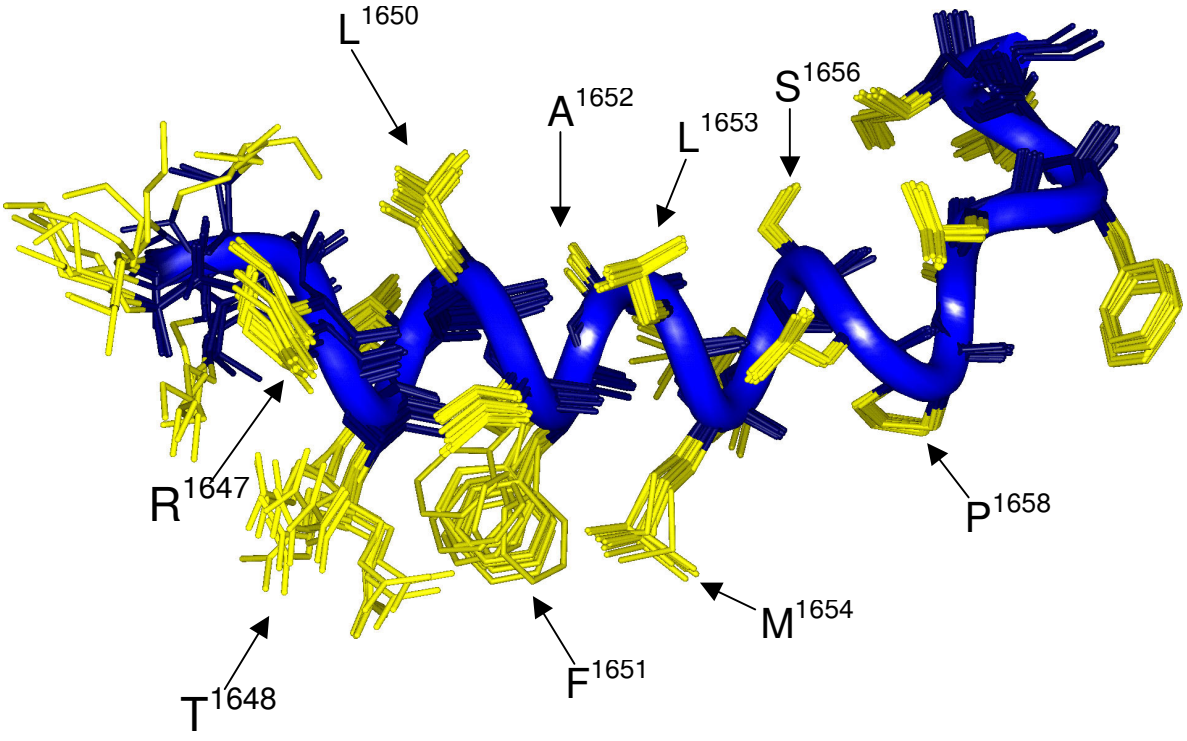

Face A

b)

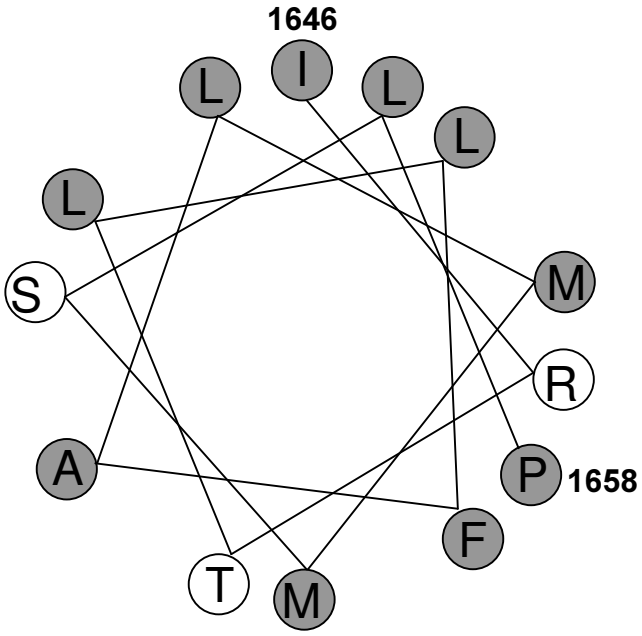

c)

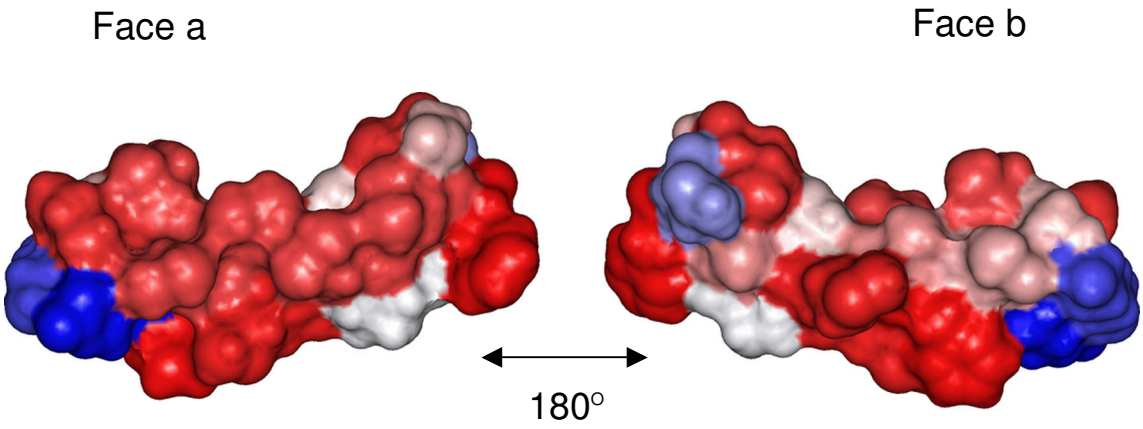

Figure 5

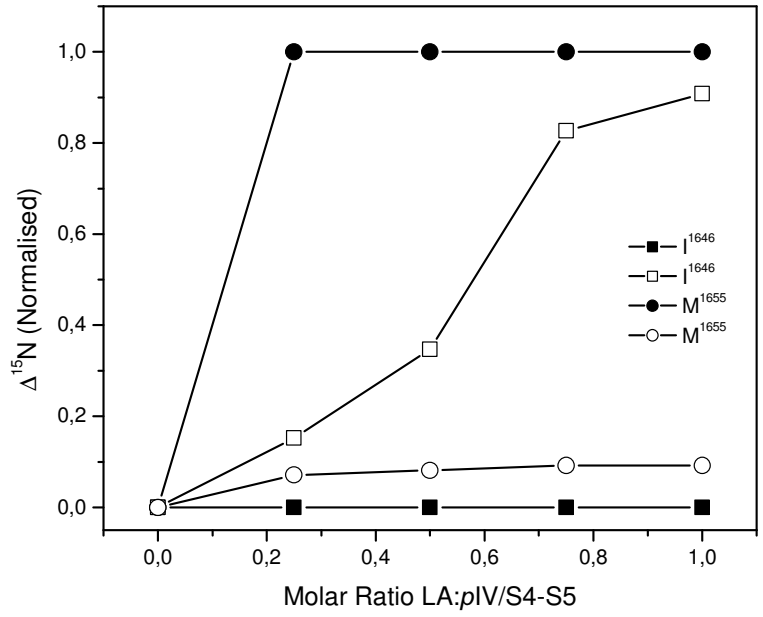

Figure 6

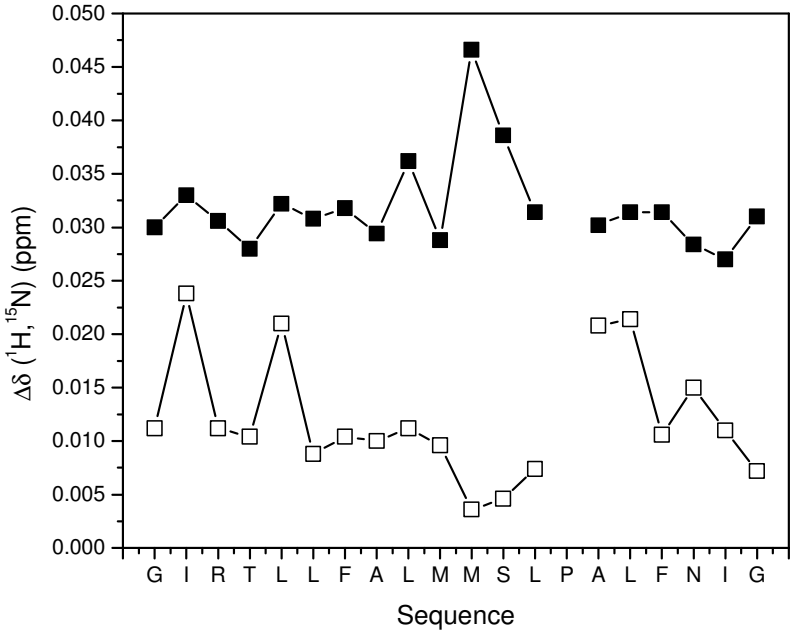

Figure 7

4 – CONCLUSÃO

Os mecanismos de ação dos anestésicos locais propostos na literatura envolvem tanto a interação com a fase lipídica membranar quanto com sítio(s) de ação na proteína canal de sódio, como representado, de maneira esquemática na **Figura 8**.

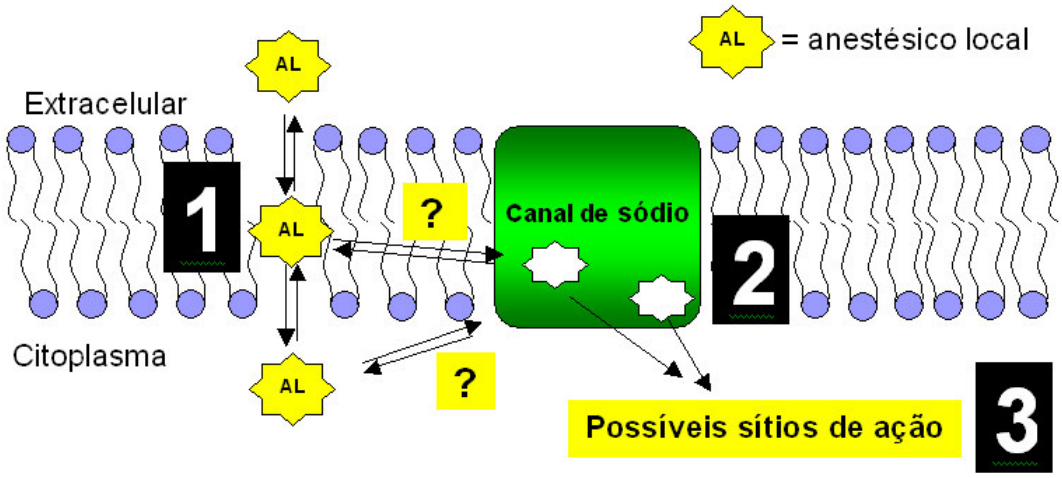

Figura 8: Esquema ilustrativo da interação de anestésicos locais com a fase lipídica e as possíveis vias de acesso destes a(os) sítio(s) de ação na proteína canal de sódio.

A partir dos resultados obtidos podemos detalhar: 1) as alterações na fase lipídica e localização preferencial dos diferentes compostos anestésicos; 2) a estrutura do segmento referente ao peptídeo estudado, importante no processo de inativação e 3) as evidências de interação deste fragmento com anestésicos locais.

1) Alterações na fase lipídica e a localização preferencial dos AL

Os anestésicos locais estudados aqui interagem com membranas modelos, lipossomos, - vesículas unilamelares e multilamelares de fosfatidilcolina de ovo - e *ghosts* de eritrócitos humanos, causando desorganização na bicamada lipídica.

Com o uso de diversas técnicas biofísicas pudemos obter informações sobre a inserção preferencial de dois anestésicos locais, benzocaína e lidocaína, no interior dessas membranas modelos e concluir que esta localização preferencial está de acordo com propriedades físico-químicas de cada anestésico, como hidrofobicidade e volume molecular. Nos dois sistemas modelo estudados (lipossomos e membranas de eritrócito) pudemos observar que a benzocaína (um anestésico neutro, com baixa solubilidade) apresentou inserção preferencial mais profunda, com o seu anel aromático próximo aos primeiros carbonos da cadeia acila e da região do glicerol. Para a lidocaína (um anestésico ionizável, com alta solubilidade) a localização preferencial foi mais superficial, próxima à cabeça polar e grupamento fosfato dos lipídios nos lipossomos e membranas de eritrócito.

Acreditamos que esta localização preferencial está diretamente relacionada à capacidade destes compostos acessarem sítio(s) hidrofóbico(s) na proteína canal de sódio. Desta forma, a interpretação do mecanismo de anestesia deixa de ter uma abordagem restrita à importância da interação com o lipídio, para uma visão mais global, em que os lipídios funcionariam como um entreposto, facilitando o acesso (concentrando e direcionado a molécula) do anestésico ao(s) sítio(s) na proteína canal de sódio, provocando a estabilização do estado inativado.

2) Segmento referente ao peptídeo e sua importância no processo de inativação

A região referente ao fragmento S4-S5, do domínio IV, do canal de sódio voltagem-dependente está envolvida no processo de estabilização do estado inativado do canal; esta região apresenta estrutura helicoidal em ambiente que mimetiza a membrana (30% trifluoretanol e micelas de SDS). Este fato é interessante pois este fragmento está ligado à hélice sensora S4 do canal, que no momento da ativação se move 5 angstrons para fora do plano da membrana, fazendo com que parte da alça S4-S5 seja inserido na membrana. Esta estrutura, determinada por nós para o peptídeo em questão é muito similar à descrita na literatura (Miyamoto *et al.*, 2001b) e pode estar relacionada a uma indução estrutural que acontece no canal, durante seu funcionamento. O peptídeo apresenta uma face hidrofóbica que, segundo Miyamoto e col. (2001b) está envolvida na estabilização da partícula de inativação (resíduos IFM) através de interações entre hélices antiparalelas, sendo estabilizada por resíduos de metionina e fenilalanina/tirosina.

3) Evidência da interação deste fragmento *p*IV/S4-S5 com anestésicos locais

Uma vez que o fragmento estudado neste trabalho está envolvido no processo de inativação do canal, propusemos que esta região poderia ser um possível sítio de ação de anestésicos locais, visto que estes têm uma grande afinidade pelo estado inativado do canal.

Nesta parte do trabalho, usando RMN, observamos que os anestésicos locais benzocaína e lidocaína interagem com o fragmento *p*IV/S4-S5 do canal de sódio. A interação observada foi maior para a benzocaína do que para a lidocaína, segundo os resultados de complexação (DOSY) e os efeitos encontrados nos deslocamentos químicos dos núcleos de ^{15}N e ^{1}H.

A benzocaína interage com resíduos específicos, principalmente com metionina (1655), do fragmento referente à região S4-S5 do domínio IV da proteína. A afinidade da benzocaína com resíduo de metionina sugere um possível sítio de ligação para o anestésico nesta região da proteína, visto que metioninas (Miyamoto *et al.*, 2001b) são importantes para a estabilização do estado inativado.

Esta interação se deve a natureza hidrofóbica da benzocaína e também à sua pequena dimensão, o que poderia facilitar o acesso (via fase lipídica membranar, provavelmente) a esta região na proteína canal de sódio, causando a estabilização do estado inativado (anestesia).

Nossos resultados abrem perspectivas para o entendimento molecular da interação de anestésicos locais com regiões importantes do canal de sódio voltagem-dependente. As informações sobre a interação específica dos anestésicos com o canal de sódio podem contribuir para a definição de um modelo de ação e auxiliar o desenvolvimento de novos compostos com potencial anestésico.

5 – REFERÊNCIAS BIBLIOGRÁFICAS

- Arias, H.R. (1998) Binding sites for exogenous and endogenous non-competitive inhibitors of the nicotinic acetylcholine receptor. **Biochim. Biophys. Acta 1376**:173-220.
- Auger, M., Jarrel, H.C., Smith, I.C.P., Wong, P.T.T., Siminovitch, D.J., Mantsch, H.H. (1987) Pressure-induced exclusion of a local anesthetic from model and nerve membranes. **Biochemistry 26**:8513- 8516.
- Auger, M., Smith, I.C.P, Mantsch, H., Wong, P.T.T. (1990) High-pressure infrared study of phosphatidylserine bilayers and their interactions with the local anesthetic tetracaine. **Biochemistry 29**:2008-2015.
- Baber, J., Ellena, J.F., Cafiso, D.S. (1995) Distribution of general anesthetics in phospholipid bilayers determined using ^{2}H NMR and ^{1}H-^{1}H NOE spectroscopy. **Biochemistry 34:**6533-6539.
- Balser, J.R., Nuss, H.B., Romashko, D.N., Marban, E., Tomaselli, G.F. (1996) Functional consequences of lidocaine binding to slow-inactivated sodium channels. **J. Gen. Physiol. 107**:643-658.
- Barry, J. A., Gawrisch, K. (1994) Direct NMR evidence for ethanol binding to the lipid-water interface of phospholipid bilayers. **Biochemistry 33**:8082-8088.
- Bianconi, M.L., Schreier, S. (1991) RPE study of membrane partitioning, orientation and membrane-modulated alkaline hydrolysis of a spin-labeled benzoic acid ester. **J. Phys. Chem. 95**:2483-2487.
- Boulanger, Y., Schreier, S., Leitch, L.C., Smith, I.C.P. (1980) Multiple binding sites for local anesthetics in membranes: characterization of the sites and their equilibria by deuterium NMR of specifically deuterated procaine and tetracaine. **Can. J. Biochem. 58:**986-995.
- Boulanger, Y., Schreier, S., Smith, I.C.P. (1981) Molecular details of anesthetic-lipid interaction as seen by deuterium and phosphorus-31 nuclear magnetic resonance. **Biochemistry 20:**6824-6830.

- Bradley, D.J., Richards, C.D. (1984) Temperature-dependence of the action of nerve blocking agents and its relationship to membrane-buffer partition coefficients: thermodynamic implications for the site of action of local anaesthetics. **Br. J. Pharmacol. 81**:161-167.
- Browning, J.L., Akutsu, H. (1982) Local anesthetics and divalent cations have the same effect on the headgroups of phosphatidylcholine and phosphatidyl ethanolamine. **Biochim. Biophys. Acta 684**:172-178.
- Butterworth, J.F. 4th., Strichartz, G.R. (1990) Molecular mechanisms of local anesthesia: a review. **Anesthesiol. 72**:711-734.
- Catterall, W.A. (1992) Cellular and molecular biology of voltage-gated Na channels. **Physiol. Rev. 72**:515-548.
- Catterall, W., Mackie, K. (1996) Anestésicos Locais, em **As Bases Farmacológicas da Terapêutica**, Guanabara Koogan, Rio de Janeiro, RJ.
- Cerbon, J. (1972) NMR evidence for the hydrophobic interaction of local anaesthetics. Possible relation to their potency. **Biochim. Biophys. Acta 290**:51-57.
- Cestèle, S., Catterall W.A. (2000) Molecular mechanisms of neurotoxin action on voltage-gated sodium channels. **Biochimie 82**:883-892.
- Choe, S., Kreusck, A., Pfaffinge, P.J. (1999) Towards the three-dimensional structure of voltage-gated potassium channels. **TIBS 24**:345-349.
- Covino, B.G., Vassalo, H.G. (1985) **Anestésicos Locais: Mecanismos de ação e uso clínico,** Grune and Stratton, New York.
- Darke, A., Finer, E.G., Flook, A.G., Phillips, M.C. (1972) Nuclear magnetic resonance study of lecithin-cholesterol interactions. **J. Mol. Biol. 63**:265-279.
- de Jong, R.H. (1994) **Local Anesthetics,** C.C. Thomas, Springfield, Illinois.
- de Paula, E., Schreier, S. (1995) Use of a novel method for determination of partition coefficient to compare the effect of local anesthetics on membrane structure. **Biochim. Biophys. Acta 1240:**25-33.
- de Paula, E., Schreier, S. (1996) Molecular and physicochemical aspects of local anesthetic-membrane interaction. **Braz. J. Med. Res. 29:**877-894.

- Doyle, A. D., Cabral, J.M., Pfuetzner, R.A., Kuo, A., Gubbis, J.M., Cohen, S.L., Chait, B.T. (1998) The structure of the potassium channel: Molecular basis of K^+ conduction and selectivity. **Science 280**:69-77.
- Filatov G.N., Nguyen T.P., Kraner S.D., Barchi R.L. (1998) Inactivation and secondary structure in the D4/S4-5 region of the SkM1 sodium channel. **J. Gen. Physiol. 111**:703-715.
- Finer, E.G., Flook, A.G., Hauser, H. (1972) Mechanism of sonication of aqueous egg yolk lecithin dispersion and nature of the resultant particles. **Biochim. Biophys. Acta. 260**:49-58.
- Fraceto, L.F., Pinto, L.M.A., Franzoni, L., Braga, A.A.C., Spisni, A., Schreier, S., de Paula, E. (2002) Spectroscopic evidence for a preferential location of lidocaine inside phospholipid bilayers. **Biophys. Chem**. **99**:229-243.
- Frazier, D. T., Narahashi, T., Yamada, M. (1970) The site of action and active form of local anesthetics. II Experiments with quaternary compounds. **J. Pharmacol. Exp. Ther. 171**:45-51.
- Frezatti Jr., W.A., Toselli, W.R., Schreier, S. (1986) Spin label study of local anesthetic-lipid membrane interactions. Phase separation of the uncharged form and bilayr micellization by the charged form of tetracaine. **Biochim. Biophys. Acta 1235**:189-196.
- Gallová, J., Balgavý, P. (1997) Interaction of local anesthetic heptacaine homologs with phosphatidylcholine bilayers: a ESR study. **Biochim. Biophys. Acta 1325**:189-196.
- Gargiulo, R.J., Giotta, G.J., Wang, H.H. (1973) Spin-labeled analogs of local anesthetics. **J. Med. Chem. 16**:707-708.
- Giotta, G.J., Chan, D.S., Wang,H.H. (1974) Binding of spin-labeled local anesthetics to phosphatidylcholine and phosphatidylserine liposomes. **Arch. Biochim. Biophys. 163**:453-458.
- Goodmam, A.G., Gilman, A.G. (1996) **As Bases Farmacológicas da Terapêutica**, Guanabara Koogan, Rio de Janeiro, RJ.
- Gupta, S.P. (1991). Quantitative structure-activity relationship studies on local anesthetics. **Chem. Rev. 91:**1109-1119.

- Guyton, A. C., Hall, J.E. (1996) **Tratado de Fisiologia Médica,** Guanabara Koogan S.A., Rio de Janeiro, RJ.
- Hamill, O.P., Marty, A., Neher, E., Sakmann, B., Sigworth, F.J. (1981) Improved patch-clamp techniques for high-resolution current recording from cells and cell-free membrane patches. **Pflügers Arch. 391**:85-100.
- Hauser, H., Dawson, R.M.C. (1968) The displacement of calcium ions from phospholipid monolayers by pharmacologically active and other organic bases. **Biochem. J.** 109:909-916.
- Hill, M.W. (1974) The effect of anaesthetic-like molecules on the phase transition in smetic mesophases of dipalmitoyllecithin I. The normal alcohol up to C=9 and three inhalation anaesthetics. **Biochim. Biophys. Acta 356:**117-124.
- Hille, B. (1977) Local anesthetics: hydrophilic and hydrophobic pathways for the drug-receptor reaction. **J. Gen. Physiol. 69**:497-515.
- Hodgkin, A.L., Huxley, A. F. (1952) A quantitative description of membrane current and its application to conduction and excitation in nerve. **J. Physiol. 117:**500-544.
- Holte, L.L., Gawrisch, K. (1997) Determining ethanol distribution in phospholipid multilayers with MAS-NOESY spectra. **Biochemistry 36**:4669-4674.
- Hondeghem, L.M., Katzung, B.G. (1977) Time- and voltage-dependent interaction of antiarrhythimic drug with cardiac sodium channels. **Biochim. Biophys. Acta 472**:373-398.
- Hornby, A.P., Cullis, P.R. (1981) Influence of local and neutral anaesthetics on the polymorphic phase preferences of egg yolk phosphatidylethanolamine. **Biochim. Biophys. Acta 647**:285-292.
- Hubbel, W.L., McConnell, H.M. (1971) Molecular motion in spin-labeled phospholipid and membranes. **J. Am. Chem. Soc. 93**:314-326.
- Hutterer, R., Kramir, K., Schneider, F.W., Hof, M. (1997) The localization of the anesthetic tetracaine in phospholipid vesicles: A fluorescence quenching and resonance energy transfer study. **Chem. Phys. Lipids 90**:11-23.
- Kaminoh, Y., Tashiro, C., Kamaya, H., Ueda, I. (1988) Depression of phase-transition temperature by AL: nonzero solid membrane binding. **Biochim. Biophys. Acta 946**:215-220.

- Kaminoh, Y, Kamaya, H., Ueda, I. (1989) Differential affinity of charged local anesthetics to solid-gel and liquid-crystalline states of dimyristoyl phosphatidic acid vesicle membranes. **Biochim. Biophys. Acta 987:**63-68.
- Katz, A.M. (1998) Selectivity and toxicity of antiarrhythmic drugs: molecular interactions with ion channels. **Am. J. Med. 104**:179-195.
- Kelusky, E.C. (1983) **Nuclear Magnetic Resonance Studies of the Interaction of Local Anesthetics with Membranes and Motions in Solid n-Alkanes,** tese de doutorado, University of Ottawa, Ottawa, Canada.
- Kelusky, E.C., Smith, I.C.P. (1984) Anesthetic-membrane interaction: a ^{2}H nuclear magnetic resonance study of the binding of specifically deuterated tetracaine and procaine to phosphatidylcholine. **Can. J. Biochem. Cell. Biol. 62:**178-184.
- Kuroda, Y., Fujiwara, Y. (1987) Locations and dynamical perturbations for lipids of cationic forms of procaine, tetracaine, and dibucaine in small unilamellar phosphatidylcholine vesicles as studied by nuclear Overhauser effects in ^{1}H nuclear magnetic resonance spectroscopy. **Biochim. Biophys. Acta 903:**395-410.
- Kuroda, Y., Ogawa, M., Nasu, H., Terashima, M., Kasahara, M., Kiyama, Y., Wakita, M., Fujiwara, Y., Fujii, N., Nakagawa, T. (1996) Locations of local anesthetic dibucaine in model membranes and the interaction between dibucaine and a Na^{+} channel inactivation gate peptide as studied by ^{2}H- and ^{1}H-NMR Spectroscopies. **Biophys. J. 71**:1911-1207.
- Kuroda Y., Maeda Y., Miyamoto K., Tanaka K., Kanaori K., Otaka A., Fujii N., Nakagawa T. (1999) ^{1}H-NMR and circular dichroism spectroscopic studies on changes in secondary structures of the sodium channel inactivation gate peptides as caused by the pentapeptide KIFMK. **Biophys J. 77:**1363-73.
- Kuroda Y., Miyamoto K., Maeda Y., Matsumoto,M., Kanaori K., Otaka A., Fujii N., Nakagawa T. (2000) Structural study of the sodium channel inactivation gate peptide including an isoleucine-phenylalanine-methionine motif and its analogous peptide (phenylalanine/glutamine) in trifluoroethanol solutions and SDS micelles. **J. Peptide Res. 56:**172-184**.**
- Lee, A.G., Birdsall, J.M. Levine, Y.K., Metcalfe, J.C. (1972) High resolution proton relaxation studies of lecithins. **Biochim. Biophys. Acta 255:**43-56.
- Lee, A.G. (1976a) Model of action of local anaesthetics. **Nature 262:**545-548.

- Lee, A.G. (1976b) Interactions between anaesthetics and lipid mixtures amines. **Biochim. Biophys. Acta 448:**34-44.
- Lee, A.G. (1978) Effects of charged drugs on the phase transition temperatures of phospholipid bilayers. **Biochim. Biophys. Acta 514**:95-104.
- Lerche, H., Peter, W., Fleischhauser, R., Pika-Hartlaub, U., Malina, T., Mitrovic, N., Lehmann-Horn, F. (1997) Role in fast inactivation of the IV/S4-S5 loop of the human muscle Na^+ channel probed by cysteine mutagenesis. **J. Physiol. 505**:345-352.
- Lever, M.J., Miller, K.W., Paton, W.D.M., Smith, E.B. (1971) Pressure reversal of anaesthesia. **Nature 231**:368-371.
- Lissi, E., Bianconi, M.L., Amaral, A.T., de Paula, E., Blanch, L.E.B., Schreier, S. (1990) Methods for determination of partition coefficients based on the effect of solutes upon membrane structure. **Biochim. Biophys. Acta 1021**:46-50.
- Malheiros, S.V.P., de Paula, E., Meirelles, N.C. (2000) Pathways involved in Trifluoperazine, Dibucaine and Praziquantel induced hemolysis. **Biophys. Chem. 83**:89-100.
- Marban, E., Yamagish, T., Tomaselli, F. (1998) Structure and function of voltage-gated sodium channels. **J. Physiol. 508**:647-657.
- Martin, D.G., Watson, C.E., Gold, M.B., Woodard, C.L.Jr., Baskin, S.I. (1995) Topical anesthetic-induced methemoglobinemia and sulfhemoglobinemia in macaques: a comparasion of benzocaine and lidocaine. **J. Appl. Toxicol. 15**:153-158.
- McPhee, J.C., Ragsdale, D.S., Scheuer, T., Catterall, W.A., (1995) A critical role for transmembrane segment IVS6 of the sodium channel alpha subunit in fast inactivation. **J Biol Chem. 270**:12025-12034.
- McPhee, J.C., Ragsdale, D.S., Scheuer, T., Catterall, W.A. (1996) Common molecular determinants of local anesthetic, antiarrhythmic, and anticonvulsant block of voltage-gated Na+ channels**. Proc. Natl. Acad. Sci. USA 93**:9270-9275**.**
- Mitrovic, N., Lerche, H., Heine, R., Fleischhauer, R., Pika-Hartlaub, U., Hartlaub, U., George, A. L., Lehmann-Horn, F. (1996) Role in fast inactivation of conserved amino acids in the IV/S4-S5 loop of the human muscle Na^+ channel. **Neuroscience Lett. 214**:9-12**.**

- Miyamoto, K., Kanaori, K., Nakagawa, T., Kuroda, Y. (2001a) Solution structures of the inactivation gate particle peptides of rat brain type-IIA and human heart sodium channels in SDS micelles **J. Peptide Res. 57:**203-214**.**
- Miyamoto, K., Nakagawa, T., Kuroda, Y. (2001b) Solution structures of the cytoplasmic linkers between segments S4 and S5 (S4-S5) in domains III and IV of human brain sodium channels in SDS micelles. **J. Peptide Res. 58:**193-203.
- Narahashi, T., Yamada, M. (1969) Cationic forms of local anaesthetics block action potentials from inside the nerve membrane. **Nature 223:**748-749.
- Noda, M., Ideda, M., Kayana T., Suzuki, H., Takeshima, H., Kurasaki, M., Takahashi, H., Numa, S. (1986) Existence of distinct sodium channel messenger RNAs in rat brain. **Nature 320:**188-192.
- Pinto, L.M.A., Yokaichiya, D.K., Fraceto, L.F., de Paula, E. (2000) Interaction of benzocaine with model membranes. **Biophys. Chem**. **87**:213-223.
- Ragsdale, D.S., McPhee, J.C., Scheuer, R., Catterall, W.A. (1994) Molecular determinants of state-dependent block of Na^+ channels by local anesthetics. **Science 265:**1724-1728.
- Ragsdale D.S., McPhee J.C., Scheuer, R., Catterall, W.A. (1996) Common molecular determinants of local anesthetic, antiarrhytmic, and anticonvulsant block of voltage-gated Na^+ channels. **Proc. Natl. Acad. Sci. USA 93**:9270-9275.
- Ragsdale, D.S., Avoli, M. (1998) Sodium channels as molecular targets for antiepiletic drugs. **Brain Res. Rev. 26**:16-28.
- Rohl, C.A., Boeckman, F.A., Baker, C., Scheuer, T., Catterall, W.A., Klevit, R.E. (1999) Solution structure of the sodium channel inactivation gate. **Biochemistry 38**:855-861.
- Schopflin, M., Fingeli, U.P., Perlia, X. (1987) A study on the interaction of local anesthetics with phospholipid model membranes by infrared ATR spectroscopy. **J. Am. Chem. Soc. 109**:2375-2380.
- Schreier, S., Frezzatti Jr., W.A., Araujo, P.S., Chaimovich, H., Cuccovia, I.M. (1984) Effect of lipid membranes on the apparent pK of the local anesthetic tetracaine. Spin label and titration studies. **Biochim. Biophys. Acta 769:**231-237.
- Schreier, S.; Amaral, A.T., Stachissini, A.S., Bianconi, M.L. (1986) Electron spin resonance study of benzoic acid esters, analogs of local anesthetics. Interaction with membranes, aggregation and hydrolysis. **Bull. Magn. Res. 8**:166-171.

- Scheuer, T. (1999) A revised view of local anesthetic action: What channel state is really stabilized? **J. Gen. Physiol. 113**:3-6.
- Scholz, A. (2002) Mechanisms of local anaesthetics on voltage-gated sodium and other ion channels. **British J. of Anaesthesia 89**:52-61.
- Seelig, A. (1987) Local anesthetics and pressure: a comparison of dibucaine binding to lipid monolayers and bilayers. **Biochim. Biophys. Acta 899**:196-204.
- Seeman, P. (1966) Erythrocyte membrane stabilization by local anesthetics and tranquilizers. **Biochem. Pharmacol. 15**:1753-1766.
- Sikaris, K.A., Sawyer, W.H. (1982) The interaction of local anaesthetics with synthetic phospholipid bilayer. **Biochem. Pharmacol. 31:**2625-2631.
- Skou, J.C. (1954) Local anesthetics. V. The action of local anesthetics on monomolecular layers of stearic acid. **Acta Pharmacol.Toxicol. 10**:317-324.
- Slater, J.S.; Kelly, M.B.; Larkin, J.D.; Ho, C.; Mazurek, A.; Taddeo, F.J.; Yeager, M.D., Stubbs, C.D. (1997) Interaction of alcohols and anesthetics with protein kinase Cα. **J. Biol. Chem. 272**:6167-6173.
- Strichartz, G.R., Ritchie, J.M. (1987) **Local Anesthetics**, **Handbook of Experimental Pharmacology**, (Strichartz, G.R. ed.), vol. 81, cap. 2, Springer-Verlag, Berlin.
- Tang, L., Kallen, R.G., Horn, R. (1996) Role of an S4-S5 linker in sodium channel inactivation probed by mutagenesis and a peptide blocker. **J.Gen. Physiol. 108**: 89-104.
- Trudell, J.R. (1977) A unitary theory of anesthesia based on lateral phase separations in nerve membranes. **Anesthesiol. 46**:5-10.
- Ueda, I., Tashiro, C., Arakawa, K. (1977) Depression of phase-transition temperature in a model cell membrane by local anesthetics. **Anesthesiol. 46**:327-332.
- Voet, D., Voet, J. (1995) **Biochemistry**, John Wiley & Sons Inc., New York.
- Wakita, M., Kuroda, Y., Fujiwara, Y., Nakagawa, T. (1992) Conformations of dibucaine and tetracaine in small unilamellar phosphatidylcholine vesicles as studied by nuclear Overhauser effects in ^{1}H nuclear magnetic resonance spectroscopy. **Chem. Phys. Lipids 62:**45-54.
- Westman, J., Boulanger, Y., Ehrenberg, A., Smith, I.C.P. (1982) Charge and pH dependent drug binding to model membranes. A ^{2}H-NMR and light absorption study. **Biochim. Biophys. Acta 685:**315-328.

- Yarov-Yarovoy, V., McPhee, J.C., Idsvoog, D., Pate, C., Scheuer T., Catterall, W.A. (2002) Role of amino acid residues in transmembrane segments IS6 and IIS6 of the Na^+ channel alpha subunit in voltage-dependent gating and drug block. **J. Biol. Chem. 277:**35393-35401.
- Yokono, S., Ogli, K., Miura, S., Ueda, I. (1989) 400MHz two-dimensional nuclear Overhauser spectroscopy on anesthetic interaction with lipid bilayer. **Biochim. Biophys. Acta 982**:300-302.

6 – ANEXO (Trabalhos em colaboração)

6.1 – Pinto, L.M.A., **Fraceto, L.F.**, Santana, M.H.A., Pertinhez, T.A., Oyama Jr, S., de Paula, E. (2003) Physico-Chemical characterization of benzocaine-β-Cyclodextrin inclusion complexes. **Submetido.**

6.2 – Pertinhez, T.A., Sherwood, A.K., **Fraceto, L.F.**, Bouchard, M., Pitkeathly, M., Smith, L.J. (2003) α and β conformational preferences in fibril-forming peptides characterized using NMR and CD techniques. Spectroscopy (*no prelo*).

6.1 – PHYSICO-CHEMICAL CHARACTERIZATION OF BENZOCAINE-β–CYCLODEXTRIN INCLUSION COMPLEXES

Physico-Chemical Characterization of Benzocaine-β-Cyclodextrin Inclusion Complexes

Luciana M. A. Pinto[a], Leonardo F. Fraceto[a,b], Maria Helena A. Santana[c], Thelma A. Pertinhez[b], Sérgio Oyama Junior[b] and Eneida de Paula[a,*]

[a] Departamento de Bioquímica, Instituto de Biologia, Universidade Estadual de Campinas, Cidade Universitária Zeferino Vaz, s/n, C.P. 6109, 13083-970, Campinas, SP, Brazil.

[b] Centro de Biologia Molecular Estrutural (CeBiME), Laboratório Nacional de Luz Síncrotron , C.P. 6192, CEP 13084-971, Campinas, SP, Brazil.

[c] Departamento de Processos Biotecnológicos, Faculdade de Engenharia Química, Universidade Estadual de Campinas, Campinas, SP, Brazil.

* Corresponding author: Tel.: + 55 19-3788-6143; Fax: + 55 19-3788-6129; E-mail address: depaula@unicamp.br (E. de Paula).

Abstract

Local anesthetics are able to induce pain relief by binding to the sodium channel of excitable membranes, blocking the influx of sodium ions and the propagation of the nervous impulse. Benzocaine (BZC) is a local anesthetic whose low water-solubility limits its application to topical formulations. The present work focuses on the characterization of inclusion complexes of BZC in β-cyclodextrin (β-CD). Differential scanning calorimetry and electron microscopy revealed the formation and the morphology of the complex. Fluorescence spectroscopy showed a BZC:β-CD 1:1 stoichiometry. Phase-solubility diagrams allowed the determination of the association constants between BZC and β-CD (549 M^{-1}) and revealed a more than 3-fold increase in BZC solubility upon complexation with β-CD. The details of BZC/β-CD molecular interaction were analyzed by ^{1}H 2D NMR allowing an inclusion model for BZC into β-CD where the aromatic ring of the anesthetic is located near the head of the β-CD cavity. Moreover, the complex seems to be less toxic than BZC alone, since it induced a decrease in the *in vitro* oxidation of human hemoglobin. These results suggest that the BZC/β-CD complex represents an effective novel formulation to enhance BZC solubility in water, turning it promising for use in infiltrative anesthesia.

Keywords: benzocaine, cyclodextrin, local anesthetic, drug delivery.

1. Introduction

Pain is one of the most extensively studied problems in medicine and biology, challenging physicians and other professionals to look for novel ways to deal with it. Anesthetics are compounds that, when administered locally or systemically, are able to induce pain relief. While general anesthetics act on the synapses, local anesthetics (LA) work along the axons, blocking the action potential (Covino and Vassalo, 1976; Strichartz and Ritchie, 1987; de Jong, 1994). Today there is a strong clinical need for long-acting LA, as well as for molecules with decreased systemic uptake that could lead to less toxic side effects.

Benzocaine (BZC, Fig. 1a) is an ester-type local anesthetic used in topical, dermal and mucous formulations, while its parenteral administration is restricted by its low water solubility (Covino and Vassalo, 1976). The interaction of this molecule with model membranes has been previously examined in our laboratory (Pinto et al., 2000) where Electron Paramagnetic Resonance studies have revealed that BZC has intermediate hydrophobicity and a relatively low effect on lipid bilayer organization compared to other LA such as lidocaine and tetracaine.

The toxicity of ester-type LA has also been reported in the literature (Covino and Vassalo, 1976) as they can be hydrolyzed by plasma esterases, generating toxic metabolites such as the p-amino benzoic derivatives. BZC has a chemical resemblance to the ethyl ether *p*-amine-propyophenone (PAPP), which induces hemoglobin oxidation (Martin et al., 1995). The literature reports increased Met-hemoglobin (Met-Hb) levels induced by BZC in different species (Guertler and Pearce, 1994; Ellis et al., 1995; Martin et al., 1995; Kern and Langevin, 2000; Karim et al., 2001; Udeh et al., 2001).

The development of local anesthetic formulations in carriers such as liposomes, glucose polymers, dextran, hyaluronic acid, biopolymers, microspheres, etc. could offer the possibility of controlling drug delivery in biological systems, prolonging the anesthetic effect and reducing its toxicity (Kuzma et al., 1997; Yu et al., 1998). Complexation with cyclodextrins (CD) provides a way to increase the solubility, stability and bioavailability of drugs (Duchêne et al., 1985; Dollo et al., 1998). CD is able to form inclusion complexes with different classes of molecules, modifying their physical, chemical and biological properties (Rajewski and Stella, 1996). These cyclic polymers are formed by glucose

molecules, linked through 1-4 bonds, consist of 6 (α-CD), 7 (β-CD) or 8 (γ-CD) glucose units and the cone-shaped cavity of CD allows the accommodation of the hydrophobic groups of molecules such as local anesthetics. Studies involving the complexation of LA molecules with CD have been reported in the literature (Dollo et al., 1996a, b; Freville et al., 1996; Dollo et al., 1998, 2000) although none of them employed benzocaine.

The aim of the present study was to obtain inclusion complexes of benzocaine with β-CD. The stoichiometry of the inclusion complex was analyzed by fluorescence spectroscopy using the continuous variation method described by Higuchi and Connors (1965). Phase-solubility diagrams were used to evaluate the solubility of BZC and its association constants with β-cyclodextrin. Differential Scanning Calorimetry (DSC) and Scanning Electron Microscopy (SEM) assays were used to observe the formation and morphology of the solid inclusion complex obtained. Finally, Nuclear Magnetic Resonance (^{1}H-NMR) experiments revealed details of the geometry of the new chlatrate formed.

2. Experimental Section

2.1 Materials

Benzocaine, β-cyclodextrin (Fig. 1 a and b) and D_2O were obtained from Sigma Chemical Co. (St. Louis, MO). All other reagents were of analytical grade. Deionized water was used throughout the experiments.

2.2 Preparation of Solid Inclusion Complex

Inclusion complexes with 1:1 and 1:2 BZC/β-CD molar ratios were prepared by shaking appropriate amounts of the anesthetic and β-CD in deionized water at room temperature (25 ± 1 °C) for 1 h. After reaching equilibrium, the solution was freeze-dried in a Labconco Freeze-dry system (Freezone 4.5) and stored at –20 °C until further use. Physical mixtures (non-complexed drugs) were obtained by mixing BZC and β-CD powders.

2.3 Phase-Solubility Studies

This methodology was based on the solubility variation of the *guest* molecule (BZC) upon increase of the *host* molecule (β-CD) concentration (Higushi and Connors, 1965). An excess amount of BZC was added to an aqueous solution with increasing β-CD concentrations (0-10 mM) at room temperature. The samples were stirred at room temperature and an aliquot was filtered through a 0.45 μm membrane filter (Millipore). The amount of soluble BZC was spectrophotometrically determined at 284 nm (Pinto et al., 2000). The association constant (K_a) was calculated from the slope of the linear portion of the phase-solubility diagram according to equation 1 (Higushi and Connors, 1965):

$$K_a = \frac{slope}{S_0\,(1 - slope)} \tag{1}$$

Where S_0 is the aqueous solubility of benzocaine. The experiment was carried out in triplicate.

2.4 Fluorescence Studies

Changes in the intrinsic fluorescence of BZC upon variation of the BZC/β-CD molar ratios of complexation were monitored with a Hitachi F-4500 spectrofluorimeter, at room temperature. Excitation wavelength was set to 284 nm and the emission spectra were recorded from 300 to 450 nm. The stoichiometry of the complex was determined by *Job-plot* analysis (Connors, 1987). Equimolar stock solutions of BZC and β-CD were prepared and mixed in order to obtain the same final value of (M) as follows:

$$[\text{BZC}]_t + [\beta\text{-CD}]_t = \text{M} \tag{2}$$

Where t = total concentration.

Changes in fluorescence intensity (ΔI) were calculated as the difference in the emission of BZC in the presence (I) and in the absence (I_0) of β-CD. Subsequently $\Delta I.[\text{BZC}]_t$ was plotted against R, the molar ratio of complexation:

$$\boldsymbol{R} = \frac{[\boldsymbol{BZC}]_t}{\boldsymbol{M}} \tag{3}$$

In the biphasic plots obtained, the concentration of the BZC/β-CD complex (measured by ΔI) will reach a maximum corresponding to the point where the derivative d[BZC/β-

CD]/dr = 0, and the value of R, independently of M, or the association constant (K_a), can be determined (Loukas et al., 1998).

2.5 Scanning Electron Microscopy (SEM)

The BZC/β-CD inclusion complexes (1:1 and 1:2 molar ratio) were morphologically analyzed by Scanning Electron Microscopy (SEM), with a JEOL JSM–T300 Scanning Microscope. Samples of BZC, β-CD and BZC/β-CD physical mixtures (1:1 and 1:2) were also prepared at the same concentration of the inclusion complexes. The samples were mounted on aluminum stubs, using double-sided sticky tabs and vacuum coated with gold for 180 s, to render them electrically conductive.

2.6 Differential Scanning Calorimetry (DSC)

The various samples (10 mg) were placed in aluminum pans and the experiments run in a Universal V2.3D TA Instruments calorimeter at a 10 °C/min heating rate over a 30-200 °C range. An empty pan served as reference and Indium was used to calibrate the temperature. Measurements were performed at BZC/β-CD 1:1 and 1:2 (molar ratio) both for the inclusion complexes and the physical mixtures; BZC and β-CD thermograms were also run.

2.7 Nuclear Magnetic Resonance (NMR)

One-dimensional ^{1}H-NMR spectra of BZC/β-CD complexes were recorded with a 500 MHz Bruker DRX500 spectrometer (Universidade de São Paulo, Brazil) at 25 ^{o}C. Samples were suspended in D_2O and degassed by bubbling N_2 directly in the NMR tubes. The chemical shifts (Δδ) are reported as ppm and are referenced to the residual water signal (4.7 ppm).

Two-dimensional (2D) rotating frame Overhauser effect spectroscopy (ROESY) experiments were performed on a Varian INOVA 600 MHz spectrometer (CeBiME, Laboratório Nacional de Luz Síncrotron, Brazil) using a spin-lock field of 3 kHz of 300 ms. The spectra were collected using 2048 complex data points in the F2 dimension and 324 increments. The spectral width was 10 ppm in both dimensions and 8 free induction decays were acquired per increment.

The spectrum was processed using the VNMR 6.1 software (Varian Inc.). The cross-peaks volumes were directly correlated with inter-nuclear distance, r, of the two observed protons, via the known r^{-6} dependence (Evans, 1995) The fixed and well-known intramolecular distances between two vicinal aromatic protons (2.48 Å) of BZC – *ortho* and *meta* – were used for calibration.

2.8 Molecular Modeling

Molecular modeling studies were performed in an Octane2 workstation (Silicon Graphics Inc.) using the InsightII package (Accelrys Inc.). All the calculations were done with the Discover module using the Consistent Valence Force Field (CVFF). The BZC model building was performed with the Builder and Biopolymer modules of InsightII. The β-CD coordinates were taken from the β-amylase/β-cyclodextrin complex crystal structure (PDB 1BFN, Adachi et al., 1998). Each molecule was first energy-minimized separately through a combination of the steepest descents and conjugate gradient algorithms, until a maximum derivative of 0.001 Kcal/mol.Å was achieved. The molecules were further manually assembled into several complexes with different relative orientations, followed by energy minimization. No distance restraints were used at any time during the calculations. The final energy-minimized complexes were compared to the experimental results obtained by ^{1}H-NMR.

2.9 Methemoglobin Formation

Freshly purified (up to 5 days after blood collection) human hemoglobin solutions – 10^{-5} M - were incubated for 30 min. with increasing amounts of BZC/β-CD complexes. Met-hemoglobin formation was followed at 630 nm (Winterbourn and Metodiewa, 1990) and $K_3Fe(CN)_6$ was used to induce 100% oxidation. The results were compared with the oxidation caused by plain BZC, as published before (Pinto et al., 2000).

3. Results and Discussion

3.1 Phase-Solubility Studies

The increase in solubility occurred as a linear function of β-CD concentration (Fig. 2) corresponding to the A_L-type profile defined by Higuchi and Connors (1965). This relationship suggests the formation of a 1:1 BZC/β-CD complex. The association constant (K_a), as described by equation 1, was calculated to be 549 M^{-1}, thus indicating the formation of a stable complex (Loukas et al., 1998).

The increased aqueous solubility of BZC in the presence of β-CD suggests that these molecules are able to form inclusion complexes. Since the complexation occurs at a 1:1 molar ratio (see section 3.2), the solubility of BZC in water is expected to be enhanced by complexation up to the limit of β-CD solubility - *ca.* 16 mM (Szejtli, 1998). In fact the results obtained here strengthen this hypothesis since, in the presence of 10 mM β-CD, benzocaine reaches a concentration at least 3 times higher (Fig. 2) than those of the free drug in water (Pinto et al., 2000).

3.2 Stoichiometry of the Complex

Complexation depends on the polarity and size of the *guest* molecule with respect to the inner cavity of the *host* CD molecule. Taken advantage of the fact that upon inclusion of a fluorescent *guest* molecule into the β-CD cavity, generally an enhancement in fluorescence is observed due to shielding from quenching and non-radioactive decay processes (Madrid et al., 1999), the stoichiometry of the BZC/β-CD complexation was obtained by fluorescence spectroscopy. The enhancement in BZC fluorescence upon complexation was quantified by the changes of the integrated fluorescence emission ratio, ΔI, as described in the Experimental Section. The *Job-plot* obtained (Fig. 3) showed a maximum ΔI at $R = 0.5$ - which is indicative of a 1:1 stoichiometry of the BZC/β-CD complex – in agreement with phase-solubility data.

3.3 Formation and Morphology of the Complex

Supporting evidence for the complexation of BZC with β-CD was also obtained from SEM, DSC and NMR data. SEM pictures showed that the shape and size of the inclusion complexes were completely different from the ones of free BZC or β-CD (Fig. 4). Typical crystals of β-CD (Duchêne, 1987) and BZC were found in many different sizes (Fig. 4a and 4b, respectively). At the two molar ratios of the BZC/β-CD inclusion complexes studied (1:1 and 1:2) a compact and homogeneous powder-like structure was observed, Fig. 4c, whose dimensions were smaller than those of the crystals of BZC or β-CD alone. The physical mixtures of BZC and β-CD powders revealed similarities with the crystals of the free molecules, (Fig. 4d) where residual β-CD crystals were easily identified (arrows). On the other hand, some agglomeration of BZC around β-CD crystals was observed both in the 1:1 (Fig. 4d) and 1:2 (not shown) BZC/β-CD physical mixture.

Representative DSC thermograms measuring the rate of heat absorbed by BZC, β-CD, BZC/β-CD inclusion complex and physical mixture, at 1:1 and 1:2 molar ratios, are shown in Fig. 5.

DSC thermograms of β-CD and free BZC detected endothermic peaks at 140.4 and 90.7 ^{o}C, respectively (Fig. 5a and 5b), corresponding to the melting point of these two compounds (Martindale, 1993; Loftsson and Brewster, 1996). The thermogram of the BZC/β-CD inclusion complex lacked the endothermic peaks of both BZC and β-CD and showed a weak and broad transition, extending from 60 to 120 ^{o}C for the 1:1 molar ratio (Fig. 5c) and from 80 to 160 ^{o}C, for the 1:2 molar ratio (Fig. 5d). The absence of the endothermic peaks in the complex strongly suggests the insertion of the guest molecule inside the β-CD cavity (Uekama et al., 1983). The increased absorption observed for the 1:2 molar ratio complex is due to some non-complexed, remaining β-CD. Finally, the curves of the physical mixtures resemble the sum of the individual curves of BZC and β-CD (Fig. 5e and 5f).

Overall, the SEM and DSC results indicate the formation of inclusion complex between BZC and β-CD and also demonstrate that no complex is formed in the physical mixture of the compounds.

3.4 Model Validation by NMR

The inclusion of BZC into the β-CD cavity was first evaluated by the changes in the chemical shifts of the protons in the complex, relatively to free BZC and β-CD (Fig. 6). Table I presents the assignment of BZC and β-CD and the chemical shifts deviations due to complexation. All the peaks belonging to BZC protons were shifted: the ethyl-CH_3 upfield and the aromatics to downfield. In the case of β-CD molecule, only H1 did not change the chemical shifts after complexation with BZC. As for the other protons, the H3 were the most significantly altered ones, followed by H6 and H5. Peak overlap did not allow evaluation of the H4 shift. H3 protons resonance shifted upfield while H5 shifted downfield, leading to an overlap with the peak of H6 protons. Similar changes in the δ of H3, H6 and H5 protons were found for the *p*-iodophenolate/α-CD complex (Schneider et al., 1998) where the aromatic ring of the drug seems to fit near the head of the cavity of CD.

To better elucidate the relative position of BZC with respect to β-CD protons we carried out ROESY experiments. Contacts were observed between protons H5 and H6 - belonging to β-CD - and the aromatic and methyl protons of BZC. These cross-peaks are intense and agree with the Δδ data (where methyl and aromatic protons were mainly changed by complexation). The volumes of the cross-peaks were measured and the inter-molecular distances calculated, as described in the Experimental Section.

Cyclodextrin has six identifiable protons in the NMR spectrum: protons H1, H2, H4 being at the outer surface of cyclodextrin, while protons H3 and H5 sit in the inner surface (or cavity) and are very important for the study of the interaction of *guest* compounds with cyclodextrins. H6 (CH_2OH – Fig. 1b) is located in the minor border cavity of β-CD (Schneider et al., 1998).

The data suggest that BZC interacts only with H5, and not with H3 protons of the inner cavity of β-CD. They indicate that BZC inserts its aromatic ring nearby the protons H5 (2.5 Å) and H6 (2.5 Å) i.e., towards the minor face (head) of the β-CD cavity. The methyl protons of BZC also get close to H5 and H6, but the distances are not so short (3.5 and 2.6 Å, respectively) as for the aromatic protons.

Molecular modeling studies revealed that a preferred final relative orientation for the BZC/β-CD complex occurs in spite of the different initial configurations arbitrarily imposed. The minimum energy complex obtained is shown in Fig. 7. It is interesting to note that although no fixed distances were imposed during the calculations, the results are in very good agreement with the distances obtained by 2D-NMR, mainly for the H_5-aromatic protons (2.66 and 2.43 Å).

Taken together, these convergent results coming from independent techniques support the existence of a unique spatial organization for the BZC/β-CD complex.

3.5 In Vitro Toxicity

In order to test the toxicity of this novel formulation, an essay using purified human hemoglobin was performed. In a previous work we have observed that the free anesthetic was able to promote Met-hemoglobin formation (Pinto et al., 2000). Here we used the same protocol to check hemoglobin oxidation induced by the BZC/β-CD complex. No significant increase in Met-Hb content was detected after incubation of Oxy-Hb with the 1:1 complex, up to 7 mM (Fig. 8), indicating that complexation could offer an additional advantage for the infiltrative administration of BZC, diminishing its toxic effects.

4. Conclusions

BZC is used in anesthesia of the skin and mucous membranes, due to its limited water solubility (Covino and Vassalo, 1976). This interesting local anesthetic molecule has also unique features – in comparison to the commercially used LA - such as the lack of an ionizable amine group (Covino and Vassalo, 1976; Pinto et al., 2000) keeping it always uncharged and the absence of use-dependent block (Butterworth and Strichartz, 1990).

The present results show that a stable BZC/β-CD complex could be prepared at a 1:1 molar ratio. This novel formulation effectively enhanced the solubility of benzocaine in water, increasing its local availability.

The complexation with β-CD generated a less toxic BZC formulation, as seen by the decreased oxidation of hemoglobin, turning this preparation promising for infiltrative use and less risky to the patient. Complexation could also delay the clearance of BZC from plasma, increasing the duration of anesthesia, as seen for other - liposomal - LA formulations (Yu et al., 1998). *In vitro* and *in vivo* toxicological tests have been carried out with this formulation and will be published in due time.

Acknowledgements

This research was supported by Fundação de Amparo à Pesquisa do Estado de São Paulo (Proc. # 96/1451-9). We thank Dr. S. Schreier for the use of the NMR equipment at University of São Paulo. We gratefully acknowledge CeBiME - Laboratório Nacional de Luz Síncrotron, for the opportunity to use the NMR facilities. LMAP (Grant # 98/15936-0) and LFF (Grant # 00/0362-0) are the recipients of fellowships from FAPESP; EP is the recipient of a fellowship from CNPq. We express our thanks to M. B. de Jesus for technical assistance.

References

Adachi, M., Mikami, B., Katsube, T., Utsumi, S., 1998. Crystal structure of recombinant soybean beta-amylase complexed with beta-cyclodextrin. J. Biol. Chem. 273, 19859-19865.

Butterworth, J.F., Strichartz, G.R., 1990. Molecular mechanisms of local anesthesia: a review. Anesthesiology, 72, 711-734.

Connors, K.A., 1987. Binding constants, the measurement of molecular complex stability, Wiley, New York.

Covino, B.G. and Vassalo, H.G., 1976. Local anesthetics: mechanisms of action and clinical use, Grune and Stratton, New York.

de Jong, R.H., 1994. Local anesthetics. C. C. Thomas, Springfield, Illinois.

Dollo, G., Le Corre, P., Chevanne, F., Le Verge, R., 1996a. Inclusion complexation of amide-typed local anesthetics with β-cyclodextrin and its derivatives. I. Physicochemical characterization, Int. J. Pharm., 131, 219-228.

Dollo, G., Le Corre, P., Chevanne, F., Le Verge, R., 1996b. Inclusion complexation of amide-typed local anesthetics with β-cyclodextrin and its derivatives. II. Evaluation of affinity constants and in vitro transfer rate constants. Int. J. Pharm., 131, 219-228.

Dollo, G., Le Corre, P., Freville, J.C., Chevanne, F., Leverge, R., 2000. Biopharmaceutics of local anesthetic-cyclodextrin complexes following loco-regional administration. Ann. Pharm. Fr. 58, 425-432.

Dollo, G., Thompson, D.O., Le Corre, P., Chevanne, F., Le Verge, R., 1998. Inclusion complexation of amide-typed local anesthetics with β-cyclodextrin and its derivatives. III. Biopharmaceutics of bupivacaine-SBE7-β-CD complex following percutaneous sciatic nerve administration in rabbits Int. J. Pharm., 164, 11-19.

Duchêne, D., Vaution, C., Glomot, F., 1985. La biodisponibilité des principes actifs par inclusion dans les cyclodextrines. STP Pharma, 4, 323-332.

Duchêne, D., 1987. Cyclodextrins and their industrial uses, Editions de Santé, Paris.

Ellis, F.D., Seiler, J.G. III, Palmore, M.M.Jr., 1995. Methemoglobinemia: a complication after fiberoptic orotracheal intubation with benzocaine spray. J. Bone Joint Surg. Amer., 77, 937-939.

Evans, J.N.S., 1995. Biomolecular NMR Spectroscopy, Oxford University Press, Oxford.

Freville, J.C., Dollo, G., Le Corre, P., Chevanne, F., Le Verge, R., 1996. Controlled systemic absorption and increased anesthetic effect of bupivacaine following epidural administration of bupivacaine-hydroxypropyl-beta-cyclodextrin complex. Pharm. Res., 13, 1576-1580.

Guertler, A.T., Pearce, W.A., 1994. A prospective evaluation of benzocaine-associated methemoglobinemia in human beings. Ann. Emerg. Medic., 24, 626-630.

Higuchi, T. and Connors, K.A., 1965. Phase-solubility techniques. Adv. Anal. Chem. Inst., 4, 117-121.

Karim, A., Ahmed, S., Siddiqui, R., Mattana, J., 2001. Methemoglobinemia complicating topical lidocaine used during endoscopic procedures. Am. J. Med., 11, 150-153.

Kern, K. and Langevin, P.B., 2000. Methemoglobinemia after topical anesthesia with lidocaine and benzocaine for a difficult intubation. J. Clin. Anesthesia, 12, 167-172.

Kuzma, P.J., Kline, M.D., Calkins, M.D., Staats, P.S., 1997. Progress in the development of ultra-long-acting local anesthetics. Reg. Anesthesia, 22,543-551.

Loftsson, T. and Brewster, M.E., 1996. Pharmaceutical applications of cyclodextrins. 1. Drug solubilization and stabilization. J. Pharm. Sci., 85, 1017-1025.

Loftsson, T. and Masson, M., 2001. Cyclodextrins in topical drug formulations: theory and practice Int. J. Pharm., 225, 15-30.

Loukas, Y.L., Vraka, V., Gregoriadis, G., 1998. Drugs, in cyclodextrins, in liposomes: a novel approach to the chemical stability of drugs sensitive to hydrolysis. Int. J. Pharm., 162, 137-142.

Madrid, J.M., Villafruela, M., Serrano, R., Mendicuti, F., 1999. Experimental thermodynamics and molecular mechanics calculations of inclusion complexes of 9-methyl anthracenoate and 1-methyl pyrenoate with β-cyclodextrin. J. Phys. Chem. B, 103, 4847-4853.

Martin, D.G., Watson, C.E., Gold, M.B., Woodard, C.L.Jr., Baskin, S.I., 1995. Topical anesthetic-induced methemoglobinemia and sulfhemoglobinemia in macaques: a comparison of benzocaine and lidocaine. J. Appl. Toxicol., 15, 153-158.

Martindale, 1993. The Extra Pharmacopoeia, The Pharmaceutical Press, London.

Pinto, L.M.A., Yokaichiya, D.K., Fraceto, L.F., de Paula, E., 2000. Interaction of benzocaine with model membranes. Biophys. Chem., 87, 213-223.

Rajewski, R.A. and Stella, V.J., 1996. Pharmaceutical applications of cyclodextrins. 2. *In vivo* drug delivery. J. Pharm. Sci., 85, 1142-1169.

Schneider, H.-J., Hacket, F., Rüdige, V., Ikeda, H.., 1998. NMR studies of cyclodextrin and cyclodextrin complexes. Chem. Rev., 98, 1755-1785.

Strichartz, G.R. and Ritchie, J.M., 1987. Local Anesthetics, Handbook of Experimental Pharmacology, (Strichartz G.R. ed.), vol. 81, chap. 2, Springer-Verlag, Berlin.

Szejtli, J., 1998. Introduction and general overview of cyclodextrin chemistry. Chem. Rev., 98, 1743-1753.

Udeh, C., Bittikofer, J., Sum-Ping, S.T.J., 2001. Severe methemoglobinemia on reexposure to benzocaine. J. Clin. Anesthesia, 13, 128-130.

Uekama, K., Narisawa, S., Hirayama, F., Otagiri, M., 1983. Improvement of dissolution and absorption characteristics of benzodiazepines by cyclodextrin complexation. Int. J. Pharm., 179, 65-71.

Winterbourn, C. C., Metodiewa, D., 1999. Reactivity of biologically important thiol compounds with superoxide and hydrogen peroxide. Free Rad. Biol. Med. 27, 322-328.

Yu, H.-Y., Sun, P., Hou, W.-Y., 1998. Prolonged local anesthetic effect of bupivacaine liposomes in rats. Int. J. Pharm., 176, 133-136.

Table I: ^{1}H-NMR: chemical shift of BZC and β-CD protons before and after complexation. Peak identification as visualized in Fig. 1.

Assignments	BZC (ppm)	β-CD (ppm)	BZC/β-CD (ppm)	Δδ (ppm)
a - Ethyl-CH_3	1.31		1.13	0.18
b - Ethyl-CH_2	4.299		4.28	0.02
c - Aromatic-3,5	6.79		6.87	-0.08
d - Aromatic-2,6	7.82		7.97	-0.15
H_1		5.04	5.04	-0.00
H_2		3.62	nd	nd
H_3		3.93	3.78	0.15
H_4		3.56	nd	nd
H_5		3.82	3.75	0.06
H_6		3.84	3.75	0.09

nd – not determined due to peak overlap.

Figure Legends

Fig. 1. Chemical structures and NMR peak identification for (a) benzocaine and (b) β-cyclodextrin - schematic representation.

Fig. 2. Phase-solubility diagram for BZC at increasing β-CD concentrations, determined at room temperature.

Fig. 3. Continuous variation plot (Job plot) for the BZC/β-CD complex obtained by fluorescence spectroscopy. $\lambda_{excitation}$ = 284 nm, $\lambda_{emission}$= 300-450 nm, room temperature.

Fig. 4. Scanning electron microscopy of (a) β-CD, (b) BZC, (c) BZC/β-CD 1:1 complex, (d) physical mixture of BZC and β-CD, 1:1, molar ratio. 1500 x magnification, bar = 10 μm.

Fig. 5. Differential scanning calorimetry thermograms of (a) β-CD, (b) BZC, (c) BZC/β-CD 1:1 complex, (d) BZC/β-CD 1:2 complex, (e) physical mixture of BZC/β-CD 1:1 and (f) physical mixture of BZC/β-CD 1:2 molar ratio.

Fig. 6. Monodimensional ^{1}H-NMR spectra of (a) BZC, (b) β-CD and (c) the BZC/β-CD complex. a) [BZC] = 3 mM, b) [β-CD] = 10 mM and c) [BZC] and [β-CD] =10 mM. Samples in D_2O, 25^{o}C.

Fig. 7. Model of BZC insertion into the β-CD cavity, proposed by molecular modeling. Distances between aromatic BZC protons and H5 protons are shown.

Fig. 8. MetHb formation induced by (+) BZC and (#) BZC/β-CD complex (1:1 molar ratio) in a purified Hb solution, 5 mM PBS buffer, pH 7.4, at room temperature.

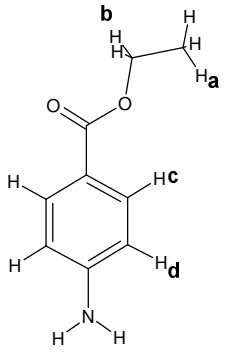

Fig. 1 - a

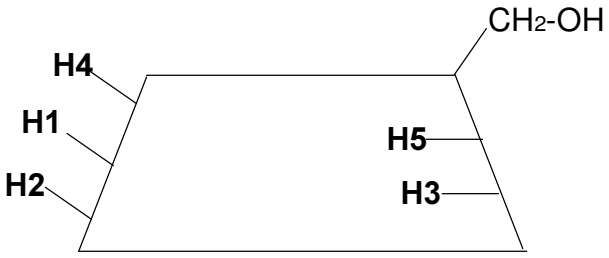

Fig. 1 - b

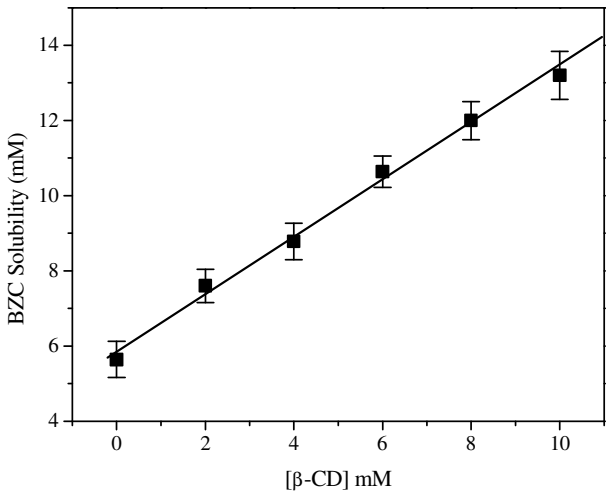
BZC Solubility (mM)
[β-CD] mM
14
12
10
8
6
4
0
2
4
6
8
10

Fig. 2

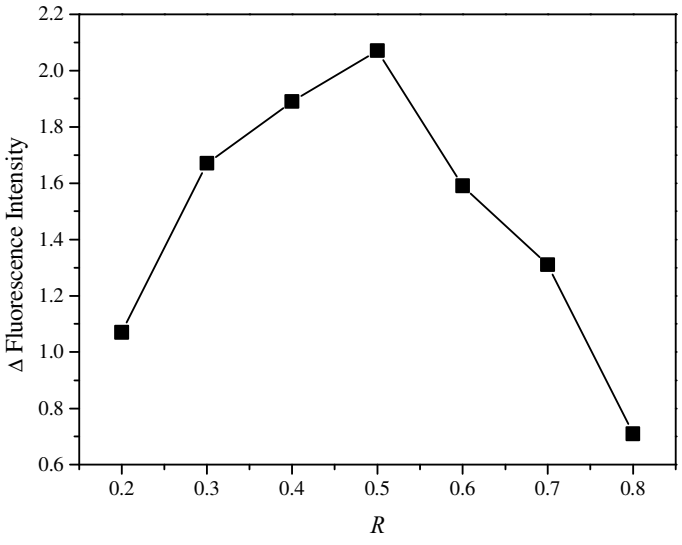
Δ Fluorescence Intensity
R
2.2
2.0
1.8
1.6
1.4
1.2
1.0
0.8
0.6
0.2
0.3
0.4
0.5
0.6
0.7
0.8

Fig. 3

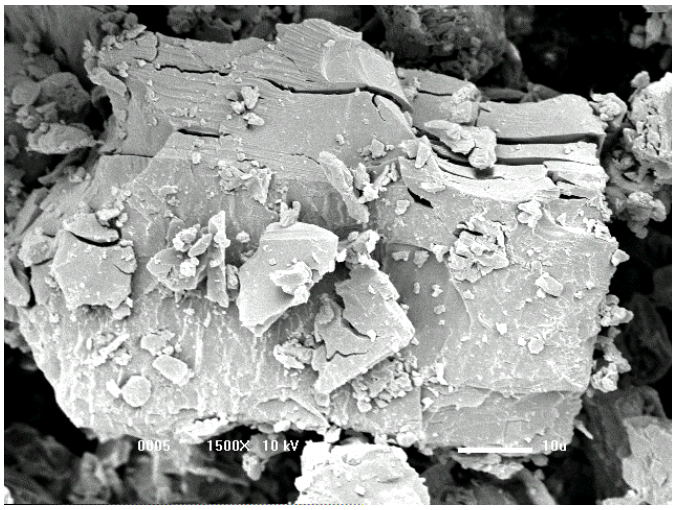

Fig. 4 – a

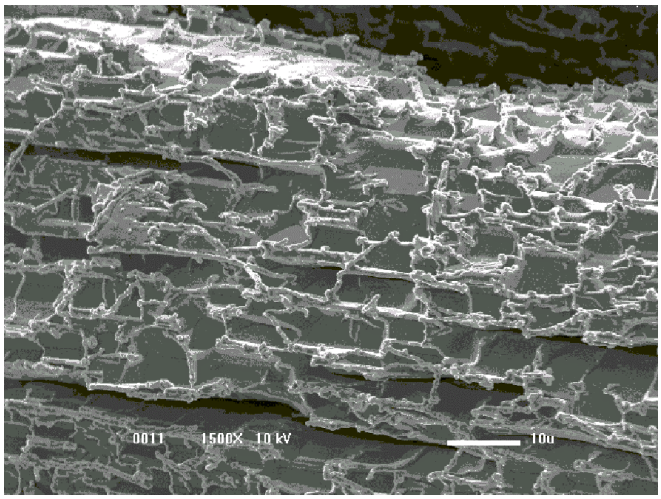

Fig. 4 - b

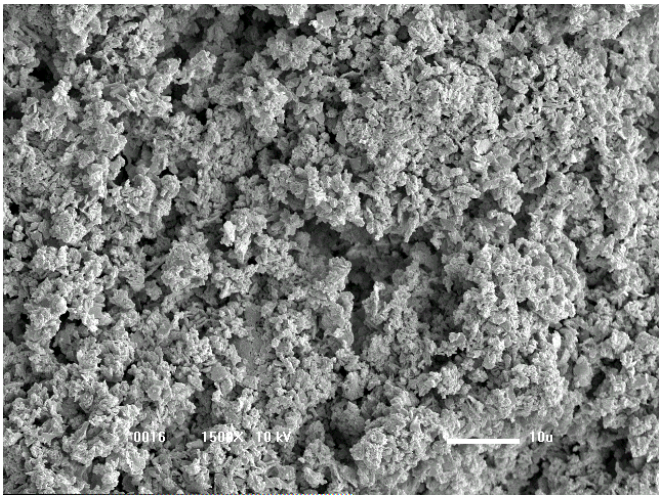

Fig. 4 - c

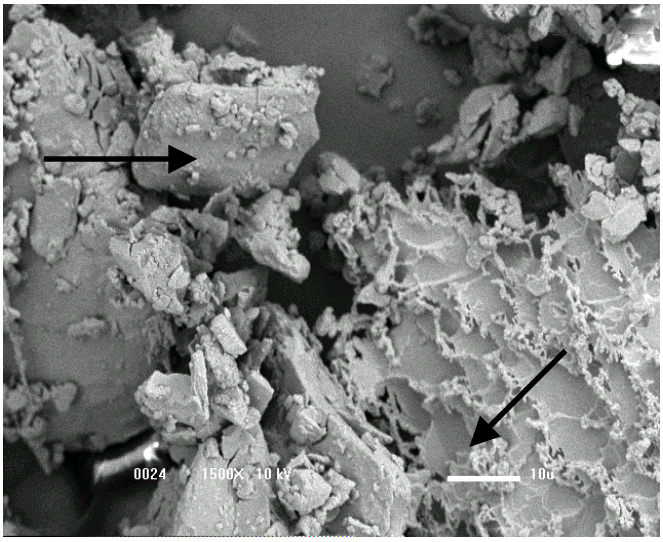

Fig. 4 - d

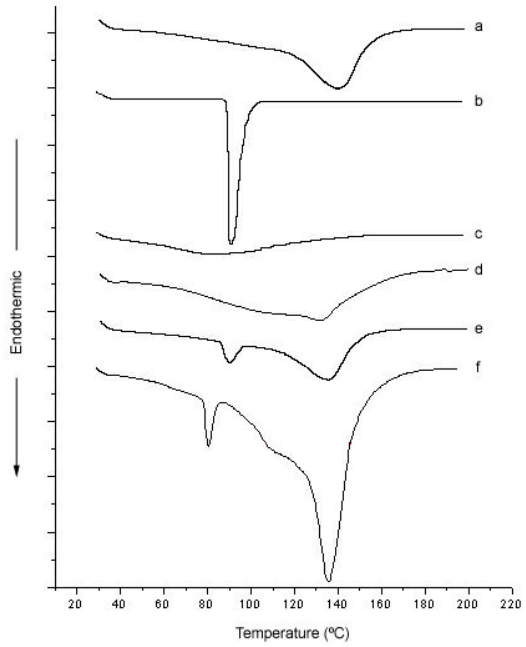
a
b
c
d
e
f
Endothermic
20 40 60 80 100 120 140 160 180 200 220
Temperature (ºC)

Fig. 5

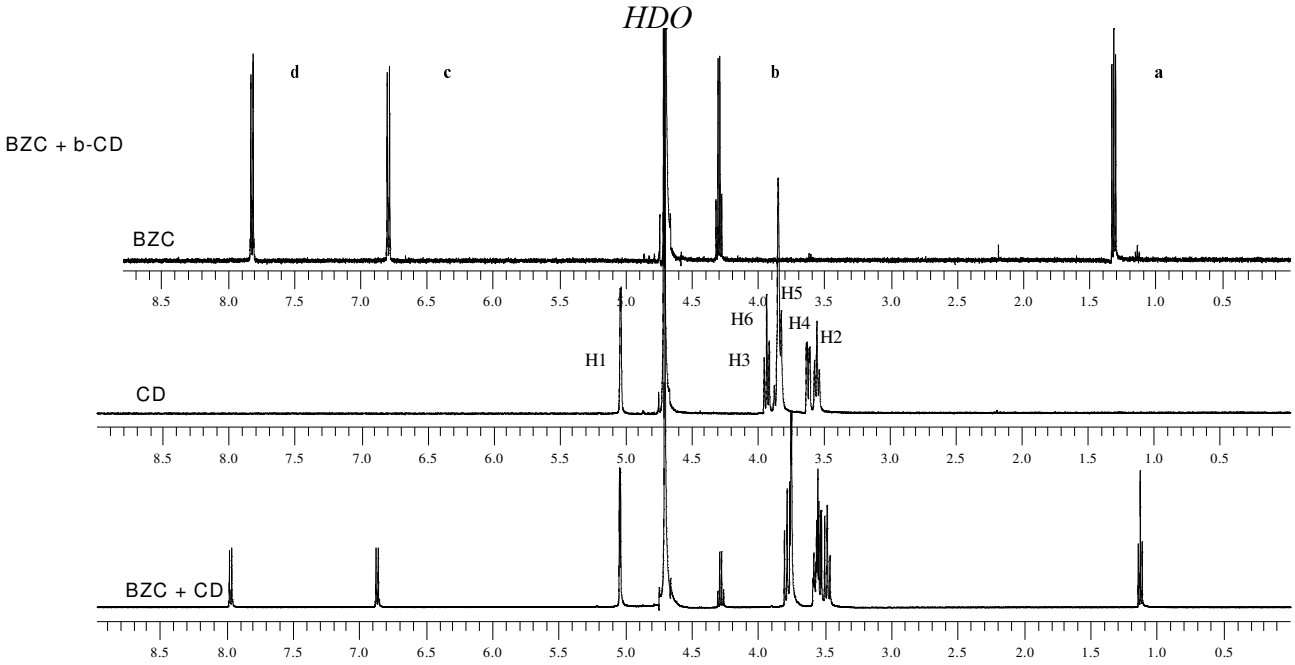
HDO
d
c
b
a
BZC + b-CD
BZC
H5
H6
H4
H2
H1
H3
CD
BZC + CD
8.5 8.0 7.5 7.0 6.5 6.0 5.5 5.0 4.5 4.0 3.5 3.0 2.5 2.0 1.5 1.0 0.5

Fig. 6

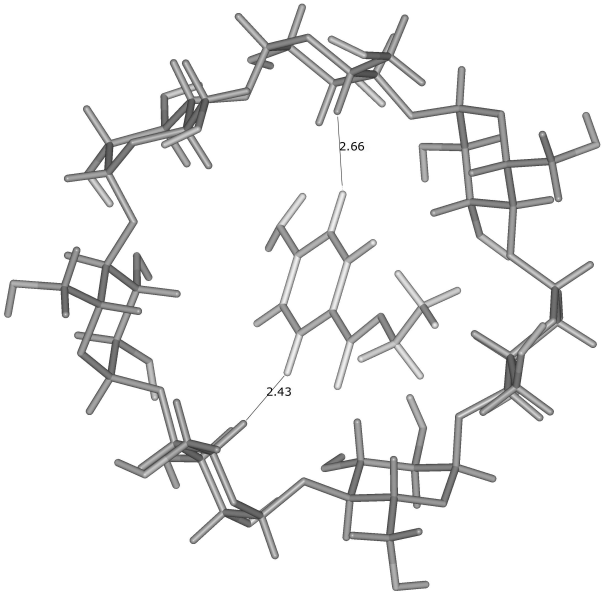
2.66
2.43

Fig. 7

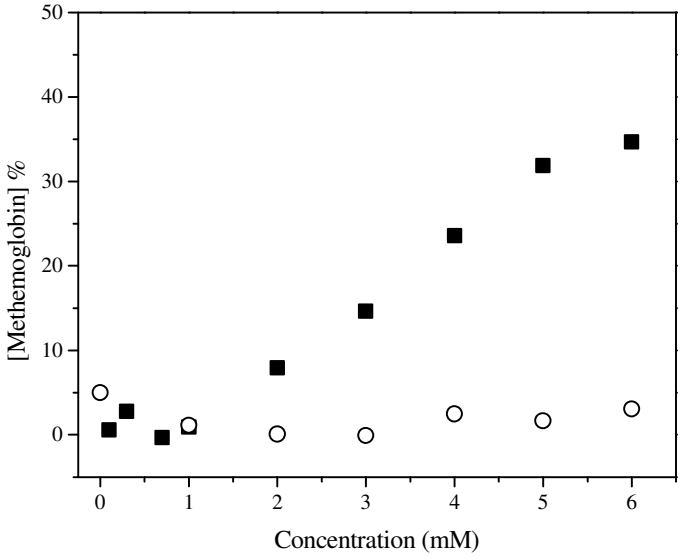
[Methemoglobin] %
Concentration (mM)
0
10
20
30
40
50
0
1
2
3
4
5
6

Fig. 8

6.2 – α AND β CONFORMATIONAL PREFERENCES IN FIBRIL-FORMING PEPTIDES CHARACTERIZED USING NMR AND CD TECHNIQUES

α and β Conformational Preferences in Fibril Forming Peptides Characterised using NMR and CD Techniques.

Thelma A. Pertinhez [1,2], Amanda K. Sherwood[1], Leonardo F. Fraceto[3], Mario Bouchard[1], Maureen Pitkeathly[1], and Lorna J. Smith [1]*

[1] Oxford Centre for Molecular Sciences, Central Chemistry Laboratory, University of Oxford, South Parks Road, Oxford, OX1 3QH, U.K. [2] Center for Molecular and Structural Biology, LNLS, CP 6192, 13084-971, Campinas, Brazil. [3] LNLS and Department of Biochemistry, University of Campinas, Campinas, Brazil.

* **Corresponding author address**: Dr. L. J. Smith, Central Chemistry Laboratory, University of Oxford, South Parks Road, Oxford, OX1 3QH, U.K. Phone: +44-1865-275961; Fax: +44-1865-275905; E-mail: lorna.smith@chem.ox.ac.uk

Abstract: Peptide fragments taken from residues 18-54 of short consensus repeat 3 (SCR3) from the human complement receptor CR1 have been found in aqueous solution to slowly aggregate and form fibrils. NMR studies of the monomeric form of these peptides show that they are essentially unfolded in aqueous solution and that they all have an increased helicity in TFE solutions. The behaviour of residues 28-31 from SCR3 is particularly interesting. These residues have a high β-sheet propensity in the native protein and a seven peptide containing their sequence is found to form fibrils despite its short length. However, NMR studies show that these residues adopt a well-defined α-helix in 80% TFE and under these conditions fibril formation has not been observed. These data demonstrate the strong dependence of conformational propensities on environment.

Abbreviations: CD, circular dichroism; EM, electron microscopy; SCR3, short consensus repeat 3 from the human complement receptor CR1; SDS, sodium dodecyl sulfate; TFE, trifluoroethanol.

1. Introduction.

A number of different proteins have been found to form amyloid fibrils *in vitro*. These include the SH3 domain of PI3 kinase, a type III domain of fibronectin, acylphosphatase, myoglobin and cytochrome c_{552} [1-5]. It is therefore becoming increasingly apparent that it is not only the 20 or so disease-associated proteins that can form the highly ordered fibrillar aggregates but rather that the propensity for this type of structure may be an intrinsic, generic property of the polypeptide backbone [6]. Indeed myoglobin and cytochrome c_{552} that are substantially α-helical in their soluble native folds have been found to form fibrils [4, 5]. It has been recognised that in general the formation of fibrils occurs when the native protein is destabilised under conditions where noncovalent interactions, particularly hydrogen bonding remains favourable [3].

In order to gain a full understanding into the process by which fibrils form it is necessary to characterise the properties of the conformers in solution from which aggregation and fibril formation occur. These conformers are often partially folded states and detailed structural studies of non-native proteins are challenging. Non-native states are in general ensembles of interconverting conformers [7]. Hence their study by NMR techniques is often hampered due to severe line broadening and lack of chemical shift dispersion [8]. One strategy therefore is to study the fibril formation of peptide fragments taken from a protein sequence since peptides can be more readily characterised at a sequence specific level using NMR techniques. This is the approach we use here. We report studies of fibril forming peptide fragments of differing lengths from the sequence of short consensus repeat 3 (SCR3) from the human complement receptor CR1 [9]. This receptor binds C3b and C4b, two complement proteins, and the peptides studied in this work include a region in SCR3/10 at which both proteins have been reported to bind. These interactions of CR1 with the complement proteins C3b and C4b form part of the catabolic and regularly pathways of the immune system [10, 11].

2. Materials and Methods

Peptides SCR3(18-34) (sequence: STNRENFHYGSVVTYRS), SCR3(34-54) (sequence: SNPGSGGRKVFELVGEPSIYS), SCR3(18-54) (sequence: STRENFHYGSVVTYRSNP GS GG RKVFELVGEPSIYS) and SCR3(27-33) (sequence: GSVVTYR) were synthesised using solid-phase methodology. The identity and purity of the final products were confirmed by FAB mass spectrometry and reversed-phase high performance liquid chromatography. The two cysteine residues (Cys 34 and Cys 54) within this region of the wild type protein sequence were replaced by serine residues. In addition in the SCR3(18-54) peptide Asn 20 has been deleted.

CD measurements were carried out on a Jasco J720 Spectropolarimeter at 25 °C using a Haake F8 temperature controller. Far UV CD spectra were acquired using cells of 1 mm path length at 0.5 nm intervals over the wavelength range 190-250 nm. The concentrations of the peptides were determined by the UV absorption of the tyrosine residue at 274 nm. Peptide solutions were prepared by dissolving lyophilised peptide in deionised water (peptide concentration 50-100 μM), and adjusting to pH 4 with small aliquots of NaOH and HCl. The H_2O/TFE cross titration experiments were carried out by mixing the appropriate aliquots of two 0.1 mM peptide stock solutions, one in water at pH 4.0 and the other in TFE. The peptide solutions in SDS were prepared by adding the peptide to a non-micellar 3mM SDS solution in water at pH 4.

Samples for NMR spectroscopy were prepared to contain approximately 2 mM peptide at pH 4 in 10%D_2O/90%H_2O, 30%TFE-d_3/70%H_2O or 80%TFE-d_3/20%H_2O. ^1H NMR experiments were performed at 25°C using NMR spectrometers at the Oxford Centre for Molecular Sciences with ^1H operating frequencies of 500.2 and 600.2 MHz and an NMR spectrometer at the Center for Molecular and Structural Biology, LNLS with a ^1H operating frequency of 500 MHz. 2D experiments were acquired with 1K complex points in t_2 and in phase-sensitive mode using time-

proportional phase incrementation (TPPI) for quadrature detection in t_1. Typically 512-750 t_1 increments with 32-64 scans were recorded for TOCSY [12] (75ms mixing time) and ROESY [13] (150ms and 200ms mixing times) experiments. For the determination of the $^3J_{HN\alpha}$ coupling constants COSY spectra [14] were recorded with 1024 t_1 increments of 4K complex data points. NMR data were processed using Felix 2.3 (Hare Research and Biosym Inc.) and Felix 2000 (Accelrys Inc.). The spectra were referenced to the internal standard DSS (2,2-dimethyl-2-silapentane 5-sulfonate) at 0.0 ppm. The spectra were assigned using standard procedures [15] and the ^{1}H resonance assignments have been submitted to BioMagRes Bank (accession number xxx).

For the electron microscopy aliquots collected from the peptide solutions during fibril formation were applied to Formvar-coated grids. These were negatively stained with a solution of 2% (wt/vol) uranyl acetate in water, washed, air-dried and then examined in a JEOL JEM1010 transmission electron microscope operating at an accelerating voltage of 80 kV.

3. Results and Discussion

In this work we concentrate on the sequence forming residues 18-54 of SCR3. Two peptides have been studied initially corresponding to residues 18-34 and 34-54 respectively (SCR3(18-34) and SCR3(34-54)). The structure of SCR3 has not yet been solved but the structures of a number of other short consensus repeat modules with a close homology to SCR3 are available [16] including the structure of the pair of modules SCR16-SCR17 from CR1 [17]. The sequences of SCR3 and SCR17 differ by only two residues in the region corresponding to the peptides studied. All these short consensus repeat modules have structures rich in β-sheet and no α-helical secondary structure [16]. Sequence alignment suggests that the peptide sequence SCR3(18-54) will form three β-strand segments in the native structure (residues 29-32, 46-47, 51-53) (Figure 1).

Comparisons in aqueous and TFE solutions

As reported previously [18] incubation of SCR3(18-34) in aqueous solution at 25°C results in the formation of amyloid fibrils after a period of days. Under similar conditions SCR3(34-54) also forms fibrils (Figure 2). To gain more insight into the properties of these peptides, and the conformations from which fibrils can form, CD and NMR studies have been performed for the two peptides in aqueous and TFE solutions.

Both the SCR3(18-34) and SCR3(34-54) peptides freshly dissolved in aqueous solution are essentially unfolded. The CD spectra (Figure 3) show strong minima at *ca* 197 nm typical of a random coil and the CαH chemical shifts for the peptides (Figure 4) are close to those seen for short unstructured GGXGG peptides [19]. Interestingly however a cluster of upfield chemical shift deviations (> 0.1 ppm) are seen for Glu 22, Asn 23, Phe 24 and His 25 in SCR3(18-34). These deviations presumably reflect a persistent hydrophobic cluster involving the aromatic side chains of two of these residues, similar to those identified in a number of denatured proteins [20-22].

CD spectra were used to follow H_2O/TFE cross-titration experiments for the peptides (Figure 3). In each case a transition to a more helical conformation, characterised by a negative band in the CD spectra near 210 nm and a shoulder at 220 nm, was observed on the addition of TFE. For SCR3(34-54) a sigmoidal increase in helical secondary structure was observed with increasing TFE concentrations indicating a cooperative induction of helicity. From the ellipticity at 222 nm SCR3(34-54) was estimated to contain 17.6% helicity in 30% TFE and 21.4% helicity in 80% TFE. The behaviour of SCR3(18-34) was different to that of SCR3(34-54). The peptide shows a regular increase in helicity throughout the titration and having 13.6% helicity in 30% TFE and 37.3% helicity in 80% TFE. To gain further insight into these changes NMR studies of SCR3(34-54) in 30% TFE and SCR3(18-34) in 30% and 80% TFE were performed.

Comparisons of the CαH chemical shifts for SCR3(18-34) and SCR3(34-54) in 30% TFE with those seen for short unstructured GGXGG peptides [19] (Figure 4) show that there are no clear pattern of chemical shift deviations for either peptide. For SCR3(18-34) deviations of more than 0.1 ppm are seen for the N-terminal residues Ser 18 and Thr 19 and for Phe 24 – Tyr 26. The deviations for the latter residues presumably reflect the persistence of the hydrophobic cluster seen in aqueous solution. For SCR3(34-54) three residues have their resonances shifts upfield (Ser 34, Val 43, Ser 51) and one downfield (Lys 42) by more than 0.1 ppm. Neither of the peptides shows any chemical shift deviations greater than 0.2 ppm (except for the N-terminal residue of SCR3(34-54)). The absence of large deviations presumably reflects the relatively small percentage helicity induced by 30% TFE (13.6% for SCR3(18-34) and 17.6% for SCR3(34-54)).

For SCR3(18-34) more significant upfield CαH chemical shift deviations (≥ 0.2ppm) are observed in 80% TFE for Val 29, Val 30 and Thr 31. As groups of upfield shifted CαH resonances are indicative of helical secondary structure [23] these data identify this 29-31 region as being the one that adopts helical conformers on the addition of TFE. Further evidence to support this comes from $^{3}J_{HN\alpha}$ coupling constant measurements (Figure 5). In particular Val 29 and Val 30 have $^{3}J_{HN\alpha}$ values of 5.5 and 5.3 Hz respectively, values reduced by approximately 2 Hz from the coupling constants measured for these residues in the peptide in aqueous solution.

This helical structure adopted in TFE is particularly interesting as comparisons with the structure of SCR17 [17] suggest that residues 29-31 are a central β-strand (residues 29-32) within an antiparallel β-sheet in the native protein. Furthermore secondary structure prediction for SCR3 identifies the 29-31 sequence as having a very high β sheet propensity. For example, with the PHD method [24] residues 29-32 are predicted to adopt extended β-strand secondary structure with the maximum value (9) of the reliability index. Similarly using the Chou and Fasman

method [25] the average conformational parameters for residues 29-32 ($<P_\alpha>$ 0.88, $<P_\beta>$ 1.36) show a strong preference for β-sheet secondary structure.

Comparison with the conformational properties of a longer peptide fragment.

The β-sheet conformation adopted by at least some parts of the SCR3(18-34) and SCR3(34-54) sequences both when in the native folded protein and also when amyloid fibrils are formed presumably results from intra or intermolecular interactions that are absent when these short peptides are studied in a monomeric form. To investigate further the role of intramolecular interactions we have also characterised by CD and NMR techniques a longer peptide with a sequence corresponding to residues 18-54 of SCR3 (SCR3(18-54)). This peptide contains the residues that form the two central strands in the antiparallel β-sheet in SCR3. This SCR3(18-54) peptide has been found to form fibrils after a period of days of incubation in aqueous solution (Figure 2D). However no fibril formation has been observed after incubation of the peptide in 80% TFE solution.

The CD spectrum the SCR(18-54) peptide freshly dissolved in aqueous solution is typical of a random coil and shows a strong minimum at *ca* 198 nm (Figure 3C). The CαH chemical shifts for the peptides (Figure 6) in aqueous solution are closely similar to those seen for the shorter SCR3(18-34) and SCR3(34-54) peptides. In addition the H_2O/TFE cross-titration experiment shows an increase in helicity on the addition of TFE similar to that observed for the shorter peptide fragments (Figure 3C). Interestingly, however, in the longer SCR3(18-54) peptide in 80% TFE slightly larger CαH chemical shifts deviations are seen than for SCR3(18-34) under the same conditions. In particular His 25, Tyr 26, Ser 28, Val 29, Val 30, Thr 31 and also Val 43 all have deviations ≥ 0.2ppm in SCR3(18-54) indicating that number of residues involved in the helicity is increased in the longer peptide.

Despite the longer peptide sequence of SCR3(18-54), there is no evidence for a significant population of β strand in the SCR3(18-54) peptide in aqueous solution or TFE. We have therefore also studied the peptide in sodium dodecyl sulfate (SDS), a detergent that is known in some cases to promote β-sheet conformers. Under these conditions the CD spectrum of SCR3(18-54) is characteristic of a β-strand conformation. In particular in 3mM SDS below the critical micellar concentration a strong band just below 210 nm and a negative band at 220nm are observed. This behaviour for SCR3(18-54) differs to that of SCR3(18-34) in SDS. Here, as we have reported previously, the peptide initially acquires an α-helical conformation in the presence of non-micellar concentrations of SDS. However under these conditions the SCR3(18-34) peptide then converts to a β-sheet and large quantities of fibrils form [18].

A short peptide fragment will also form fibrils.

In SDS both the SCR3(18-54) and SCR3(18-34) peptides are observed, under certain conditions, to adopt β conformers. However under the conditions of the NMR studies of the peptides in aqueous solution and TFE there was no evidence for β conformers. Therefore to obtain more information on a residue specific level as to which residues in the 18-54 sequence may be important in the fibril formation we have also characterised a shorter peptide fragment taken from this sequence of SCR3. The peptide corresponds to residues 27-33 (SCR3(27-33)), one of the regions that comparisons with the structure of SCR17 suggests contains a β-strand in the native folded structure. Reflecting this, residues in the centre of the peptide sequence are predicted to adopt β-strand secondary structure with the maximum reliability index (with the PHD method [24]). However the peptide also contains the group of four residues which in the SCR3(18-54) peptide in TFE have upfield chemical shift deviations ≥ 0.2 ppm characteristic of α-helical conformations (for residues 28-31).

SCR3(27-33) was found to be essentially unfolded in aqueous solution, the CD spectrum resembling that expected for a random coil. On incubation the peptide in aqueous solution was found to form fibrils (Figure 2C) after a period of days. The CD spectrum of SCR3(27-33) showed evidence for an increase in helicity on the addition of TFE but NMR studies indicate that the helical secondary structure is less persistent that in the longer peptides. In particular in 80% TFE the only CαH chemical shift deviation ≥ 0.1 ppm is for Thr 31 (-0.10 ppm) (Figure 4C). This presumably reflects the fact the short peptide length does not give possibilities for many helix-stabilising hydrogen bonding interactions. However under these conditions in 80% TFE SCR3(27-33) was not found to form fibrils.

4. Conclusions

The 18-54 sequence from SCR3 has a clear propensity to form fibrils. Indeed all the peptides reported here have been found to form fibrils when in aqueous solution including even a short peptide of just seven residues (SCR3(27-33)). In aqueous solution the peptides are essentially unfolded and therefore, as in a model random coil, each residue will be interconverting between α and β main chain conformations [26]. The sequence, however, has a β propensity and the native SCR3 fold is rich in β-sheet. Amyloid fibrils have also been shown to contain extensive β structure [27]. Therefore for the isolated peptide fragments aggregation and formation of fibrils lead to the stabilisation of preferred β conformers in the absence of the tertiary interactions that would be present in the full protein structure. The results for these SCR3 peptides therefore support hypothesis that the ability to adopt amyloid fibrils is an inherent property of the polypeptide backbone [6].

In TFE solutions studies of both SCR3(18-54) and SCR3(27-31) have not given any evidence of fibril formation. CD studies show that the peptides have an increased helicity under these conditions. For most parts of the sequence however the NMR chemical shift deviations for

the peptides in TFE from the values expected of a random coil are relatively small. This indicates that the helical secondary structure adopted by the peptides in TFE must be fluctuating and dynamic in nature. Studies of acylphosphatase have shown that for this protein fibril formation is accelerated in 25% TFE. However at higher concentrations of TFE (>35%) fibril formation does not occur [28]. For acylphosphatase it is proposed that at the higher TFE concentrations aggregation is not favoured because of increased intramolecular hydrogen bonding and reduced hydrophobic effects [28]. These factors are presumably also responsible for the inhibition of fibril formation for this sequence in TFE. As any intramolecular hydrogen bonds will be very fluctuating for the peptides it is likely that the reduced hydrophobic effects may be the dominant factor. Indeed the SCR3 18-54 sequence has a high hydrophobicity containing 12 residues with aromatic side chains or other significantly hydrophobic side chains (Val, Leu, Ile). In addition in aqueous solution residues 22-25 have been identified to form a hydrophobic cluster.

It is interesting that the part of the SCR3 sequence studied which the NMR studies shows has the highest α-helicity in TFE (residues 28-31) has a high β-sheet preference and a significant propensity to form fibrils. A number of other studies have identified sequences that adopt β-strands in native protein folds but α-helices in TFE including parts of β-lactoglobulin and hen lysozyme [29-31]. In the cases of these proteins though, in contrast to the SCR3 residues, the sequences have a high α-helical propensity. This local helical preference dominates in the absence of longer-range intramolecular contacts. Some understanding into the helicity observed in SCR3 despite the high β-sheet propensity comes from the results of studies in the changes in the conformational propensities of different amino acids in TFE [32, 33]. These have shown that increases in helical preference under these conditions are context dependent but there is a significant increase in the helical propensity of amino acids with nonpolar β-branched side chains such as valine. As the 28-31 sequence contains two valines (sequence SVVT) it is therefore

presumably these residues that are at least in part responsible for the helicity in TFE. Interestingly though these same valine residues are also likely to be important in determining the β-sheet preference in the native protein and the propensity to form fibrils. The variety of conformations observed for this sequence therefore provide a clear example of the manner in which the environment can significantly influence conformational preferences of a polypeptide chain.

5. Acknowledgements

We thank Chris Dobson and Richard Smith for encouragement and helpful discussions. This work was supported in part by FAPESP, Brazil

6. References

[1] J.I. Guijarro, M. Sunde, J.A. Jones, I.D. Campbell and C.M. Dobson, Amyloid fibril formation by an SH3 domain, Proc. Natl. Acad. Sci. USA 95 (1998), 4224-4228.

[2] S.V. Litvinovich, S.A. Brew S. Aota, S.K. Akiyama, C. Haudenschild and K.C. Ingham, Formation of amyloid-like fibrils by self-association of a partially unfolded fibronectin type III module, J. Mol. Biol. 280 (1998), 245-258.

[3] F. Chiti, P. Webster, N. Taddei, A. Clark, M. Stefani, G. Ramponi and C.M. Dobson, Designing conditions for in vitro formation of amyloid protofilaments and fibrils, Proc. Natl. Acad. Sci. USA 96 (1999), 3590-3594.

[4] M. Fandrich, M.A. Fletcher and C.M. Dobson, Amyloid fibrils from muscle myoglobin - Even an ordinary globular protein can assume a rogue guise if conditions are right, Nature 410 (2001), 165-166.

[5] T.A. Pertinhez, M.L. Bouchard, E.J. Tomlinson, R. Wain, S.J. Ferguson, C.M. Dobson and L.J. Smith, Amyloid fibril formation by a helical cytochrome, FEBS Lett. 495 (2001), 184-186.

[6] C.M. Dobson, The structural basis of protein folding and its links with human disease, Phil. Trans. Roy. Soc. London Ser. B 356 (2001), 133-145.

[7] A.R. Dinner, A. Sali, L.J. Smith, C.M. Dobson and M. Karplus, Understanding protein folding via free-energy surfaces from theory and experiment, Trends Biochem. Sci. 25 (2000), 331-339.

[8] D.R. Shortle, Structural analysis of non-native states of proteins by NMR methods, Curr. Opin. Struc. Biol. 6 (1996), 24-30.

[9] N.S. Clark, I. Dodd, D.E. Mossakowska, R.A.G. Smith and M.G. Gore, Folding and conformational studies on SCR1-3 domains of human complement receptor 1, Protein Eng. 9 (1996), 877-884.

[10] M. Krych, R. Hauhart and J.P. Atkinson, Structure-function analysis of the active sites of complement receptor type 1, J. Biol. Chem. 273 (1998), 8623-8629.

[11] M. Krych-Goldberg and J.P. Atkinson, Structure-function relationships of complement receptor type 1 Immunological Reviews 180 (2001), 112-122.

[12] L. Braunschweiler and R.R. Ernst, Coherence transfer by isotropic mixing - application to proton correlation spectroscopy, J Magn. Reson. 53(1983), 521-528.

[13] C. Griesinger and R.R. Ernst, Frequency offset effects and their elimination in NMR rotating-frame cross-relaxation spectroscopy, J.Magn. Reson.75 (1987), 261-271.

[14] A. Bax and R. Freeman, Investigation of complex networks of spin-spin coupling by two-dimensional NMR, J.Magn. Reson. 44 (1981), 542-561.

[15] K. Wüthrich, NMR of proteins and nucleic acids, Wiley, New York (1986).

[16] M.D. Kirkitadze and P.N. Barlow, Structure and flexibility of the multiple domain proteins that regulate complement activation, Immunological Reviews 180 (2001), 146-161.

[17] B.O. Smith, R.L. Mallin, M. Krych-Goldberg, X.F. Wang, R.E. Hauhart, K. Bromek, D. Uhrin, J.P. Atkinson and P.N. Barlow, Structure of the C3b binding site of CR1 (CD35), the immune adherence receptor, Cell 108 (2002), 769-780.

[18] T.A. Pertinhez, M. Bouchard, R.A.G. Smith, C.M. Dobson and L.J. Smith, Stimulation and inhibition of fibril formation by a peptide in the presence of different concentrations of SDS, FEBS Lett. 529 (2002), 193-197.

[19] G. Merutka, H.J. Dyson and P.E. Wright, Random coil H-1 chemical shifts obtained as a function of temperature and trifluoroethanol concentration for the peptide series GGXGG, J. Biomol. NMR 5 (1995), 14-24.

[20] D. Neri, M. Billeter, G. Wider and K. Wüthrich, NMR determination of residual structure in a urea-denatured protein, the 434-repressor, Science 257 (1992), 1559-1563.

[21] W. Peti, L.J. Smith, C. Redfield and H. Schwalbe, Chemical shifts in denatured proteins: Resonance assignments for denatured ubiquitin and comparisons with other denatured proteins, J. Biomol. NMR 19 (2001), 153-165.

[22] J. Klein-Seetharaman, M. Oikawa, S.B. Grimshaw, J. Wirmer, E. Duchardt, T. Ueda, T. Imoto, L.J. Smith, C.M. Dobson and H. Schwalbe, Long-range interactions within a nonnative protein, Science 295 (2002), 1719-1722.

[23] D.S. Wishart, B.D. Sykes and F.M. Richards, Relationship between nuclear magnetic resonance chemical-shift and protein secondary structure, J. Mol. Biol. 222 (1991), 311-333.

[24] B. Rost, and C. Sander, Prediction of protein secondary structure at better than 70-percent accuracy, J. Mol. Biol. 232 (1993), 584-599.

[25] P.Y. Chou and G.D. Fasman, Empirical predictions of protein structure, Annu. Rev. Biochem. 47 (1978), 251-276.

[26] L.J. Smith, K.M. Fiebig, H. Schwalbe, and C.M. Dobson, The concept of a random coil - Residual structure in peptides and denatured proteins, Fold. Des. 1 (1996), R95-R106.

[27] M. Sunde, L.C. Serpell, M. Bartlam, P.E. Fraser, M.B. Pepys and C.C.F. Blake, Common core structure of amyloid fibrils by synchrotron X-ray diffraction, J. Mol. Biol. 273 (1997), 729-739.

[28] F. Chiti, N. Taddei, M. Bucciantini, P. White, G. Ramponi and C.M. Dobson, Mutational analysis of the propensity for amyloid formation by a globular protein, EMBO J. 19 (2000), 1441-1449.

[29] K. Shiraki, K. Nishikawa and Y. Goto, Trifluoroethanol induced stabilization of the alpha-helical structure of beta-lactoglobulin - implication for non-hierarchical protein folding, J. Mol. Biol. 245 (1995), 180-194.

[30] D. Hamada, Y. Kuroda, T. Tanaka, Y. Goto, High helical propensity of the peptide-fragments derived from beta-lactoglobulin, a predominantly beta-sheet protein, J. Mol. Biol. 254 (1995), 737-746.

[31] M. Buck, H. Schwalbe and C.M. Dobson, Characterization of conformational preferences in a partly folded protein by heteronuclear NMR spectroscopy - Assignment and secondary structure analysis of hen egg-white lysozyme in trifluoroethanol, Biochemistry 34 (1995), 13219-13232.

[32] C.A. Rohl, A. Chakrabartty and R.L. Baldwin, Helix propagation and N-cap propensities of the amino acids measured in alanine-based peptides in 40 volume percent trifluoroethanol, Protein Sci. 5 (1996), 2623-2637.

[33] J.K. Myers, C.N. Pace and J.M. Scholtz, Trifluoroethanol effects on helix propensity and electrostatic interactions in the helical peptide from ribonuclease T-1, Protein Sci. 7 (1998), 383-388.

[34] P.J. Kraulis, MOLSCRIPT - a program to produce both detailed and schematic plots of protein structures, J. Appl. Crystallog. 24 (1991), 946-950.

[35] D.S. Wishart, C.G. Bigam, A. Holm, R.S. Hodges and B.D. Sykes, H-1, C-13 and N-15 random coil NMR chemical shifts of the common amino acids 1. Investigations of nearest neighbor effects, J. Biomol. NMR 5 (1995), 67-81.

Figure legends

Figure 1: The structure of complement control protein 17 of CR1 [17] indicating in grey the residues corresponding to residues 18-34 of SCR3 and in black the residues corresponding to residues 35-54 of SCR3. The figure was generated using the program Molscript [34].

Figure 2: Electron micrographs of fibrils formed by A) SCR3(18-34), B) SCR3(34-54), C) SCR3(27-33) and D) SCR3(18-54). In each case the fibrils were formed in 0.5mM samples of the peptide in aqueous solution at pH 4 that had been incubated at room temperature for approximately 6 months (SCR3(18-34) and SCR3(34-54)), 3 months (SCR3(18-54)) or 1 month (SCR3(27-33)). Bar = 200 nm.

Figure 3: Far-CV CD spectra of A) SCR3(18-34), B) SCR3(34-54) and C) SCR3(18-54).
In each case the bold line shows the spectrum of the peptide in aqueous solution and the dashed lines show the spectra for the peptide in increasing concentrations of TFE. Panel D) shows the percentage of helicity present in each of the peptides in TFE solutions calculated from the elipticity at 222 nm (symbols: SCR3(18-34) triangle; SCR3(34-54) circle; SCR3(18-54) square). In all the CD experiments a peptide concentration of 0.1mM was used at pH 4 and 25°C.

Figure 4: Secondary CαH chemical shifts of A) SCR3(18-34), B) SCR3(34-54) and C) SCR3(27-33). The open bars show the data for the peptides in aqueous solution, the filled bars the data for the peptides in 30% TFE and the dashed bars the data for the peptides in 80% TFE (pH 4 and 25°C). A positive secondary shift ($\Delta C\alpha H=\delta_{measured}-\delta_{coil}$) indicates a downfield chemical shift relative to the random coil values. The random coil chemical shifts of Merutka et al. [19] for GGXGG peptides

have been used expect for the residues that precede prolines. For these residues the values for GGXPGG peptides of Wishart et al. [35] have been used.

Figure 5: $^{3}J_{HN\alpha}$ coupling constant values for SCR3(18-34) in aqueous solution (open symbols) and in 80% TFE (filled symbols) at pH 4. The coupling constants were measured at 35°C in aqueous solution and at 25°C in TFE.

Figure 6: Secondary CαH chemical shifts of SCR3(18-54) The open bars show the data for the peptides in aqueous solution and the filled bars the data for SCR3(18-34) in 80% TFE (pH 4 and 25°C). A positive secondary shift ($\Delta C\alpha H=\delta_{measured}-\delta_{coil}$) indicates a downfield chemical shift relative to the random coil values. The random coil chemical shifts of Merutka et al. [19] for GGXGG peptides have been used expect for the residues that precede prolines. For these residues the values for GGXPGG peptides of Wishart et al. [35] have been used.

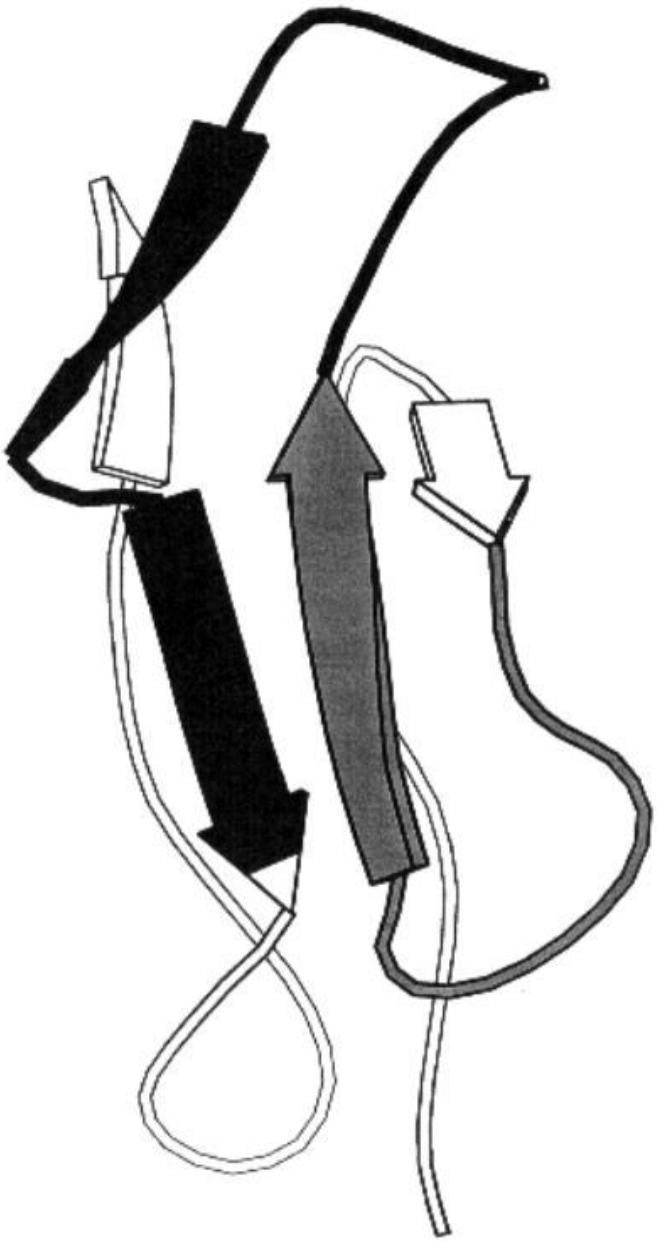

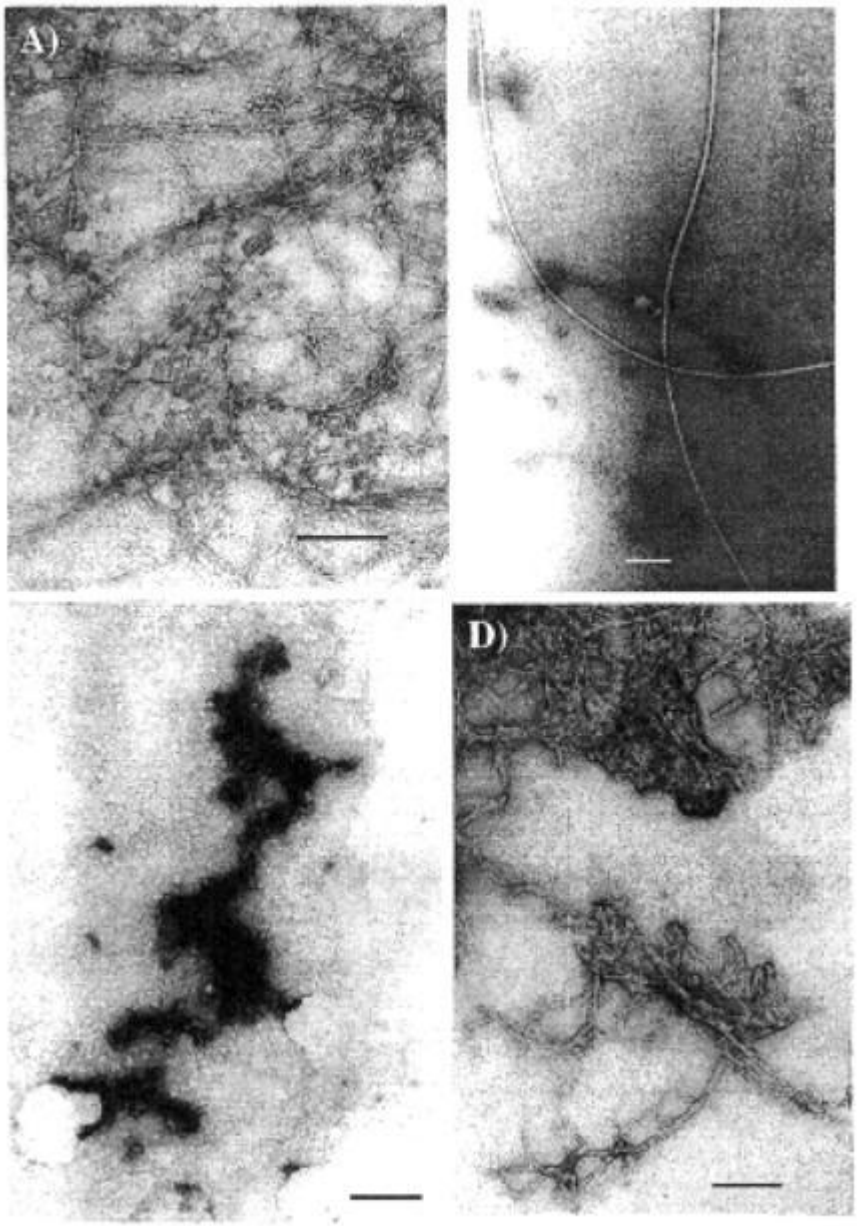
A)
D)

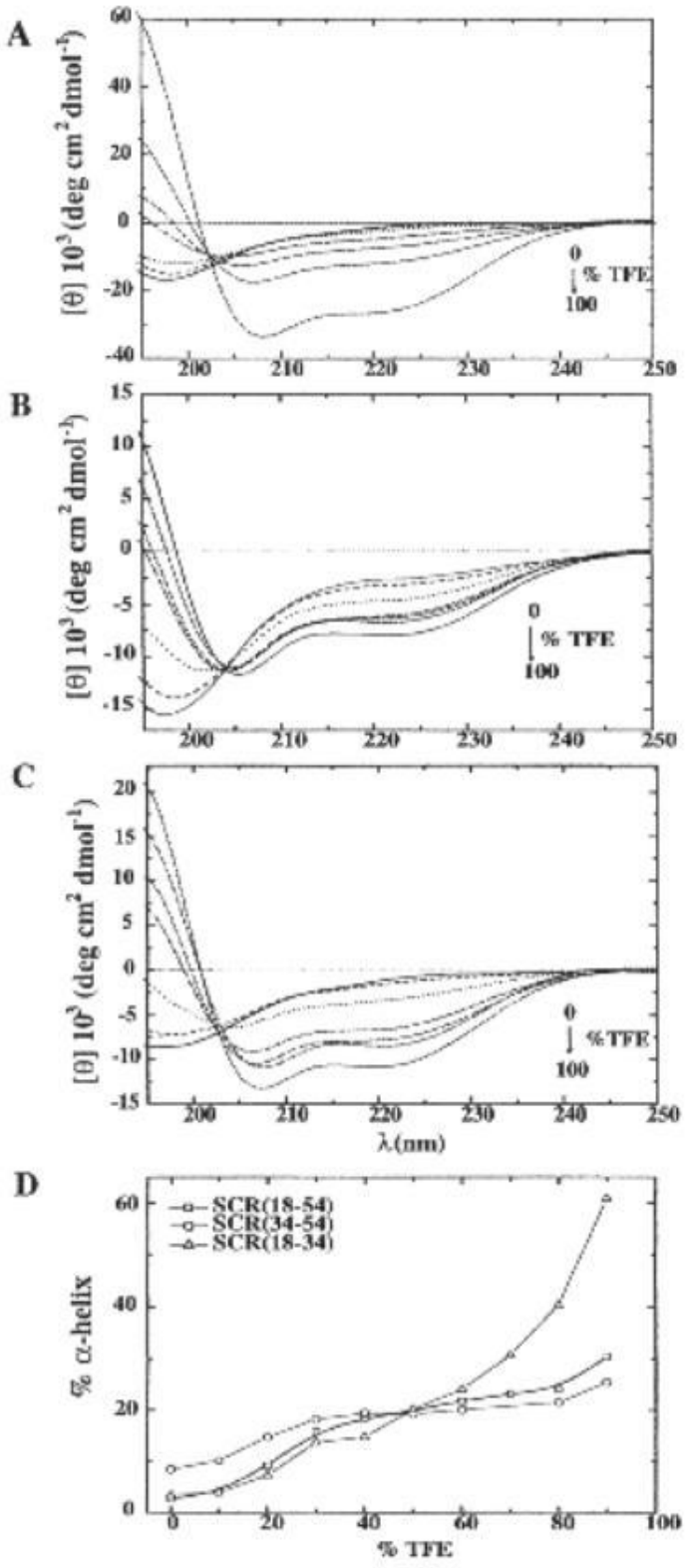
A
B
C
D
[θ] 10^-3 (deg cm^2 dmol^-1)
0
% TFE
100
λ(nm)
% α-helix
% TFE
SCR(18-54)
SCR(34-54)
SCR(18-34)

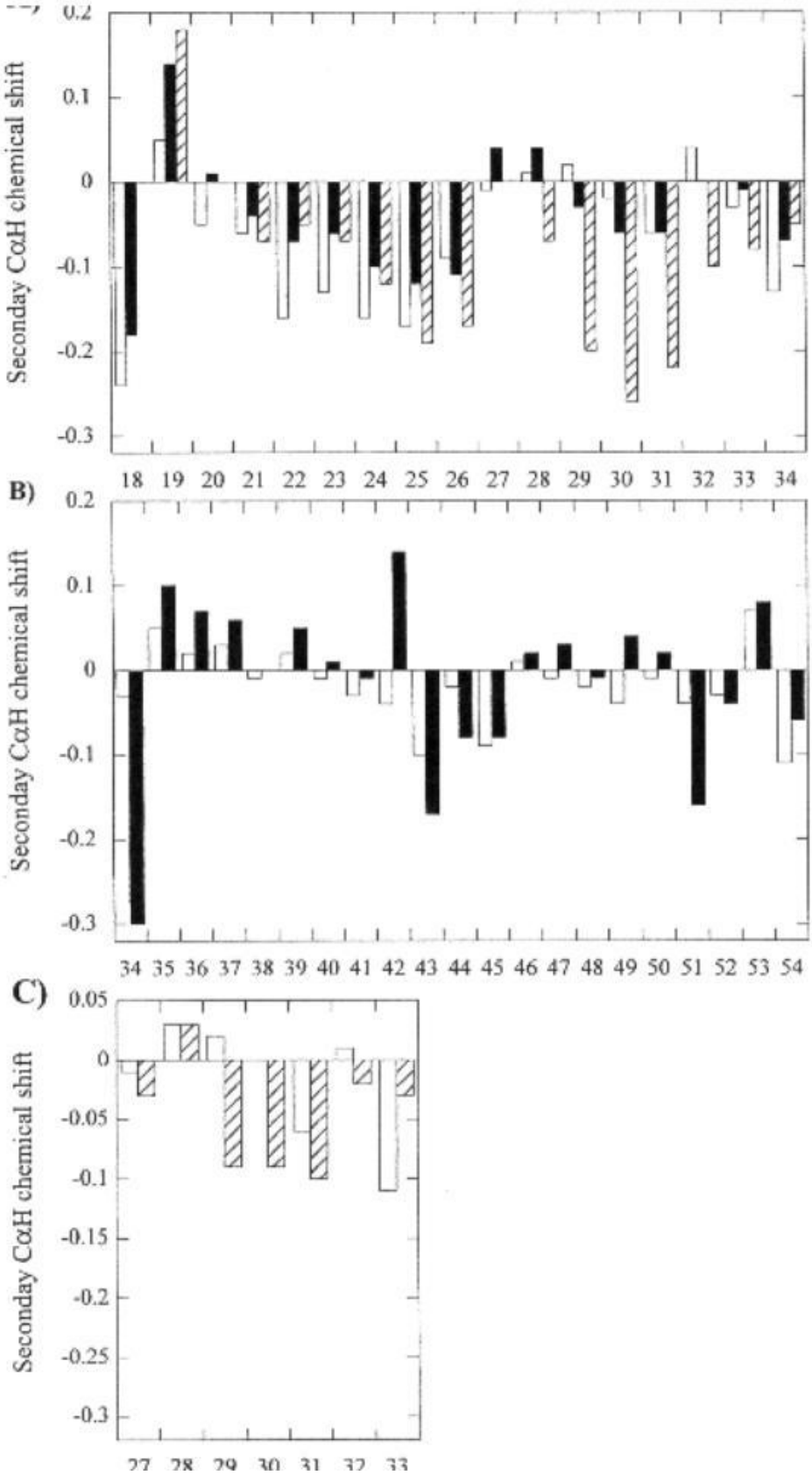
Seconday CαH chemical shift
0.2
0.1
0
-0.1
-0.2
-0.3
18 19 20 21 22 23 24 25 26 27 28 29 30 31 32 33 34
B)
Seconday CαH chemical shift
0.2
0.1
0
-0.1
-0.2
-0.3
34 35 36 37 38 39 40 41 42 43 44 45 46 47 48 49 50 51 52 53 54
C)
Seconday CαH chemical shift
0.05
0
-0.05
-0.1
-0.15
-0.2
-0.25
-0.3
27 28 29 30 31 32 33

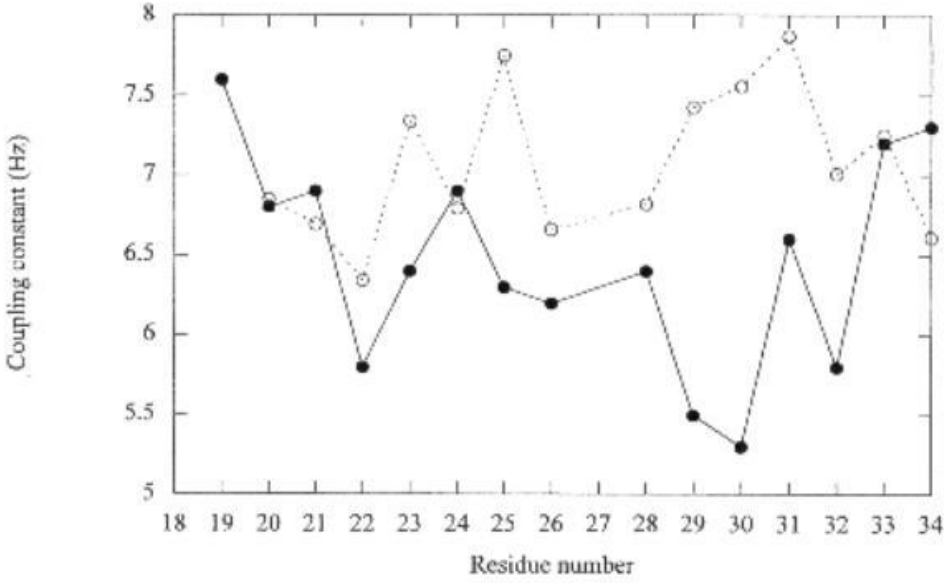
Coupling constant (Hz)
8
7.5
7
6.5
6
5.5
5
18 19 20 21 22 23 24 25 26 27 28 29 30 31 32 33 34
Residue number

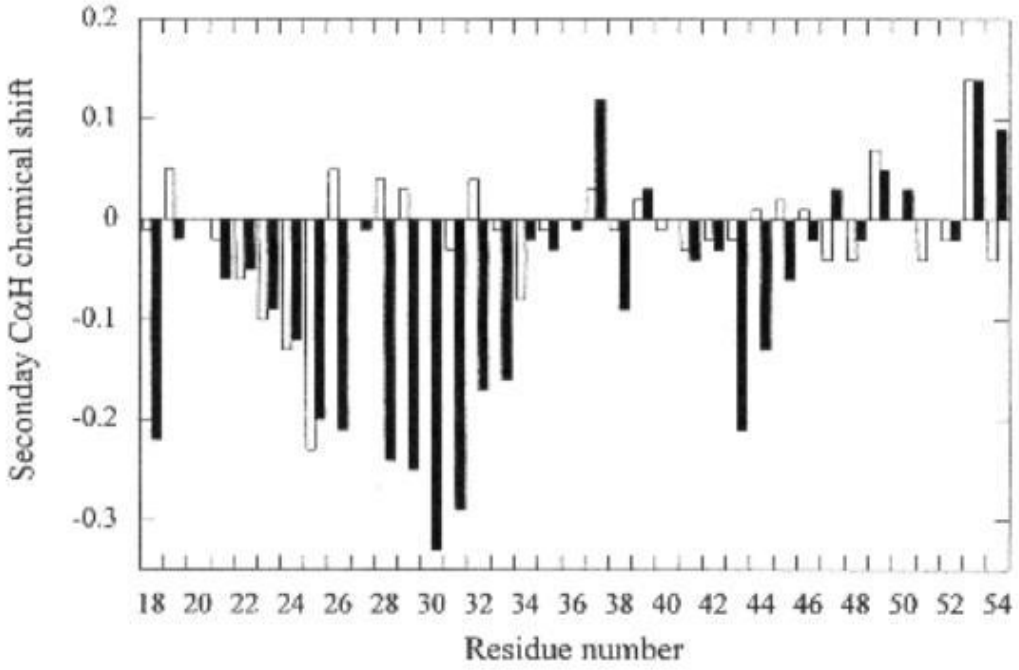
Seconday CαH chemical shift
0.2
0.1
0
-0.1
-0.2
-0.3
18 20 22 24 26 28 30 32 34 36 38 40 42 44 46 48 50 52 54
Residue number